ACTIVITY-DEPENDENT MICROTUBULE INVASIONS REGULATE CHANGES IN THE POSTSYNAPTIC MOLECULAR COMPOSITION OF DENDRITIC SPINES

By

Xindao Hu

A dissertation submitted in partial fulfillment of the requirements for the degree of

Doctor of Philosophy

(Neuroscience)

at the

UNIVERSITY OF WISCONSIN-MADISON

2012

Date of final oral examination: 08/10/12

The dissertation is approved by the following members of the Final Oral Committee:

Erik Dent, Associate Professor, Neuroscience

Corinna Burger, Assistant Professor, Neurology

Timothy Gomez, Professor, Neuroscience

Zhen Huang, Assistant Professor, Neurology/Neuroscience

Meyer Jackson, Professor, Neuroscience

Katherine Kalil, Professor, Neuroscience

TABLE OF CONTENTS

Chapter 1

Introduction

Microtubule Structure and Function in Neurons

In eukaryotic cells the cytoskeleton plays a central role in a number of cellular functions, including mitosis, maintenance of cell morphology, intracellular transport and cell motility (Conde and Caceres, 2009). Microtubules (MT), along with actin filaments and neurofilaments, constitute the major components of the cytoskeleton. MTs are polarized cylindrical polymers composed of α-tubulin and β-tubulin heterodimers, assembled into a linear array of alternating α- and β-subunits termed protofilaments (Dent and Gertler, 2003). MTs constitute a hollow tubular structure by parallel bundling of 11-15 protofilaments (Luduena, 1998; Dent and Gertler, 2003). This structural arrangement allows tubulin side chains to be exposed on the outside of individual MT polymers where posttranslational modifications can change conformation and binding characteristics of these side chains (Alexander et al., 1991; Rudiger et al., 1992; Redeker et al., 1994; Cambray-Deakin and Burgoyne, 1987; Janke and Bulinski, 2011). The surface of MT polymers provide binding sites for motor proteins, as well as MT-associated proteins (MAPs) that can bundle MT polymers into thick array. In developing neurons, MTs are abundant in the cell body and form dense parallel bundles in axons and dendrites via MAPs (Dent and Gertler, 2003). Ultrastructural studies have revealed that the orientation of MTs is different in axons and dendrites (Baas et al., 1988). In axons, MTs are uniformly oriented with their plus-ends facing the distal axon tip, whereas in dendrites MTs have mixed polarity (Conde and Caceres, 2009). The establishment of correct MT polarity has been demonstrated to play important roles when neurites assume their axonal or dendritic identity during development (reviewed by Georges et al., 2008; Baas and Lin, 2011).

MTs are also capable of rapid polymerization (growth) and depolymerization (shrinkage) from their plus-ends in a process termed dynamic instability (Mitchison and Kirschner, 1984).

Conversion from growth to shrinkage is termed ‘catastrophe’ whereas the opposite switch from shrinkage to growth is called ‘rescue’ (Conde and Caceres, 2009). GTP-bound tubulin dimers facilitate the polymerization of MTs while the exchange of GTP for GDP results in MT depolymerization from the plus-end. Dynamic instability allows MTs to rapidly explore the entire cytoplasm and has been extensively studied in non-neuronal cells (Holy and Leibler, 1994). Studies investigating MT dynamics in the axonal growth cone have found that dynamic MTs are important for growth cone motility, pathfinding and synapse formation (reviewed by Dent and Gertler, 2003; Dent et al., 2010). MTs and actin interactions have also been shown to play crucial roles during neuritogenesis and axon branching (Dent and Kalil, 2001; Dent et al., 2004). The dynamics of MTs in different regions of the growth cone has been further examined by live cell imaging. The rate of both MT polymerization and depolymerization in neurons averages 7-15um/min (Kabir et al., 2001; Dent and Kalil., 2001). Time-lapse imaging of fluorescently-labeled MTs in growth cones has shown that MTs are capable of rapid extension into and retraction from all areas of the growth cone, even to the tip of peripheral filopodia (Dent and Kalil, 2001; Schaefer et al., 2002; Suter et al., 2004). Thus, in developing neurons MTs are very dynamic and are capable of exploring all intracellular areas of the neuron.

Structure and Function of Dendritic Spines

Dendritic spines were first identified as small protrusions along neuronal dendrites by Ramon y Cajal more than a hundred years ago (Yuste and Tank, 1996; Rochefort and Konnerth, 2012). Today, it is accepted that spines function as the postsynaptic sites for most excitatory and some inhibitory inputs in the central nervous system (Yuste, 1995; Yuste and Tank, 1996; Ethell and Pasquale 2005). Serial section electron microscopy (EM) studies revealed that spines

typically consist of an enlarged “head” structure connected to a narrow “neck” (Harris 1999, Sorra and Harris 2000), although spine morphologies can exhibit a variety of shapes (Yuste and Bonhoeffer 2004). From EM studies it has been estimated that the majority of spines have a thin long neck and a bulbous head (~65%), whereas ~15% are mushroom-shaped with a large spine head and short neck. The remainder of dendritic protrusions appear to be either stubby spines or filopodial protrusions (Bourne and Harris, 2007).

The major cytoskeletal component of dendritic spines is filamentous actin (Matus, 2000). Immunocytochemistry and imaging studies visualizing GFP-tagged actin showed that spines are rich in actin whereas the neighboring dendritic shaft is actin poor (Matus, 2000). These postsynaptic structures emerge during synaptogenesis and can undergo morphological and structural changes based on actin rearrangement throughout neural development (Zito et al., 2004; Ethell and Pasquale, 2005). In hippocampal neurons, it is generally believed that spinogenesis begins with the formation of numerous filopodial protrusions during the early postnatal weeks. The protrusions then go through selective “pruning” as some filopodia form stable synaptic spines (Fiala et al., 1998, Marrs et al., 2001). However, a recent two-photon *in vivo* imaging study in the cortex also provided evidence that *de novo* spinogenesis could be induced by focal glutamate uncaging along the dendritic shaft (Kwon and Sabatini, 2011), indicating spines may not be required to develop from filopodial precursors. EM studies have shown that larger spine heads often associate with larger postsynaptic densities (PSDs) and are more likely to contain organelles (Spacek and Harris, 1997; Sorra and Harris, 2000). The PSD in the spine head contains NMDA and AMPA receptors, along with hundreds of other postsynaptic proteins (Sheng and Hoogenraad, 2007). Changes in spine structure and composition have been observed to closely correlate with changes in neuronal activity. During long term potentiation

(LTP - an enduring form of plasticity), spine head enlargement occurs through recruitment of NMDA and AMPA receptors to the PSD, whereas long term depression (LTD) results in spine shrinkage from the endocytosis of PSD proteins (Tada and Sheng, 2006). Depolymerization of actin filaments reduces spine formation and abolishes the LTP-induced increase in spine volume (Star et al., 2002; Halpain 2000). Thus, spine plasticity relies on an active actin network.

Loss of dendritic spines and abnormal spine morphology has been implicated in a variety of neurological disorders (Penzes et al., 2011). Post-mortem tissue histology has shown that spine density is severely reduced in Alzheimer's patients brains (DeKosky and Scheff, 1990; Penzes et al., 2011). Using *in vivo* imaging methods, a study modeling Alzheimer's disease by overexpression of human amyloid-beta precursor proteins (APP) in mice neurons also showed decreased spine numbers near formations of neurofibrillary tangles (Tsai et al., 2004). Spine pathology is prevalent in many developmental disorders. Cortical and hippocampal neurons in schizophrenia patients undergo spine pruning defects, where filopodial protrusions are excessively eliminated during synapse formation and stabilization, resulting in reduced synapse number (Sweet et al., 2009; Kolomeets et al., 2005). In autism spectrum disorder (ASD), post mortem tissue examination revealed increased spine numbers in the cortex, possibly due to increased synapse formation and early maturation during development (Hutsler and Zhang, 2010; Geschwind and Levitt, 2007). Similar synapse pathology can be observed in mouse models of Fragile X syndrome (Irwin et al., 2001), which is considered to be a form of ASD caused by mutation in the translational repressor fmr1 gene. Genetic mutations in adhesion molecules neuroligin and neurexin-1, which resulted in increased spine density, could also be explained by insufficient synapse pruning in ASD (Chih et al., 2004; Dudanova et al., 2007). It has become more and more evident that spine plasticity plays an important role in a variety of neurological

disorders. Further understanding of the cellular mechanisms that regulate spine formation and structural changes could provide valuable insight in the treatment of these diseases.

MTs in Dendrites and Dendritic Spines

In neurons, MTs function to transport intracellular cargos and regulate cell shape and motility during development. Dynamic MTs are required for neurite initiation, axon elongation and branch formation (Dent et al., 1999; Dent et al., 2001). Stabilizing MTs to prevent depolymerization after axotomy in *C. elegans* sensory neurons has been shown to promote axon regrowth and pathfinding (Chen et al., 2011). Global upregulation of MT plus-end dynamics was also identified as a neural protective mechanism following axon injuries in *Drosophila* (Chen et al., 2012). In mouse spinal cord lesions, MT stabilization with taxol improved axonal regeneration and locomotive recovery over time (Hellal et al., 2011). In dendrites, disrupting MT dynamics by genetic knock down of CLIP-170, an important component of the plus-end complex, resulted in reduced dendrite length and complexity (Swiech et al., 2011). Moreover, depletion of the structural MT-associated proteins MAP2 or MAP1A also led to a reduced dendritic network (Teng et al., 2001). MT dynamics are also required for normal cortical migration of neural precursor cells (Tsai et al., 2010) and MT-based motor proteins have been shown to act as an intracellular filter for trafficking of pre- versus post-synaptic cargos to their correct destinations (Song et al., 2009). Thus, MTs serve many functions in neurons but have heretofore thought to be specifically excluded from dendritic spines (Kaech et al., 2001). Nevertheless, based on the data presented above it is tempting to speculate that dynamic MTs could also play an important role in the postsynaptic spines during synapse formation and maintenance. In my thesis I investigated this possibility and discovered that MTs are involved in

various postsynaptic events in spines.

First, it was important to establish whether dynamic or stable MTs are present in spines. Over the last fifty years, myriad spine ultrastructural studies using transmission electron microscopy (TEM) and a variety of tissue fixation protocols supported the notion that spines are devoid of MTs. Among these studies, the presence of MTs in spines was documented only in a handful of cases. One study identified the presence of MTs in EM images of dendritic spines in cortical neurons (Gray et al., 1982). However, the method these authors used to prepare the samples (dissection in high albumin solution) was thought to induce artifacts. Another study found that MTs were present in some of the unusual highly branched spines in rat CA3 hippocampal neurons (Chicurel and Harris, 1992). A decade later, the same group also identified MTs in dendritic spines in rat hippocampal slices that were prepared at 4°C and warmed to 37°C (Fiala et al., 2003). In these slices, MTs only appeared in spines within the first 30 minutes after warming, but no MTs were detected in spines 3 hours post-warming. Furthermore, no MTs were discovered in hippocampal spines after direct perfusion of rats with fixative, indicating that under normal conditions spines do not contain MTs. Therefore the documentation of MTs in dendritic spines has been attributed to unusual circumstances or experimental artifacts due to unconventional tissue treatment.

Another methodology that has been utilized to visualize MTs in cells is to fluorescently label MT-associated proteins (MAPs) as a proxy for direct labeling of MTs with tubulin, which tends to have high background levels in neurons. Time-lapse imaging of either fluorescently-labeled MAP2 in dissociated hippocampal cultures or in hippocampal slices from GFP-MAP2c transgenic mice failed to detect MTs in the actin-rich dendritic spines (Kaech et al., 1997; Kaech et al., 2001). However, it should be noted that MAP2 is known to stabilize MTs (Kaech et al.,

1996). Therefore the decreased MT dynamics caused by over-expression of MAP-2 in neurons might have contributed to the absence of MTs in dendritic spines during time-lapse observation. This group's imaging regimen of collecting images at 30 second intervals using wide-field microscopy (Kaech et al., 2001) would also reduce the possibility of detecting fast MT dynamics within the micron-sized dendritic spines. Finally, the absence of evidence does not necessarily indicate evidence of absence.

In the first chapter of my thesis, I employed the relatively new methodology of total internal reflectance microscopy (TIRFM) to visualize MT dynamics in mature hippocampal spines. Using TIRFM, we were able to frequently acquire (10 second intervals) high-resolution images of EGFP-labeled tubulin for several hours, without any photodamage to the neurons. We used EGFP-α-tubulin to label MTs and DsRed2 to label the cytoplasm, and thus morphology, of neurons. Surprisingly, our experiments demonstrated that MTs were capable of polymerizing into and retracting from dendritic spines in mature cortical and hippocampal neurons (Hu et al., 2008). These MT excursions were infrequent and transient, targeting mature mushroom-shaped spines more than immature filopodial protrusions. Furthermore, we found that MTs target synaptic sites and neuronal depolarization induced by addition of a high-concentration of KCl effectively elevated the level of MT entry into dendritic spines, providing the first evidence that MT invasions are regulated by neuronal activity. Our results were corroborated by another study that used confocal microscopy to examine MTs in hippocampal cultures fixed in a specific MT-stabilizing buffer (Gu et al., 2008). A third study also found that MTs, labeled with the MT tip-binding protein EB3, invaded dendritic spines in cultured hippocampal neurons (Jaworski et al., 2009). This group further demonstrated that EB3 interaction with an actin-associated, cortactin-binding protein (p140cap) is important for spine morphological changes, indicating that MT-

actin interactions are significant in spines (Jaworski et al., 2009). These recent findings reveal that MTs might be involved in spine morphology and synaptic activity. It is therefore temping to speculate that MT entry into dendritic spines may play important roles in shuffling synaptic components into and out of spines, and that MTs may affect changes in spine shape via interaction with synaptic structural components such as actin filaments.

PSD-95 Dynamics in Dendritic Spines and Synaptic Plasticity

One of the most prominent and well-understood postsynaptic density proteins is the scaffolding protein PSD-95. PSD-95 is a multi-domain protein that can link several synaptic players together and anchor them to postsynaptic density. The postsynaptic proteins that have been demonstrated to directly associate with PSD-95 complex include NMDAR and AMPAR subunits, the cell adhesion molecule N-cadherin, the actin-binding proteins SHANK3 and cortactin, and the Rho GEF Kalirin-7 (Sheng and Hoogenraad, 2007). PSD-95 overexpression promotes spine formation and synapse stabilization (El-Husseini, 2000), whereas loss of PSD-95 affects LTP and spine morphological plasticity through defects in AMPAR recruitment to the synapse (Ehrich and Malinow, 2004; Ehrich et al., 2007). The N-terminal domain of PSD-95 contains side chains that can be palmitoylated (Topinka and Bredt, 1998), and PSD-95 palmitoylation is required for anchorage at the postsynaptic density as well as recruitment of AMPARs to the synapse (Noritake et al., 2009). Using a focal glutamate uncaging, Steiner and colleagues found that transient retrieval of PSD-95 is required for LTP-induced spine growth through CaMKII dependent phosphorylation at the serine 73 site (Steiner et al., 2008). Therefore, it is well established that normal function of PSD-95 is crucial for the formation and growth of synapses.

PSD-95 has been observed to undergo both ongoing slow turnover (Okabe, 1999) and rapid formation and movement within spines and spine precursors (Marrs et al., 2001). In an *in vivo* imaging study using photo-activatable GFP-PSD95 Gray and colleagues demonstrated that neighboring spines share a common pool of PSD-95 molecules, where PSD-95 molecules freely diffuse throughout the dendritic shaft and are retained in spines for minutes to hours (Gray et al., 2006). Interestingly, PSD-95 can bind to EB3, a MT tip binding protein (Sweet et al., 2011) and PSD-95 trafficking throughout the dendritic compartment is increased by neuronal activity induced by brain-derived neurotophic factor (BDNF) and NMDAR activation (Yoshi and Constantine-Paton, 2008). It is therefore reasonable to test for the possible connection between MT entries into spines and retention of PSD-95 molecules in those same spines.

In the second chapter of my thesis I used acute BDNF treatment as a plasticity inducing protocol. BDNF belongs to a family of small secreted proteins known as neurotrophins. In the nervous system, BDNF is widely expressed in developing and mature brains, where it functions to promote cell proliferation, differentiation, survival and growth cone pathfinding in axons (Davies and Wright, 1995; Shen and Cowan, 2010). Substantial evidence supports the role of BDNF as a crucial factor during synaptic development and plasticity through regulation of local translation, protein phosphorylation and strengthening of presynaptic terminals (Lu et al., 2008; Waterhouse and Xu, 2009). BDNF can be secreted in an activity-dependent manner from both pre and postsynaptic terminals (Hartmann et al., 2001; Kohara et al., 2001; Kojima et al., 2001), and act in a cell-autonomous fashion to regulate synaptic strength (Dean et al., 2009). Long-term treatment of hippocampal slices with BDNF increased spine density and the number of synapses in apical dendrites of CA1 pyramidal neurons (Tyler and Pozzo-Miller, 2001), whereas a regimen of several low doses of BDNF treatment over time resulted in enlargement of spine heads (Ji et

al., 2010). BDNF application also potentiates EPSPs in cultured hippocampal neurons (Lessmann et al., 1994), as well as long lasting LTP that is dependent on local protein translation in dendrites (Kang and Schuman, 1995; Kang and Schuman, 1996). BDNF application paired with theta-burst stimulation has been shown to induce actin-based spine formation through phosphorylation of p21-activated kinase and cofilin, indicating that BDNF can promote spine plasticity through regulation of actin dynamics (Rex et al., 2007). When paired with focal uncaging of glutamate, Tanaka and colleagues demonstrated that BDNF is required for a long lasting form of spine enlargement (Tanaka et al., 2008), further supporting the notion that BDNF is crucial for long lasting spine plasticity.

Interestingly, BDNF treatment was linked to activity induced trafficking of PSD-95 in dendrites (Yoshii and Constantine-Paton, 2008). Within 60 minutes of BDNF application, increases in both the size of PSD-95 puncta and PSD-95 fluorescence intensity were observed in visual cortical dendrites. This BDNF-induced PSD potentiation is dependent on activation of the BDNF receptor TrkB, facilitated by PI3K and can be enhanced by NMDAR activation. Moreover, treatment with colchicine, a microtubule destabilizing agent, abolished the increase in PSD-95 trafficking following BDNF treatment, indicating that PSD-95 trafficking to the postsynaptic site is dependent on an intact MT network (Yoshii and Constantine-Paton, 2008). In another study, cAMP was identified as a downstream BDNF signaling component that facilitated TrkB phosphorylation, translocation to the synapse, and association with PSD-95 (Ji et al., 2005), providing another pathway where BDNF could affect synaptic strength by regulating PSD-95.

In the second chapter of my thesis, I found that acute BDNF treatment increased MT invasion event length in spines within 5 minutes of application. This effect was dependent on

TrkB signaling, as the tyrosine kinase inhibitor k252a could block BDNF-induced MT retention in spines. Moreover, treatment with k252a for 24hrs also blocked basal levels of MT invasions, suggesting that endogenous BDNF is required for dynamic MT entries under basal conditions. BDNF increased PSD-95 fluorescence intensity by 20 minutes of treatment, but had yet to induce morphological changes in spines. Interestingly, the post-BDNF MT invasions were crucial for the accumulation of PSD-95, and inclusion of low concentrations of MT depolymerizing drugs abolished the increase in PSD-95. These results provided new connections between the function of BDNF and PSD-95 plasticity, suggesting that dynamic MTs play important roles in the retention of PSD-95 in a subset of spines. It is possible that these spines may be specific synapses "tagged" by BDNF induced synaptic potentiation.

MT-mediated cargo transport in spines

Neuronal MTs serve as the structural backbone that maintains the shape of dendrites, as well as a stable railway for intracellular transport of various cargos. In general, cargos are transported along MTs by forces generated by motor proteins through ATP hydrolysis (Vale, 2003; Schiwa and Woehlke, 2003). The motor proteins involved in MT-based transport are the minus-end directed cytoplasmic dynein and plus-end directed kinesin superfamily of proteins. Cargos can form a transport complex along MTs by direct interaction with motors or association with adaptor proteins. MTs function as the major platform for long distance transport, which is particularly important in highly polarized neurons, while short distance transport is thought to be facilitated by myosin-driven transport along actin filaments. In axons and dendrites, cargo is transported bi-directionally, from the cell body to the distal neurite tips (anterograde) and from the distal end of neurites back to the cell body (retrograde). It has been well established that in

axons, because of the uniform polarity of MTs (plus-end distal), anterograde transport is mediated exclusively by kinesins whereas retrograde transport is mediated by cytoplasmic dynein. In the dendrite, however, MTs have mixed polarity, allowing kinesins to move both distally and proximally.

A variety of molecules and intracellular organelles have been identified as cargos recognized by specific motors in the dendritic compartment. Anterograde trafficking of known cargos mainly involves two members of the kinesin superfamily proteins. KIF5, a kinesin-1 family protein, has been associated with transport of AMPARs, GABARs, mitochondria and mRNA-containing complexes (Setou et al., 2002; Twelvetrees et al., 2010; Kanai et al., 2004; Hirokawa et al., 2010). KIF5 binds to a scaffolding protein GRIP, which in turn associates with AMPAR containing vesicles, and directs these vesicles into dendrites (Nakata and Hirokawa, 2003). Transport of GABA receptors depends on Huntingtin-associated protein 1 (HAP1) as an adaptor, whereas Miro has been identified as an adaptor for binding of mitochondria to KIF5. Interestingly, the presence of mitochondria in spines can be elevated by KCl-induced depolarization (Li et al., 2004), suggesting that mitochondria are needed in spines following activity induction and for the subsequent spine morphological changes. The motor complex for mRNA-containing vesicles has not been fully dissected. In a study focused on FMRP, a RNA-associated transcriptional repressor that is downregulated in Fragile X syndrome, it was shown to directly bind to kinesin light chain (KLC) (Dictenberg et al., 2008). Since KLC is required for the KIF5 mediated transport complex, it is likely that translocation of FMRP to synapses depends on KIF5. This suggests an interesting hypothesis where disruption of KIF5-mediated trafficking of FMRP could be involved in the pathogenesis of Fragile X syndrome (Hirokawa et al., 2010).

Another member of the kinesin super-family of proteins that have been extensively studied

is the kinesin-2 family protein KIF17. KIF17 is exclusively located in the dendritic compartment. This specific subcellular localization of KIF17 is regulated by its cargo-binding tail domain, as chimeric KIF17 vectors expressing the motor domain of KIF5b resulted in axonal entry of NR2B containing vesicles (Setou et al., 2002; Song et al., 2009). The NMDA receptor subunit NR2B has been identified as the major cargo of KIF17, suggesting an important function of KIF17-based transport in NMDA-dependent synaptic plasticity. Expression of dominant negative KIF17 proteins in hippocampal neurons decreased mobility of NR2B-containing packets (Setou et al., 2000), whereas, KIF17 overexpressing mice showed enhanced spatial learning, most likely due to upregulated expression and trafficking of NR2B (Wong et al., 2002). Conversely, KIF17 knockout mice showed impaired learning and memory consolidation in several tasks (Yin et al., 2011). On the molecular level, NR2B vesicles are recognized by KIF17 through binding to the adaptor complex Mint1(LIN10) (Guillaud et al., 2008). Upon reaching the vicinity of its postsynaptic destination, the Mint1 complex can be released from KIF17 by CaMKII-alpha mediated phosphorylation of KIF17. It was hypothesized that CaMKII is activated by postsynaptic Ca2+ influx in the spine, and diffuses out of the spine into the dendritic shaft, where it phosphorylates KIF17 and releases the NR2B-containing cargo from the MT track (Guillaud et al., 2008). The exact mechanism by which NR2B vesicles subsequently move into the spine, however, has not been demonstrated.

Although kinesin-based transport in the dendritic shaft has been well defined, the exact mechanisms by which cargos move into spines remain largely unknown. Since spines are rich in actin filaments, myosin-based transport has been shown to be involved in delivery of several types of cargos. Myosin Va is localized to the postsynaptic density fractions in the brain. Myosin Va is normally inhibited through head-to-tail interactions but can be activated by LTP

and has been implicated in AMPAR trafficking in the spines (Correia et al., 2008; Krementsov et al., 2004; Hirokawa et al., 2010). Myosin Vb has also been identified as a motor for AMPA receptors in spines in response to synaptic activity. It was discovered that Ca2+ influx induces myosin Vb mediated delivery of AMPAR-containing recycling endosomes into spines, where exocytosis and AMPAR insertion can lead to LTP (Lise et al., 2006; Wang et al., 2008). Other than myosin V, myosin II and myosin IV have also been implicated in transport at postsynaptic regions and in LTP expression (Ryu et al., 2006; Yano et al., 2006).

In chapter three of my thesis, I investigated the possibility that dynamic MT invasions may be directly involved in cargo transport events in dendritic spines. I used synaptotagmin-IV (syt-IV) as a marker for vesicles that are transported in dendrites and can potentially be shuffled into and out of dendritic spines. Synaptotagmins are a family of proteins identified as regulators of vesicle fusion and release events as part of the SNARE complex. All 14 identified synaptotagmin proteins have one transmembrane domain that spans the vesicle membrane (Chapman, 2002). The cytoplasmic domain of synaptotagmin consists of two calcium sensing C2-domains connected by a short linker sequence (Chapman, 2002). Sequencing studies identified that all the Ca2+ binding residues are preserved in the C2B domain of synaptotagmin-IV (syt-IV) in *Drosophila* and rat. However, protein-binding assays showed that while *Drosophila* syt-IV can effectively undergo Ca2+-dependent phospholipid binding, neither C2 domain of rat syt-IV is capable of Ca2+ or phospholipid binding (Dai et al., 2004). It was therefore suggested that, based on crystallography studies, subtle changes in the orientation of Ca2+ sensing residues may have abolished the full Ca2+ binding sites in rat syt-IV (Dai et al., 2004). Moreover, it has been demonstrated in PC12 cells that syt-IV reduced the frequency of fusion events and gave rise to prolonged opening of fusion pores (Bhalla et al., 2005), suggesting

that syt-IV can negatively regulate Ca2+-induced fusion events.

The syt-IV gene has been mapped to a region on human chromosome 18 that is related to several developmental disorders, raising considerable interest in the possibility that syt-IV expression may be involved in normal neural development (Ferguson et al., 2000). Syt-IV is an immediate early gene that is downregulated in most brain regions during development, but syt-IV expression can be upregulated by induction of neuronal activity. Syt-IV knockout mice showed defects in contextual fear conditioning and motor balance behavior, indicating that syt-IV expression in hippocampal neurons, albeit at low levels, is important for learning and memory, whereas cerebellar expression of syt-IV is crucial for fine motor behavior (Ferguson, 2001). Syt-IV expression remains abundant throughout development in the hypothalamus (Zhang et al., 2011). A recent study of oxytocin secreting neurons in the mouse hypothalamus revealed that syt-IV can affect energy balance by negatively regulating hypothalamic oxytocin release. Overexpression of syt-IV led to dietary obesity in a similar way to centrally antagonizing oxytocin, whereas inhibition of syt-IV prevented dietary obesity by balancing energy consumption through normalized oxytocin release in chronic nutritional excess (Zhang et al., 2011). These studies established the important role of syt-IV in various brain regions by regulating vesicular content release.

The cellular localization and mechanism of action of syt-IV in hippocampal neurons has been addressed in several recent studies. Using a combination of fluorescent imaging and eletrophysiological recordings, Dean and colleagues demonstrated that syt-IV is localized to both axons and dendrites in cultured hippocampal neurons (Dean et al., 2009). Interestingly, a subset of syt-IV is co-localized to the same vesicles as BDNF, and co-trafficking of the two molecules can be increased by activity. Syt-IV knockout neurons showed enhanced BDNF release, and syt-

IV overexpression inhibited BDNF release from vesicles, assessed by measuring changes in phluorin-BDNF fluorescence intensity. By measuring the FM-dye destaining rate from wild-type presynaptic terminals, it was also demonstrated that postsynaptic syt-IV negatively affected synaptic strength through regulation of BDNF release (Dean et al., 2009). Interestingly, a follow up study also showed that distinct groups of syt-IV/BDNF-containing vesicles are sorted to axons and dendrites upon activity induction (Dean et al., 2012). Given the specific motor proteins that regulate transport in axons versus dendrites, it is therefore tempting to speculate that dendrite-specific microtubule-based motors could be responsible for trafficking of syt-IV-containing vesicles to the postsynaptic site, where syt-IV could exert its effect on synaptic strength by negatively regulating vesicular release of BDNF.

In the third chapter of my thesis, I used TIRFM to study the intracellular dynamics of syt-IV puncta in hippocampal dendrites and spines concomitantly with MT dynamics. I found that syt-IV puncta are capable of rapidly moving along the dendritic shaft in mature neurons. The rate of transport of these puncta corresponds to the velocity of kinesin/dynein based transport (Hirokawa et al., 2010). I also observed that syt-IV puncta entered into and exited from dendritic spines coincident with the presence of MTs in the spine. Nanomolar taxol treatment blocked MT-based dynamics in spines and abolished syt-IV movement in spines, indicating that this type of syt-IV motility is dependent on dynamic MT invasions. I also examined the possibility that KIF17 might function to directly mediate syt-IV puncta transport by imaging KIF17 and syt-IV simultaneously. Interestingly, in young hippocampal dendrites, KIF17 puncta co-localized with fast moving syt-IV puncta, but not with stationary syt-IV puncta. These results provide the first direct evidence that dynamic MT invasions can mediate the delivery of cargo into and out of spines and syt-IV is one of potentially many cargos.

References:

Alexander JE, Hunt DF, Lee MK, Shabanowitz J, Michel H, Berlin SC, MacDonald TL, Sundberg RL, Rebhun LI, Frankfurter A. (1991) Characterization of posttranslational modifications in neuron-specific class III beta-tubulin by mass spectrometry. Proc Natl Acad Sci USA. 88(11): 4685-9

Baas PW, Deitch JS, Black MM, Banker GA. (1988) Polarity orientation of microtubules in hippocampal neurons: uniformity in the axon and nonuniformity in the dendrite. Proc Natl Acad Sci USA 85(21): 8335-9

Baas PW, Lin S (2011) Hooks and comets: The story of microtubule polarity orientation in the neuron. Dev Neurobiol. 71(6):403-18

Bhalla A, Tucker WC, Chapman ER. (2005) Synaptotagmin isoforms couple distinct ranges of Ca2+, Ba2+, and Sr2+ concentration to SNARE-mediated membrane fusion. Mol Biol Cell. 16(10):4755-64

Bourne J, Harris KM. (2007) Do thin spines learn to be mushroom spines that remember? Curr Opin Neurobiol. 17(3): 381-6

Cambray-Deakin MA, Burgoyne RD. (1987) Posttranslational modifications of alpha-tubulin: acetylated and detyrosinated forms in axons of rat cerebellum. J Cell Biol. 104: 1569-74

Chapman ER. (2002) Synaptotagmin: a Ca2+ sensor that triggers exocytosis? Nat Rev Mol Cell Biol. 37:498-508

Chen L, Wang Z, Ghosh-Roy A, Hubert T, Yan D, O'Rourke S, Bowerman B, Wu Z, Jin Y, Chisholm AD. (2011) Axon regeneration pathways identified by systematic genetic screening in C. elegans. Neuron 71(6):1043-57

Chen L, Stone MC, Tao J, Rolls MM. (2012) Axon injury and stress trigger a microtubule-based neuroprotective pathway. Proc Natl Acad Sci USA. 109(29):11842-7

Chicurel ME, Harris KM. (1992). Three-dimensional analysis of the structure and composition of CA3 branched dendritic spines and their synaptic relationships with mossy fiber boutons in the rat hippocampus. J Comp Neurol. 325:169-82

Chih B, Afridi SK, Clark L, Scheiffele P. (2004) Disorder-associated mutations lead to functional inactivation of neuroligins. Hum Mol Genet. 13:1471-77

Correia SS, Bassani S, Brown TC, Lise MF, Backos DS, El-Husseini A, Passafaro M, Esteban JA. (2008) Motor protein-dependent transport of AMPA receptors into spines during long-term potentiation. Nat Neurosci. 11(4):457-66

Conde C, Cáceres A. (2009) Microtubule assembly, organization and dynamics in axons and

dendrites. Nat Rev Neurosci. 10(5): 319-32

Dai H, Shin OH, Machius M, Tomchick DR, Sűdhof TC, Rizo J. (2004) Structural basis for the evolutionary inactivation of Ca2+ binding to synaptotagmin 4. Nat Struct Mol Biol. 119:844-9

Davies AM, Wright EM (1995) Neurotrophic factors. Neurotrophin autocrine loops. Curr Biol. 5(7):723-6

Dean C, Liu H, Staudt T, Markus TA, Siv V, Buckers J, Kamin D, Engelhardt J, Jackson M, Hell SW, Chapman ER (2012) Distinct subsets of Syt-IV/BDNF vesicles are sorted to axons versus dendrites and recruited to synapses by activity. J. Neurosci 32(16):5398-5413

Dean C, Liu H, Dunning FM, Chang PY, Jackson MB, Chapman ER (2009) Synaptotagmin-IV modulates synaptic function and long-term potentiation by regulating BDNF release. Nat Neurosci. 12(6):767-76

DeKosky ST, Scheff SW. (1990) Synapse loss in frontal cortex biopsies in Alzheimer's disease: correlation with cognitive severity. Ann. Neurol. 27:457-64

Dent EW, Barnes AM, Tang F, Kalil K. (2004) Netrin-1 and semaphoring 3A promote or inhibit cortical axon branching, respectively, by reorganization of the cytoskeleton. J Neurosci. 24(12): 3002-12

Dent EW, Callaway JL, Szebenyi G, Baas PW, Kalil K. (1999) Reorganization and movement of microtubules in axonal growth cones and developing interstitial branches. J Neurosci. 19: 8894-8908

Dent EW, Gupton SL, Gertler FB. (2011) The growth cone cytoskeleton in axon outgrowth and guidance. Cold Spring Harb Perspect Biol. 3(3),pii:a001800

Dent EW, Kalil K. (2001) Axon branching requires interactions between dynamic microtubules and actin filaments. J Neurosci. 21(24):9757-69

Dent EW, Gertler FB. (2003) Cytoskeletal dynamics and transport in growth cone motility and axon guidance. Neuron 40(2): 209-27

Dictenberg JB, Swanger SA, Antar LN, Singer RH, Bassell GJ. (2008) A direct role for FMRP in activity-dependent dendritic mRNA transport links filopodial-spine morphogenesis to fragile X syndrome. Dev Cell. 14(6):926-39

Dudanova I, Tabuchi K, Rohlmann A, Sudhof TC, Missler M. (2007) Deletion of alpha-neurexins does not cause a major impairment of axonal pathfinding or synapse formation. J Comp Neurol. 502:261-274

El-Husseini AE, Schnell E, Chetkovich DM, Nicoll RA, Bredt DS (2000) PSD-95 involvement

in maturation of excitatory synapses. Science 290:1364–1368.

Ehrlich I, Klein M, Rumpel S, Malinow R (2007) PSD-95 is required for activity-driven synapse stabilization. Proc Natl Acad Sci USA 104:4176-81

Ehrlich I, Malinow R (2004) Postsynaptic density 95 controls AMPA receptor incorporation during long-term potentiation and experience-driven synaptic plasticity. J Neurosci. 244:916-27

Ethell IM, Pasquale EB. (2005) Molecular mechanisms of dendritic spine development and remodeling. Prog Neurobiol. 75(3): 161-205

Ferguson GD, Anagnostaras SG, Silva AJ, Herschman HR. (2000) Deficits in memory and motor performance in synaptotagmin IV mutant mice. Proc Natl Acad Sci. USA 97(10):5598-603

Fiala JC, Feinberg M, Popov V, Harris KM. (1998) Synaptogenesis via dendritic filopodia in developing hippocampal area CA1. J Neurosci. 18(21):8900-11

Fiala JC, Kirov SA, Feinberg MD, Petrak LJ, George P, Goddard CA, Harris KM. (2003) Timing of neuronal and glial ultrastructure disruption during brain slice preparation and recovery in vitro. J Comp Neurol. 465(1): 90-103

Georges PC , Hadzimichalis NM, Sweet ES, Firestein BL. (2008) The yin-yang of dendrite morphology: unity of actin and microtubules. Mol Neurobiol. 38(3): 270-84

Geschwind DH, Levitt P. (2007) Autism spectrum disorders: developmental disconnection syndromes. Curr. Opin Neurobiol. 17:103-111

Gray EG, Westrum LE, Burgoyne RD, Barron J. (1982) Synaptic organization and neuron microtubule distribution. Cell Tissue Res. 226:579-588

Gray NW, Weimer RM, Bureau I, Svoboda K (2006) Rapid redistribution of synaptic PSD-95 in the neocortex in vivo. PLoS Biol. 4(11):e370

Gu J, Firestein BL, Zheng JQ. (2008) Microtubules in dendritic spine development. J Neurosci. 28:12120-12124

Guillaud L, Wong R, Hirokawa N (2008) Disruption of KIF17-Mint1 interaction by CaMKII-dependent phosphorylation: a molecular model of kinesin-cargo release. Nat Cell Biol. 10(1): 19-29

Halpain S (2000) Actin and the agile spine: how and why do dendritic spines dance? Trends Neurosci. 23(4):141-6

Harris KM. (1999) Structure, development and plasticity of dendritic spines. Curr Opin

Neurobiol. 9(3):343-8

Hartmann M, Heumann R, Lessmann V (2001) Synaptic secretion of BDNF after high-frequency stimulation of glutamatergic synapses. EMBO J. 20(21): 5887-97

Hellal F, Hurtado A, Ruschel J, Flynn KC, Laskowski CJ, Umlauf M, Kapitein LC, Strikis D, Lemmon V, Bixby J, Hoogenraad CC, Bradke F. (2011) Microtubule stabilization reduces scarring and causes axon regeneration after spinal cord injury. Science 331(6019):928-31

Hirokawa H, Niwa S, Tanaka Y. (2010) Molecular motors in neurons: transport mechanisms and roles in brain function, development, and disease. Neuron 68(4):610-38

Holy TE, Leibler S. (1994) Dynamic instability of microtubules as an efficient way to search in space. Proc Natl Acad Sci USA 91(12): 5682-5

Hu X, Viesselmann C, Nam S, Merriam E, Dent EW. (2008) Activity-dependent dynamic microtubule invasions of dendritic spines. J Neurosci. 28:13094-105

Hutsler JJ, Zhang H. (2010) Increased dendritic spine densities on cortical projection neurons in autism spectrum disorders. Brain Res. 1309:83-94

Irwin SA, Patel B, Idupulapati M, Harris JB, Crisostomo RA, Larsen BP, Kooy F, Willems PJ, Cras P, Kozlowski PB, Swain RA, Weiler IJ, Greenough WT. (2001) Abnormal dendritic spine characteristics in the temporal and visual cortices of patients with fragile-X syndrome: a quantitative examination. Am. J. Med Genet. 98:161-167

Janke C, Bulinski JC (2011) Post-translational regulation of the microtubule cytoskeleton: mechanisms and functions. Nat Rev Mol Cell Biol. 12(12):773-86

Jaworski J, Kapitein LC, Gouveia SM, Dortland BR, Wulf PS, Grigoriev I, Camera P, Spangler SA, Di Stefano P, Demmers J, Krugers H, Defilippi P, Akhmanova A, Hoogenraad CC. (2009) Dynamic microtubules regulate dendritic spine morphology and synaptic plasticity. Neuron 61:85-100

Ji Y, Pang PT, Feng L, Lu B (2005) Cyclic AMP controls BDNF-induced TrkB phosphorylation and dendritic spine formation in mature hippocampal neurons. Nat Neuroscie. 8(2):164-72

Ji Y, Lu Y, Yang F, Shen W, Tang TT, Feng L, Duan S, Lu B (2010) Acute and gradual increases in BDNF concentration elicit distinct signaling and functions in neurons. Nat Neurosci. 13(3):302-9

Kabir N, Schaefer AW, Nakhost A, Sossin WS, Forscher P. (2001) Protein kinase C activation promotes microtubule advance in neuronal growth cones by increasing average microtubule growth lifetimes. J Cell Biol. 152(5): 1033-44

Kaech S, Ludin B, Matus A (1996) Cytoskeletal plasticity in cells expressing neuronal microtubule-associated proteins. Neuron 17(6):1189-99

Kaech S, Fischer M, Doll T, Matus A. (1997) Isoform specificity in the relationship of actin to dendritic spines. J Neurosci. 17(24):9565-72

Kaech S, Parmar H, Roelandse M, Bornmann C, Matus A. (2001) Cytoskeletal microdifferentiation: a mechanism for organizing morphological plasticity in dendrites. Proc Natl Acad Sci USA. 98(13):7086-92

Kanai Y, Dohmae N, Hirokawa N. (2004) Kinesin transports RNA: isolation and characterization of and RNA-transporting granule. Neuron 43(4):513-25

Kang H, Schuman EM (1995) Long-lasting neurotrophin-induced enhancement of synaptic transmission in the adult hippocampus. Science 267(5204):1658-62

Kang H, Schuman EM (1996) A requirement for local protein synthesis in neurotrophin-induced hippocampal synaptic plasticity. Sicnece 273(5280):1402-6

Kohara K, Kitamura A, Morishima M, Tsumoto T (2001) Activity-dependent transfer of brain-derived neurotrophic factor to postsynaptic neurons. Science 291(5512):2419-23

Kolomeets NS, Orlovskaya DD, Rachmanova VI, Uranova NA. (2005) Ultrastructural alterations in hippocampal mossy fiber synapses in schizophrenia: a postmortem morphometric study. Synapse 57:47-55

Kojima M, Takei N, Numakawa T, Ishikawa Y, Suzuki S, Matsumoto T, Katoh-Semba R, Nawa H, Hatanaka H. (2001) Biological characterization and optical imaging of brain-derived neurotrophic factor green fluorescent protein suggest an activity-dependent local release of BDNF in neuritis of cultured hippocampal neurons. J Neurosci. Res. 64(1):1-10

Krementsov DN, Kremontsova EB, Trybus KM (2004) Myosin V: regulation by calcium, calmodulin, and the tail domain. J Cell Biol. 164(6): 877-86

Kwon HB, Sabatini BL. (2011) Glutamate induces de novo growth of functional spines in developing cortex. Nature 474(7349):100-4

Lessmann V, Gottmann K, Heumann R (1994) BDNF and NT-4/5 enhance glutamatergic synaptic transmission in cultured hippocampal neurons. Neuroreport. 30(6):21-5

Li Z, Okamoto K, Hayashi Y, Sheng M. (2004) The importance of dendritic mitochondria in the morphogenesis and plasticity of spines and synapses. Cell 119(6):873-87

Lisė MF, Wong TP, Trinh A, Hines RM, Liu L, Kang R, Hines DJ, Lu J, Goldenring JR, Wang YT, El-Husseini A. (2006) Involvement of myosin Vb in glutamate receptor trafficking. J Biol. Chem. 281(6):3669-78

Lu Y, Christian K, Lu B (2008) BDNF: a key regulator for protein synthesis-dependent LTP and long-term memory? Neurobiol Learn Mem. 89(3):312-23

Ludueña RF. (1998) Multiple forms of tubulin: different gene products and covalent modifications. Int Rev Cytol. 178: 207-75

Marrs GS, Green SH, Dailey ME. (2001) Rapid formation and remodeling of postsynaptic densities in developing dendrites. Nat Neurosci. 4(10):1006-13

Matus A. (2000) Actin-based plasticity in dendritic spines. Science 290(5492): 754-8

Mitchison T, Kirschner M (1984) Dynamic instability of microtubule growth. Nature 312: 237-242

Noritake J, Fukata Y, Iwanaga T, Hosomi N, Tsutsumi R, Matsuda N, Tani H, Iwanari H, Mochizuki Y, Kodama T, Matsuura Y, Bredt DS, Hamakubo T, Fukata M (2009) Mobile DHHC palmitoylating enzyme mediates activity-sensitive synaptic targeting of PSD-95. J Cell Biol. 186:147-60

Okabe S, Kim HD, Miwa A, Kuriu T, Okado H (1999) Continual remodeling of postsynaptic density and its regulation by synaptic activity. Nat Neurosci. 2(9):804-11

Penzes P, Cahill ME, Jones KA, VanLeeuwen JE, Woolfrey KM. (2011) Dendritic spine pathology in neuropsychiatric disorders. Nat Neurosci. 14(3):285-93

Rex CS, Lin CY, Kramar EA, Chen LY, Gall CM, Lynch G (2007) Brain-derived neurotrophin factor promotes long-term potentiation-related cytoskeletal changes in adult hippocampus. J Neurosci. 27(11):3017-29

Redeker V, Levilliers N, Schmitter JM, Le Caer JP, Rossier J, Adoutte A, Brė MH. (1994) Polyglycylation of tubulin: a posttranslational modification in axonemal microtubules. Science 266(5191): 1688-91

Rochefort NL, Konnerth A. (2012) Dendritic spines: from structure to in vivo function. EMBO Rep. doi:10.1038

Rűdiger M, Plessman U, Kloppel KD, Wehland J, Weber K. (1992) Class II tubulin, the major brain β tubulin isotype is polyglutamylated on glutamic acid residue 435. FEBS Lett. 308:101-5

Ryu J, Liu L, Wong TP, Wu DC, Burette A, Weinberg R, Wang YT, Sheng M (2006) A critical role for myosin IIb in dendritic spine morphology and synaptic function. Neuron 49(2):175-82

Schaefer AW, Kabir N, Forscher P. (2002) Filopodia and actin arcs guide the assembly and transport of two populations of microtubules with unique dynamic parameters in neuronal

growth cones. J Cell Biol. 158(1): 139-52

Schliwa M, Woehlke G (2003) Molecular motors. Nature 422(6933):759-65

Setou M, Seog DH, Tanaka Y, Takei Y, Kawagishi M, Hirokawa N. (2002) Glutamate-receptor-interacting protein GRIP1 directly steers kinesin to dendrites. Nature 417(6884):83-7

Setou M, Nakagawa T, Seog DH, Hirokawa N. (2000) Kinesin superfamily motor protein KIF17 and mLin-10 in NMDA receptor-containing vesicle transport. Science 288(5472):1796-802

Shen K, Cowan CW (2010) Guidance molecules in synapse formation and plasticity. Cold Spring Harb Perspect Biol. 2(4):a001842

Sheng M, Hoogenraad CC. (2007) The postsynaptic architecture of excitatory synapses: a more quantitative view. Annu Rev Biochem. 76:823-47

Song AH, Wang D, Chen G, Li Y, Luo J, Duan S, Poo MM (2009) A selective filter for cytoplasmic transport at the axon initial segment. Cell 136(6): 1148-60

Sorra KE, Harris KM. (2000) Overview on the structure, composition, function, development, and plasticity of hippocampal dendritic spines. Hippocampus 10(5): 501-11

Spacek J, Harris KM. (1997) Three-dimensional organization of smooth endoplasmic reticulum in hippocampal CA1 dendrites and dendritic spines of the immature and mature rat. J Neurosci. 17(1):190-203

Star EN, Kwiatkowski DJ, Murthy VN (2002) Rapid turnover of actin in dendritic spines and its regulation by activity. Nat Neurosci. 5(3):239-46

Steiner P, Higley MJ, Xu W, Czervionke BL, Malenka RC, Sabatini BL (2008) Destabilization of the postsynaptic density by PSD-95 serine 73 phosphorylation inhibits spine growth and synaptic plasticity. Neuron 60(5):788-802

Sweet RA, Henteleff RA, Zhang W, Sampson AR, Lewis DA (2009) Reduced dendritic spine density in auditory cortex of subjects with schizophrenia. Neuropsychopharmacology 34:374-89

Sweet ES, Previtera ML, Fernandez JR, Charych EI, Tseng CY, Kwon M, Starovoytov V, Zheng JQ, Firestein BL (2011) PSD-95 alters microtubule dynamics via an association with EB3. J Neurosci. 31(3):1038-47

Swiech L, Blazejczyk M, Urbanska M, Pietruszka P, Dortland BR, Malik AR, Wulf PS, Hoogenradd CC, Jaworski J. (2011) CLIP-170 and IQGAP1 cooperatively regulate dendrite morphology. J Neurosci. 31(12):4555-68

Suter DM, Schaefer AW, Forscher P. (2004) Microtubule dynamics are necessary for SRC family kinase-dependent growth cone steering. Curr Biol. 14(13):1194-9

Tada T, Sheng M. (2006) Molecular mechanisms of dendritic spine morphogenesis. Curr Opin Neurobiol. 16(1):95-101

Tanaka J, Horiike Y, Matsuzaki M, Miyazaki T, Ellis-Davies GC, Kasai H (2008) Protein synthesis and neurotrophin-dependent structural plasticity of single dendritic spines. Science 319(5870):1683-7

Teng J, Takei Y, Harada A, Nakata T, Chen J, Hirokawa N. (2001) Synergistic effects of MAP2 and MAP1B knockout in neuronal migration, dendritic outgrowth and microtubule organization. J Cell Biol. 155(1):65-76

Topinka JR, Bredt DS (1998) N-terminal palmitoylation of PSD-95 regulates association with cell membranes and interaction with K+ channel Kv1.4. Neuron 201:125-34

Tsai JW, Lian WN, Kemal S, Kriegstein AR, Vallee RB (2010) Kinesin 3 and cytoplasmic dynein mediate interkinetic nuclear migration in neural stem cells. Nat Neurosci. 13(12):1463-71

Tsai J, Grutzendler J, Duff K, Gan WB (2004) Fibrillar amyloid deposition leads to local synaptic abnormalities and breakage of neuronal branches. Nat Neurosci. 7(11):1181-3

Twelvetrees AE, Yuen EY, Aranciba-Carcamo IL, MacAskill AF, Rostaing P, Lumb MJ, Humbert S, Triller A, Saudou F, Yan Z, Kittler JT. (2010) Delivery of GABAARs to synapses is mediated by HAP1-KIF5 and disrupted by mutant huntingtin. Neuron 65(1):53-65

Tyler WJ, Pozzo-Miller LD (2001) BDNF enhances quantal neurotransmitter release and increases the number of docked vesicles at the active zones of hippocampal excitatory synapses. J Neurosci. 21(12):4249-58

Vale RD (2003) Myosin V motor proteins: marching stepwise towards a mechanism. J Cell Biol. 163(3):445-50

Wang Z, Edwards JG, Riley N, Provance DW Jr. Karcher R, Li XD, Davison LG, Ikebe M, Mercer JA, Kauer JA, Ehlers MD. (2008) Myosin Vb mobilizes recycling endosomes and AMPA receptors for postsynaptic plasticity. Cell 135(3): 535-48

Waterhouse EG, Xu B (2009) New insights into the role of brain-derived neurotrophic factor in synaptic plasticity. Mol Cell Neurosci. 42(2):81-9

Wong RW, Setou M, Teng J, Takei Y, Hirokawa N. (2002) Overexpression of motor protein KIF17 enhances spatial and working memory in transgenic mice. Proc Natl Acad Sci. USA 99(22):14500-5

Yano H, Ninan I, Zhang H, Milner TA, Arancio O, Chao MV (2006) BDNF-mediated neurotransmission relies upon a myosin VI motor complex. Nat Neurosci. 98:1009-18

Yin X, Takei Y, Kido MA, Hirokawa N. (2011) Molecular motor KIF17 is fundamental for memory and learning via differential support of synaptic NR2A/2B levels. Neuron 70(2): 310-25

Yoshii A, Constantine-Paton M (2007) BDNF induces transport of PSD-95 to dendrites through PI3K-AKT signaling after NMDA receptor activation. Nat Neurosci. 10(6):702-11

Yuste R, Tank DW. (1996) Dendritic integration in mammalian neurons: a century after Cajal. Neuron 16(4): 701-16

Yuste R, Denk W. (1995) Dendritic spines as basic functional units of neuronal integration. Nature 375(6533): 682-4

Yuste R, Bonhoeffer T. (2004) Genesis of dendritic spines: insights from ultrastructural and imaging studies. Nat Rev Neurosci. 5(1):24-34

Zhang G, Bai H, Zhang H, Dean C, Wu Q, Li J, Guariqlia S, Meng Q, Cai D. (2011) Neuropeptide exocytosis involving synaptotagmin-4 and oxytocin in hypothalamic programming of body weight and energy balance. Neuron 69(3):523-35

Zito K, Knott G, Shepherd GM, Shenolikar S, Svoboda K. (2004) Induction of spine growth and synapse formation by regulation of the spine actin cytoskeleton. Neuron 44(2):321-34

Zito K, Scheuss V, Knott G, Hill T, Svoboda K. (2009) Rapid functional maturation of nascent dendritic spines. Neuron 61(2): 247-58

Chapter 2

Activity-Dependent Dynamic Microtubule Invasion of Dendritic Spines

ABSTRACT

Dendritic spines are the primary sites of contact with presynaptic axons on excitatory hippocampal and cortical neurons. During development and plasticity spines undergo marked changes in structure that directly affect the functional communication between neurons. Elucidating the cytoskeletal events that induce these structural changes is fundamental to understanding synaptic biology. Actin plays a central role in the spine cytoskeleton, however the role of microtubules in spine function has been studied little. Although microtubules have a prominent role in transporting material throughout the dendrite that is destined for spines, they are not thought to directly influence spine structure or function. Using total internal reflectance fluorescent microscopy (TIRFM) we discovered that microtubules rapidly invade dendritic protrusions of mature CNS neurons (up to 63 days *in vitro*), occasionally inducing marked changes in spine morphology in the form of transient spine head protrusions (tSHPs). Two microtubules can occupy a spine simultaneously and microtubule targeting can occur from both the proximal and distal dendrite. A small percentage of spines are targeted at a time and all targeting events are transient, averaging only a few minutes. Nevertheless, over time many spines on a dendrite are targeted by microtubules. Importantly, we show that increasing neuronal activity enhances both the number of spines invaded by microtubules and the duration of these invasions. This study provides new insight into the dynamics of the neuronal cytoskeleton in mature CNS neurons and suggests that microtubules play an important, direct role in spine morphology and function.

INTRODUCTION

During development spines undergo marked changes in structure ranging from motile filopodial protrusions to stable mushroom-shaped spines. The morphology of spines can directly affect functional communication between neurons (Hayashi and Majewska, 2005; Alvarez and Sabatini, 2007; Bourne and Harris, 2007; Harms and Dunaevsky, 2007). Enlarged spine heads correlate with an increased size of the post-synaptic density, while simplification of spine morphology and loss of entire dendritic spines can occur in developmental and adult neurological disorders, including mental retardation, autism and epilepsy (Calabrese et al., 2006; Tada and Sheng, 2006). Actin filaments play prominent roles in the formation, maintenance and plasticity of dendritic spine structure (Ethell and Pasquale, 2005). However, the role of microtubules (MTs) in spine architecture has been studied little. Generally, spines are thought to be devoid of MTs because electron micrographs have shown MTs in spines only in extremely rare circumstances (Gray et al., 1982; Chicurel and Harris, 1992; Fiala et al., 2003). Furthermore, live-cell imaging with fluorescently-labeled microtubule associated proteins has failed to detect the presence of MTs in spines (Kaech et al., 2001).

Prominent in dendrite shafts, MTs are assumed to function exclusively as stable railways for long distance intracellular transport. However, MTs exhibit bouts of rapid polymerization and depolymerization, termed dynamic instability (Mitchison and Kirschner, 1984). MTs have been shown to rapidly explore all regions of developing neurons (Stepanova et al., 2003), including the tips of growth cone filopodia (Dent and Kalil, 2001; Schaefer et al., 2002). We hypothesized that MTs remain dynamic in mature neurons and are capable of exploring intracellular space through dynamic polymerization and depolymerization. To test this idea we

imaged MTs in dendrites of mature hippocampal and cortical neurons, fluorescently labeled with either EGFP-α-tubulin or EB3-EGFP. EGFP-α-tubulin incorporates throughout MTs allowing us to image all microtubules within a living neuron. However, EB3-EGFP, a MT plus end tracking protein (+TIP), labels the fast growing plus ends of polymerizing MTs, but not paused or depolymerizing MTs (Stepanova et al., 2003). We can document MT dynamics (polymerization, depolymerization, pausing) in dendritic protrusions with EGFP-α-tubulin-labeled MTs, while imaging EB3-EGFP-labeled plus ends of MTs allow us to follow MT polymerization in both the shaft and protrusions.

We used total internal reflection fluorescence microscopy (TIRFM) to track MT dynamics in spines that were positioned near or on the coverslip. TIRFM is a laser-based microscopy technique that only illuminates ~100-400nm above the glass substrate (Schneckenburger, 2005). We obtained high signal-to-noise images of MTs entering micron-sized structures (dendritic protrusions) and imaged two fluorophores at rapid intervals (10 seconds) for long periods of time (1 hour). Surprisingly, we discovered that MTs are capable of extending rapidly into and out of dendritic protrusions (filopodia and spines) and remain dynamic throughout neuronal development (up to DIV63). Importantly, we also discovered that MT invasion of dendritic protrusions was dependent on neuronal activity. These results indicate that MTs may have a hitherto unappreciated role as a central player in spine function.

MATERIALS AND METHODS

Plasmids and Reagents

GFP-α-tubulin (human) in a pCAX vector and mCherry-β-actin (human) in a C1 vector (Clontech) have been described elsewhere (Dent et al., 2007). DsRed2 (Clontech) was cloned into a pCAX vector (Osumi and Inoue, 2001) using standard techniques. EB3-EGFP was a generous gift of Niels Galjart (Erasmus Medical Center, Rotterdam, Netherlands). Newly-polymerized, dynamic microtubules were labeled with rat anti-tyrosinated tubulin at 1:1000 (YL1/2 clone, Millipore, Temeluca, CA). Presynaptic terminals were labeled with anti-synaptophysin at 1:5000 (Millipore). All Alexa-conjugated secondary antibodies and Alexa-conjugated phalloidin, to label actin filaments, were from Invitrogen.

Hippocampal and Cortical Neuron Culture and Transfection

All mouse procedures were approved by the University of Wisconsin Committee on Animal Care and were in accordance with NIH guidelines. Cortical (E14.5-16.5) and hippocampal (E15.5-17.5) neuron cultures were prepared from Swiss Webster mice (Taconic, Hudson, NY) essentially as described (Lebrand et al., 2004; Dent et al., 2007). Briefly, cortices and hippocampi were dissected, trypsinized and dissociated. Dissociated cortical or hippocampal neurons were resuspended in Nucleofector solution (Mouse Neuron Kit - Amaxa Biosystems, Gaithersburg, MD) and transfected with an Amaxa Nucleofector according to the manufacturer's directions. Transfected neurons were plated at densities of $2\text{-}4\text{x}10^4$ neurons/cm^2 on 1.0mg/ml poly-D-lysine (Sigma, St. Louis, MO) coated glass coverslips adhered to the bottom of 35mm plastic culture dishes that had a 15mm hole drilled through the bottom of the chamber. Neurons were plated in plating medium (PM) which consisted of Neurobasal medium with 5% FBS

(Hyclone, Logan, UT), B27 supplement, 2mM glutamine, 37.5mM NaCl and 0.3% glucose. After one hour this medium was replaced with serum free medium (SFM), which was PM without FBS.

Live-cell TIRF Imaging

The TIRFM microscope consisted of a Nikon TE2000E base with TIRF illuminator (Nikon, Melville, NY), a Nikon 100x/1.49NA Plan Apo TIRF objective, a Nikon perfect focus system for continuous automatic focusing of the sample during time-lapse imaging, a Nikon z-motor, a motorized x-y stage (Prior Scientific, Rockland, MA), a Lumen Pro200 fluorescent illumination system consisting of a 200W metal halide lamp and six-position excitation filter wheel and a fiber optic illuminator (Prior Scientific), a ten-position emission filter wheel and a Coolsnap HQ cooled interline CCD camera (Photometrics, Tuscon, AZ). For TIRF illumination two lasers were used: a 40mW Argon laser for GFP illumination and a 10mW solid state 561nM laser for DsRed2 and mCherry illumination (both Melles-Griot, Carlsbad, CA). Laser power was attenuated to 6.25% with neutral density filters. The microscope was equipped with a dual wavelength (EGFP/mCherry) dichroic mirror (z488/561rdc, Chroma, Rockingham, VT) for both TIRF and wide-field illumination. Wide-field fluorescent illumination was accomplished with the aid of a Lumen Pro 200 (Prior Scientific), containing an excitation filter wheel with GFP and mCherry excitation filters, a metal halide illuminator and a liquid light guide. This system allowed us to collect two-color TIRF, two-color widefield and a DIC image in quick succession. Usually, we only collected wide-field images at the beginning and end of a time-lapse. All images were collected, measured and compiled in Metamorph imaging software (Molecular Devices, Downingtown, PA). Figures were compiled in Photoshop (Adobe, San Jose, CA).

During time-lapse microscopy neurons were kept at 37ºC with in an incubation chamber (Solent Inc., Segensworth, UK) custom fitted to the microscope. For fluorescent live-cell imaging the chamber was closed with a glass ring, coverslip and silicone grease.

Induction of Activity in Hippocampal Cultures

To induce global activation of hippocampal cultures we briefly added high concentrations of KCl to the cultures essentially as described (Li et al., 2004). We modified this approach for both live-cell and fixed-cell imaging. Briefly, for live-cell imaging we slowly exchanged the SFM media with ECS (140mM NaCl, 5mM KCl, 2mM $CaCl_2$, 2mM $MgCl_2$, 5mM HEPES, 20mM Glucose, 315mOsm) of the same osmolarity and temperature as SFM in cultures that were previously transfected with EGFP-α-tubulin/DsRed2. A custom silicone insert was placed in the 35mm dish to allow for rapid addition/removal of media and inlet and outlets (Bioscience Tools, San Diego, CA) were positioned in the dish. After 30 minutes of imaging in ECS, ECS with 75mM KCl (osmolarity balanced by removing NaCl) was manually perfused into the chamber and left for 3 minutes. Excess media was removed with a small vacuum pump. Fresh ECS was exchanged for the high KCl-ECS and left for 10 minutes. This was repeated three times in total. Neurons were then imaged for an additional 30 minutes. For fixed cell imaging we slowly exchanged SFM for ECS and let the cells recover for 10 minutes. We then conducted the same exchanges of 75mM KCl (3 min. on/10 min. off (x3)) and then fixed the cultures 20 minutes after the final KCl removal for quantitation of MT invasion in dendritic protrusions. Controls for both experiments included all the same exchanges with ECS instead of ECS with 75mM KCl. In some experiments 1μM tetrodotoxin (TTX) was included in all solutions (with or without KCl).

Quantitative Analysis of Protrusions and MT Kinetics

All MT measurements were made with the aid of Metamorph software. Morphological criteria for determining protrusion type were essentially as described (Chapleau et al., 2008). Briefly, spines were defined as protrusions <3µm in length, while filopodia were 3-10µm in length. For all protrusions the head width at widest point (H), neck width at the junction of the protrusion and dendrite (N) and protrusion length from dendrite/protrusion junction to distal extent of protrusion (L) were measured with Metamorph software. Stubby spines were defined as having parameters (H~N~L), thin spines were defined as (H~N, H<L, N<L) and mushroom-shaped spines were defined as (H>N, H~L). Filopodia were longer than spines and did not possess an enlargement (head) at their distal ends. Live-cell images were collected at a resolution of 0.126µm/pixel. All images used for quantifications (n=69 spines, n=23 filopodia) were collected at 10 second intervals for a period of 1 hour (361 images). This collection scheme resulted in 33,212 quantifiable images.

Immunocytochemistry

Neurons were fixed in 4% paraformaldehyde/KREBs/sucrose or 4% paraformaldehyde/PHEM medium at 37ºC (Dent et al., 2007). Cultures were rinsed in PBS and blocked with 10% BSA/PBS, permeabilized in 0.2% Triton X-100/PBS and labeled with primary (see above) and secondary antibodies at 1:500 (Invitrogen, Carlsbad, CA). Phalloidin coupled to Alexa 350, 488 or 568 (Invitrogen) was used to label actin filaments (1:25-1:100). Images of fixed and labeled neurons were collected in both widefield and TIRFM at a resolution of 0.063µm/pixel.

Statistics and Graphing

All statistical tests were preformed with Graphpad Prism 4.0c (La Jolla, CA). For each data set parametric or non-parametric statistical tests and post hoc tests were performed depending upon the variance of the data sets. Graphs were compiled in Microsoft Excel (Redmond, WA) or Prism.

RESULTS

To determine whether and how MTs are capable of entering dendritic protrusions we imaged MT dynamics with time-lapse TIRFM. Because TIRFM only excites fluorophores within a few hundred nanometers of the cell/coverslip interface we were able to acquire high signal-to-noise images of MT dynamics in spines within dense neuronal cultures **(Fig. 1e-g)**. Furthermore, TIRF imaging allowed us to image sections of dendrites labeled with EGFP-α-tubulin and DsRed2 (as a volume marker) at rapid intervals (10-30 second intervals) for extended periods of time (8-20 hours), without any obvious deleterious effects to the neurons. We were able to image neurons with standard wide-field microscopy (WFM) but the images were of lower quality with higher background fluorescence **(Fig. 1a-c)**. Furthermore, the much higher level of illumination required to obtain usable WFM images limited our total imaging time to 20-30 minutes before phototoxic damage to the neurons occurred. Therefore, all live-cell imaging was conducted with TIRFM. However, we used WFM to obtain z-stacks of fixed cultures to detect MTs in protrusions after fixation (see below). All of our studies were performed on cultures that were transfected by electroporation before plating. Because all the neurons that we imaged expressed the transfected proteins for their entire time in culture (DIV12-63) and developed normally, it is unlikely that transfection of EGFP-α-tubulin or EB3-EGFP induced spurious cytoskeletal dynamics in our cultures. Surprisingly, we discovered that MTs remained dynamic in mature cultures of both hippocampal and cortical neurons (DIV12-63). However, for quantitative analysis of MT dynamics in spines we imaged EGFP-α-tubulin-labeled MTs (and DsRed2) in DIV20-28 hippocampal neurons at 10 second intervals for one hour, resulting in 361 images for analysis of each protrusion.

Microtubules transiently invade dendritic protrusions

In all types of dendritic protrusions examined (filopodia, stubby spines, thin spines and mushroom-shaped spines) MTs were capable of rapidly extending into and out of the full extent of the protrusion. Furthermore, at least two MTs could occupy one spine at a time (Fig. 1i). The first MT polymerized (green arrowheads) into the spine at the beginning of the montage (51:45) and continued polymerizing coincident with the formation of a transient spine head protrusion (tSHP) (52:45-53:25) (Fig. 1i). This MT then depolymerizes out of the spine coincident with retraction of the tSHP (53:35-54:05), while a second MT (magenta arrowheads) polymerizes into the spine without inducing a tSHP. tSHPs were seen in a subset of spines that were targeted by MTs (6.0%, 4 of 69 spines, DIV20-28) and appeared to extend along other neuronal processes near the spine (Fig. 1h, boxed region). MT polymerization/depolymerization always accompanied tSHP extention/retraction (Fig. 1j), yellow arrow) indicating an important association of MTs and tSHPs. In fact, in DIV20-28 cultured tSHPs only occurred when MTs polymerized beyond the spine head (7/7 tSHPs from 4 different spines). Furthermore, we did not observe tSHPs in spines that were not targeted by MTs (0/76 randomly selected untargeted spines). tSHPs were always transient, with an average lifetime of 40+/-12 seconds (n=7).

Because we used DsRed2 as a marker of cell volume we may have missed tSHPs that were entirely actin-based filopodial protrusions. Indeed, based on our imaging of very mature neurons (DIV63), that were transfected with mCherry-β-actin instead of DsRed2, we document transient actin-based protrusions that did not contain MTs (see Fig. 6). Thus, there may be both MT- and f-actin-based extensions from spine heads. Our current imaging technique does not allow us to determine if MTs perforated the post-synaptic density or if these protrusions extend

into or along the outside of the presumptive presynaptic ending associated with these spines. Nevertheless, the vast majority of spines in our cultures are associated with synaptophysin puncta in both DIV20-28 untransfected cultures (94.7+/-0.8%, n=1459 spines) and DsRed2/EGFP-α-tubulin-transfected cultures (93.9+/-1.3%, n=1098 spines), indicating the presence of a morphological presynaptic ending associated with most spines. Similar values for transfected and non-transfected cultures ($p>0.05$, Student's t-test with Welch's correction) also suggests that long-term transfection with DsRed2 and EGFP-α-tubulin does not affect synaptogenesis in our cultures.

To represent, in a single image, the frequency and extent of MT polymerization in protrusions over one hour imaging intervals we compiled kymographs. These kymographs consisted of taking the maximum pixel value from a five pixel-wide line drawn parallel to the long axis of the protrusion for each frame (Fig. 1k) and arranging them horizontally, yielding images where the x-axis represents time and the y-axis represents distance (Fig. 1j). The maximum value within a five pixel-wide line (instead of using a single pixel-wide line) was used to assure that we recorded all MT invasions within each motile spine. The kymograph of this spine shows that MTs enter protrusions by discrete invasions (Fig. 1j, white arrows) and polymerize/depolymerize coincident with extension/retraction of a tSHP (Fig 1j, yellow arrow). We measured MT invasions into spines (n=69 spines, 24,909 images) and plotted them graphically (Fig 2a shows four examples). These four examples show the variability of MT invasion; some spines are targeted frequently, while others are targeted rarely or not at all (not shown). To determine if MT invasion varied over one hour of imaging we compiled a cumulative graph of MT invasion of spines after binning MT invasions in 10 minute intervals for

each of the 69 spines (Fig. 2b). This graph shows that the percentage of time a MT is present in a spine does not vary over the one hour of imaging, indicating that TIRF imaging does not affect the likelihood of MT invasion into dendritic spines ($p=0.567$, repeated measures ANOVA and $p=0.189$, post test for linear trend). We did not find significant morphological changes (area, spine length, spine head width) in dendritic spines when MTs invaded these protrusions, except when the invasion resulted in a tSHP (Fig. 1l). These increases in spine area were always transient, coinciding with the presence of the MT in the spine (Fig. 1l). However, because TIRF imaging does not allow us to image the full extent of the spine in the z-axis changes in spine volume may be occurring during MT invasion.

Microtubule kinetics differ in spines vs. filopodia

Overall, we found MTs explored 8.9+/-1.0% of protrusions (spines and filopodia) per hour (104 of 1163 protrusions from 10 independent experiments), indicating only a subset of spines are visited in a given time period. However, this number may be an underestimate of the actual number of protrusions invaded by MTs because TIRF imaging only allows us to image MTs that are within the ~400nm distance above the coverslip. To determine the kinetics of MT invasion of dendritic protrusions we quantified MT dynamics in filopodia (n=23) and spines (thin and mushroom-shaped) (n=69) from DIV20-28 hippocampal neurons transfected with EGFP-α-tubulin/DsRed2 (Fig. 3). Spines and filopodia were differentiated by strict morphological criteria (see Materials and Methods). All filopodia in which MT invasion was quantified maintained a relatively fixed length (+/-0.3μm) for the entire hour of imaging (the few filopodia that were dynamic during the one hour interval were not quantified). Stubby spines were not quantified owing to the difficulty of discerning MT entry into a spine directly apposed

to the brightly fluorescent dendritic shaft. Furthermore, we combined the data for thin and mushroom-shaped spines because they were statistically similar.

We quantified a number of different dynamic parameters including: the percent of time MTs were present in protrusions (Fig. 3a), the average event time (defined as the cumulative time it takes an individual MT to enter and exit a protrusion) (Fig. 3b), the percentage of time a MT within a spine was extending, pausing and retracting (Fig. 3c), the number of both full (extension to the tip of the protrusion) and partial MT invasions per hour (Fig. 3d), and the average polymerization/depolymerization rates (Fig. 3e, f) of MTs in spines. Only spines that were invaded by MTs were quantified. MTs spent a significantly higher percentage of time in spines (9.9+/-1.3%) compared to filopodia (5.3+/-0.8%) (Fig. 3a). This higher percentage of time spent in spines may be due to both longer event times (141+/-11 seconds for spines vs. 86+/-9 seconds for filopodia) (Fig. 3b), which were dependent on MTs pausing more in spines (42+/-3% of time in spines vs. 32+/-4% of time in filopodia) (Fig. 3c) and the slightly, but not significantly, higher number of invasion per hour (3.2+/-0.5 spines vs. 2.6+/-0.5 filopodia) (Fig. 3d). Furthermore, the likelihood of full MT invasion was similar between spines (68.4%, n=212 events) and filopodia (69.5%, n=59 events), indicating that MTs were just as likely to polymerize to the end of spines as filopodia, even though filopodia were considerably longer. Similarly, polymerization and depolymerization rates of MTs in spines and filopodia did not differ from each other (Fig. 3e, f) or from values documented in newly plated cortical neurons (Dent and Kalil, 2001). These data indicate that MTs target spines slightly more frequently and spend more time per targeting event by pausing more in spines compared to filopodia, resulting in MTs spending a higher overall percentage of time in spines.

Microtubules enter dendritic protrusions from both the proximal and distal dendrite

Since MTs in dendrites are of mixed polarity (arrayed with their plus (dynamic) ends facing both proximal and distal directions (Baas et al., 1988)) we wondered if MT entry into protrusions occurred from both the proximal and distal dendrite. Indeed, we documented that EGFP-α-tubulin-labeled MTs can enter protrusions from both the proximal and distal dendrite with live-cell TIRFM (Supplemental Figure 1). To confirm these results we also labeled the polymerizing ends of MTs with the +TIP protein EB3 (Stepanova et al., 2003). Unlike EGFP-α-tubulin, EB3-EGFP only allows the detection of polymerizing MTs, not pausing or depolymerizing MTs, so we could not use these data in our quantifications above. Nevertheless, an advantage of using EB3-EGFP is that MT polymerization within dendritic shafts, as well as dendritic protrusions, can be documented. This allowed us to unequivocally show that MTs were capable of entering protrusions from both proximal and distal dendritic domains (Fig. 4). Most of the invasions occurred from the proximal dendrite (84.8%), while fewer occurred from the distal dendrite (15.2%) (n=92 invasions). These percentages are different than the percentages of MTs arrayed with plus ends facing away from the cell body or toward the cell body in both hippocampal (~60% away/40% toward) (Baas et al., 1988) and Purkinje (~65% away/35% toward) (Stepanova et al., 2003) dendrites. However, both of these studies found most (~95%) MTs in the distal dendritic regions, where we focused much of our imaging, faced away from the cell body (Baas et al., 1988; Stepanova et al., 2003), indicating the percentages of MT invasions we documented are in line with the with the polarity of MTs in the these regions of the dendrite. These data indicate that MTs of either polarity are capable of entering dendritic protrusions.

In addition to polymerizing into and depolymerizing out of spines, we documented a single case where a MT polymerized into a spine followed by a depolymerizion from its minus (trailing) end while in a spine (Supplemental Fig. 2). This observation indicates that relatively short MTs are capable of polymerizing into spines. We never observed a MT originating (nucleating) in a spine and polymerizing out of it into the dendrite shaft, as has been suggested by others (van Rossum and Hanisch, 1999). However, this type of MT behavior is formally possible.

EGFP-labeled and endogenous microtubules target spines with morphological synapses

Even though our DIV20-28 cultures were mature and likely contained presynaptic endings adjacent to spines we wanted to establish if MTs were capable of entering spines containing a morphological synapse. Furthermore, we wanted to determine if we could image MTs in spines away from the coverslip interface with standard wide-field imaging to determine if MT invasion of dendritic protrusions only occurred in spines adjacent to the coverslip. First, we fixed DIV20-28 cultures previously transfected with EGFP-α-tubulin/DsRed2, stained them for presynaptic endings with anti-synaptophysin and imaged them by taking z-series stacks (10 images, 0.2μm distance between images, 100X/1.49NA objective) with wide field imaging (Fig. 5a, b). MTs in EGFP-α-tubulin/DsRed2-transfected neurons (not directly on the coverslip) entered spines and targeted morphological synapses. These data are consistent with another study that used confocal imaging in fixed cultures and documented the presence of MTs in spines (Gu et al., re-submitted to the Journal of Neuroscience). From our live-cell analysis we determined MTs usually enter spines at non-right angles relative to the dendrite shaft, as we have shown for MTs entering axon branches from the parent axon (Dent et al., 1999; Kalil et al., 2000;

Dent and Kalil, 2001; Dent et al., 2003). MTs predominantly targeted spines at an obtuse angle, relative to the dendrite shaft. Therefore, in fixed neurons we could determine whether MTs targeted spines from proximal vs. distal dendrites by the angle they formed in the spine neck, relative to the dendrite shaft (Fig. 5a, b). We found that most spines (90%, n=10) in transfected and fixed neurons were targeted from the proximal dendrite (spines targeted by MTs at right angles were disregarded). This value is similar to the percentage of spines targeted from the proximal dendrite (85%) in our live-cell imaging studies (see above).

However, EGFP-α-tubulin-containing MTs may exhibit aberrant MT behavior. Therefore, as a second approach we determined if endogenous MTs from untransfected neurons enter dendritic spines. We fixed untransfected DIV20-28 hippocampal cultures and stained them for endogenous, newly polymerized MTs (anti-tyrosinated MTs), dendritic spines (phalloidin to label high concentrations of f-actin in spines) and presynaptic endings (anti-synaptophysin). We imaged these labeled cultures in TIRFM to distinguish endogenous MT invasion of spines from the highly tubulin-labeled dendrites and axons in the culture. Endogenous MTs extended into dendritic protrusions from both proximal (86%) and distal (14%) dendrites as well (n=22 spines) (Fig. 5c, d). Thus, by live-cell imaging of transfected neurons with TIRFM, fixed-cell imaging of transfected neurons with wide-field microscopy and fixed cell-imaging of endogenous MTs with TIRFM we consistently found that ~85% of protrusions were targeted from the proximal dendrite and ~15% of protrusions were targeted from the distal dendrite. It should be noted that we fixed all of our cultures in a fixative that preserves dynamic MTs and f-actin and stained them for tyrosinated-tubulin to detect newly polymerized/dynamic MTs (Dent et al., 2007).

In fixed cultures endogenous MTs targeted spines at a similar frequency to EGFP-labeled MTs. Overall, 1.1+/-0.3% of spines contained endogenous MTs (n=3477 spines) and 0.9+/-0.3% of spines contained EGFP-α-tubulin-labeled MTs (n=1098 spines) ($p>0.05$, Student's t-test). Endogenous MTs can extend to the tips of spines as well. Importantly, the percentage of spines containing MTs in fixed cultures is in accordance with another study by Zheng and colleagues (Gu et al., resubmitted to J. Neuroscience) in which confocal imaging of living rat hippocampal neurons was used to show 1-2% of spines contained MTs. Together with our data, these results indicate similar MT behavior in both mouse (this study) and rat hippocampal neurons (Gu et al., resubmitted), regardless of imaging technique employed (TIRFM, widefield or confocal). These data also indicate that EGFP-α-tubulin-labeled MTs do not induce spurious MT behavior in mature dendrites. Additionally, MTs are present in a very small fraction of dendritic protrusions in fixed specimens, consistent with their extremely rare incidence in electron micrographs of spines in culture or in hippocampus (Gray et al., 1982; Chicurel and Harris, 1992; Fiala et al., 2003). However, we discovered that 8.9% of spines are targeted per hour (see above), indicating many spines on a neuron may be targeted by MTs over a period of a day. Our live cell imaging data correspond very well with our fixed cell data. We discovered that 8.9% of spines are targeted by MTs per hour and in these spines MTs are present 9.9% of the time (Fig. 3a). Thus, if a single frame of a one hour time-lapse was chosen at random the likelihood of finding a MT in a spine would be 0.88%, which compares favorably with our results from transfected and fixed cultures (0.9%).

Microtubules remain dynamic throughout the life of the neuron

Surprisingly, we discovered that even in very mature cultures (DIV63) MTs were still

very dynamic (Fig. 6). We labeled these cultures with EB3-EGFP, a protein that specifically binds to the polymerizing ends of MTs (Stepanova et al., 2003). We discovered that in very mature cultures (DIV63) MTs were capable of rapid polymerizing anterogradely and retrogradely throughout dendritic shafts (Fig. 6b and c, arrows point to EB3 puncta) and axons (data not shown), as shown previously in younger hippocampal (DIV2-6) and Purkinje (DIV10-17) cell cultures (Stepanova et al., 2003). We documented EB3-labeled MTs extending into spines in these very mature hippocampal cultures as well (Fig. 6a-c, boxed region). tSHPs formed coincidently with EB3-labeled MTs (Fig. 6d), like EGFP-α-tubulin-labeled MTs (Fig. 1i). Interestingly, a mushroom-shaped spine from this hippocampal neuron showed prominent increases in actin signal coincident with MT invasion (Fig. 6d,e), suggesting that signaling between these two polymer systems may occur in spines, as shown previously in axonal filopodia (Dent and Kalil, 2001; Schaefer et al., 2002; Zhou et al., 2002; Dent et al., 2007). These increases in actin signal and formation of transient filopodia protruding from the spine head (see mCh-Actin frames 1:31:10 – 1:32:30hr) indicate that tSHPs can occur without MTs (Fig. 6d). However, many of the protrusions from these spines contain prominent EB3 label without detectable actin label (Fig. 6d, yellow arrowheads), indicating MTs may be capable of inducing tSHPs independently of actin polymerization, as has been demonstrated in axonal growth cones (Goldberg and Burmeister, 1992). Based on their infrequent and transient nature further study will be required to determine if MT-based tSHPs require coincident f-actin polymerization.

MT Invasion of Dendritic Protrusions is Regulated by Activity

As a first step toward understanding the functional significance of MT invasion of

dendritic spines we experimentally manipulated cultures by stimulating activity with high KCl. We used a regime of perfusion of 75mM KCl 3 times for 3 minutes, separated by 10 minute rest intervals (Fig. 7a); an established technique to elevate activity in cultured neurons globally but transiently (Wu et al., 2001; Li et al., 2004). We then fixed the neurons after 30 minutes and quantified the percentage of protrusions containing a MT. KCl treatment resulted in a significant increase of protrusions containing a MT from 0.74+/-0.30% (n= 15 neurons/1960 protrusions) to 3.05+/-0.53% (n= 13 neurons/1818 protrusions), an increase of over 400% (Fig. 7b). Conversely, when we globally inhibited activity in the cultures by including 1μM tetrodotoxin (TTX) in the perfusate we decreased the percentage of protrusions containing a MT from 0.74+/-0.30% to 0.42+/-0.22% (n= 11 neurons/1982 protrusions), although this decrease was not significantly different from controls (Fig. 7b). Furthermore, by including TTX in all solutions while stimulating with KCl (Fig. 7b) we abolished the increase in MT invasion produced by KCl, resulting in 1.05+/-0.52% (n=12 neurons/1364 protrusions) protrusions invaded by MTs (Fig. 7b). This value was not significantly different from control or TTX-treated cultures ($p>0.05$, Kruskal-Wallis test with Dunn's post hoc tests). These data indicate that global activation of synaptic activity increases the proportion of spines containing MTs and this increase in MT invasion can be inhibited by TTX.

To understand the dynamic aspects of MT entry into dendritic protrusions after KCl treatment we imaged EGFP-α-tubulin and DsRed2 transfected neurons before and after KCl application. We used a similar protocol to the one used in fixed cultures (above) and compared MT invasion in the 20 minute interval before the first KCl treatment and the 20 minute interval after the final 10 minute rest period after the third KCl treatment (Fig. 7c, d). We quantified

these results by determining the percent of time MTs remained in protrusions (Fig. 7e), the average MT event time (Fig. 7f), the number of MT invasions (Fig. 7g) and the area of protrusions (Fig. 7h) before and after KCl treatment. When we compared the mean values for all these quantitative measurements we found the percent of time MTs spent in protrusions increased from 16+/-6% before KCl to 46+/-7% after KCl (Fig. 7e) (n=34 protrusions for all measurements in c-f). Also, each MT invasion (event time) persisted for a longer period of time (183+/-67 seconds before KCl, 468+/-83 seconds after) (Fig. 7f) and the number of invasions doubled from 0.44+/-0.13 to 0.97+/-0.14 (Fig. 7g). All measurements made were statistically significant when the means before and after KCl treatment were compared. Interestingly, we discovered that virtually all protrusions (n=21/22) that exhibited MT invasion after KCl treatment had no activity before KCl treatment (Fig 7c shows one example) and virtually all protrusions (n=11/12) that exhibited MT invasion before KCl treatment did not exhibit any MT invasions after KCl treatment (Fig. 7d shows one example). A subset of protrusions changed spine type, i.e. filopodia to thin spine or thin spine to mushroom-shaped spine (13%, 4/30). Importantly, the spines that changed type only had MT invasion after KCl treatment (see Fig. 7c for example). Finally, KCl induced a significant increase in area for all protrusions, as documented previously (Wu et al., 2001). This increase in protrusion size occurred whether or not MT invasion took place before or after KCl treatment (Fig. 7h), indicating the enlargement was probably not due to MT invasion directly.

DISCUSSION

Our findings suggest that dendritic MTs are dynamic and can rapidly and transiently polymerize into dendritic protrusions throughout the life of cortical and hippocampal neurons.

Interestingly, MTs can penetrate the entire extent of the spine and even induce transient spine head protrusions (tSHPs). Although MTs were only documented in ~1% of dendritic protrusions in fixed cultures (DIV20-28) under basal conditions, it is likely that many spines are targeted over relatively short periods of time. Indeed, our one hour time-lapse imaging of MTs at frequent intervals (10 seconds) showed that ~9% of protrusions (spines and stable filopodia) are targeted by MTs. Thus, over a period of a day it is possible that all spines on a dendrite could be targeted by MTs. However, MT invasion of spines is likely to serve specific functions and is therefore not a random event. Indeed, we found that increasing activity substantially increased the number of protrusions that were invaded by MTs and the time MTs remained in those protrusions, while decreasing activity induced an opposite trend.

Why are spines thought to be devoid of MTs?

Our results are surprising based on the many light microscopic studies and hundreds of electron microscopic studies that have not documented the presence of MTs in spines. However, there have been a handful of studies that have documented MTs in spines. The first studies that showed MTs in dendritic spines are those by Westrum and Gray (Westrum and Gray, 1976; Westrum et al., 1980; Gray et al., 1982; Westrum et al., 1983). However, the occurrence of MTs in spines was dependent on dissection of tissue in up to 20% bovine serum albumin. This technique was, for good reason, dismissed by many researchers. More recent work showed MTs in complex, branched spines of the CA3 region of hippocampus that contained greater than four heads (Chicurel and Harris, 1992), indicating MT entry only under unusual circumstances. Moreover, a recent study from the same lab showed that the presence of MTs in dendritic spines was likely to be an artifact of warming hippocampal slices and was not documented in freshly

perfused tissue (Fiala et al., 2003). These findings at the EM level were confirmed with light microscopy by imaging EGFP-MAP2b and -MAP2c with time-lapse fluorescent microscopy (Kaech et al., 2001). It is unclear why these investigators failed to detect MTs in spines (or much dynamic MAP2 movement) after imaging for several hours. One possibility is that overexpression of MAP2 stabilized MTs. However, this group imaged hippocampal slices from EGFP-MAP2c-expressing mice that did not exhibit any morphological or behavioral abnormalities, making this argument less convincing.

We suggest that the failure to detect MTs in spines can be explained by their inherently dynamic nature. In preparation of samples for electron microscopy MTs are not usually stabilized against depolymerization during fixation. As we show here in mature neurons and have documented in immature neurons (Dent and Kalil, 2001; Dent et al., 2004; Dent et al., 2007), MTs are extremely dynamic polymers that are exquisitely sensitive to perturbation. Therefore, only studies that have purposefully stabilized MTs against depolymerization have detected MTs in spines by EM (Westrum and Gray, 1976; Westrum et al., 1980; Gray et al., 1982; Westrum et al., 1983; Mitsuyama et al., 2008). Obviously, fixation freezes any dynamic movement in time. Therefore, if only ~1% of spines possess MTs at a time when MTs are stabilized against depolymerization (this study) it is very unlikely MTs would be detected in electron micrographs, unless several hundred spines were examined in serial sections. Similarly, the lack of detection of MAP2 in spines in time-lapse microscopy (Kaech et al., 2001) could be due to the fact that MAP2 does not label the dynamic ends of MTs (data not shown), but rather the more stable sections of MT polymers that are present in the dendritic shaft. Therefore, dynamic imaging or labeling dendrites with antibodies to MAP2 would not show MTs in spines.

This suggestion is consistent with the lack of movement of EGFP-MAP2c in the dendrite shaft by time-lapse imaging (Kaech et al., 2001), even though a population of MTs is very dynamic in dendrite shafts of mature Purkinje (Stepanova et al., 2003) and hippocampal/cortical neurons (this study). Thus, the aforementioned studies are not inconsistent with the present results.

Potential Functions of MT Invasion of Dendritic Protrusions

MTs target spines more frequently and for longer periods of time than stable filopodia. These results suggest that MT invasion of spines may function in maintaining spine structure. However, it does not preclude the possibility that MT invasion of filopodia may be important for maturation of filopodia into spines (Hayashi and Majewska, 2005; Alvarez and Sabatini, 2007; Bourne and Harris, 2007; Harms and Dunaevsky, 2007). This hypothesis is consistent with the results from Zheng and colleagues (Gu et al. resubmitted to Journal of Neuroscience) where they show that inhibiting MT dynamics throughout the neuron inhibits BDNF-induced increases in spine numbers and knock-down of the +TIP protein EB3 with shRNA also decreases spine numbers.

Because MTs are the main route of transport of materials from the cell body to peripheral neuronal processes their transient invasion of dendritic spines could be an important pathway for delivery of material to nascent and established dendritic spines. Although all the MT invasions we documented were transient, they were more than long enough (avg. time in spines ~2.5 min.) for kinesin to transport material into spines and dynein/kinesin to transport material out of spines before MT depolymerization (Vale and Fletterick, 1997). Furthermore, we found MTs enter spines from both proximal and distal regions of the dendrite. Thus, it is likely that anterogradely

as well as retrogradely transported material can enter spines via MTs. This result is intriguing because MT-based transport could provide a direct route for communication between distal and proximal spines, as well as between the cell body and specific spines. Presumably, any material that is transported on MTs (Hirokawa and Takemura, 2005) could be directed to specific spines via MTs that polymerize from the dendrite shaft directly into the distal extent of the spine. Indeed, it is tempting to speculate that the dynamic nature of postsynaptic protein redistribution (Gray et al., 2006; Tsuriel et al., 2006) may depend at least in part on MT dynamics.

The function that tSHPs play in synaptic activity is unclear. Protrusions from the spine head, in the form of spinules (Westrum and Blackstad, 1962; Toni et al., 1999; Spacek and Harris, 2004), spine head protrusions (SHPs) (Richards et al., 2005), and lazypodia (Zha et al., 2005) have been documented previously. Oftentimes, these structures are associated with pronounced activity, in the form of LTP induction (Toni et al., 1999), focal application of glutamate (Richards et al., 2005) or bath application of a $GABA_A$ inhibitor to induce epileptiform activity (Zha et al., 2005). However, spine head protrusions also form after application of tetrodotoxin (TTX), which reduces neuronal activity (Richards et al., 2005). Because tSHPs that we document here are so ephemeral (average lifetime of 40 seconds) and rare (only 4/69 spines showed tSHPs) they may differ from spinules, SHPs and lazypodia. Furthermore, we did not detect any transendocytosis of MTs/tubulin, as has been shown for spinules (Spacek and Harris, 2004), suggesting spinules and tSHPs are distinct structures. Further studies will be required to discern the function of these structures and there dependence on MT and actin dynamics.

We document here for the first time that neuronal activity affects the ability of MTs to polymerize into spines. We found that inducing global activity in hippocampal cultures by an established technique ((Wu et al., 2001; Li et al., 2004) increased the number of dendritic protrusions that contained a MT by over 400% (0.7% before KCl treatment and 3.1% after KCl treatment). If we blocked action potential-derived activity with TTX we abolished the ability of KCl to induce increased invasion of MTs into dendritic protrusions. Furthermore, we discovered MTs that polymerized into these protrusions remained in the protrusions over 250% longer (3:03 minutes before KCl and 7:48 minutes after). These data show that global activity increases both the number of protrusions targeted by MTs and the time MTs remain in protrusions. Interestingly, we found that most spines that had MT invasion before global activation did not have any MT invasion after activation. Furthermore, most spines that had MT invasions after activation did not have any MT invasions before activation (at least in the 30 minutes prior to KCl treatment). These data, along with the data showing TTX decreases MT invasions of dendritic protrusions, suggest that MT invasion may coincide with a specific amount of synaptic activation. Further studies are needed to determine if focal activity is sufficient to cause MT polymerization into individual activated spines and what mechanisms are necessary for MT invasion of spines.

Figure 1. Two microtubules can occupy a spine and induce transient spine head protrusions. **(a-c)** Widefield (WF) and **(e-g)** total internal reflection fluorescent (TIRF) images of a DIV20 hippocampal neuron transfected with DsRed2 **(a,e)** and EGFP-α-Tubulin **(b,f)** at the time of plating. **(c,g)** Overlay images of WF **(a,b)** and TIRF **(e,f)** images with DsRed2 in red and EGFP-Tubulin in green. **(d)** DIC image of same region. **(h)** DIC image merged with TIRF overlay image **(g)**. **(i)** Montage of images (~4 minutes) from a one hour TIRF time-lapse of the spine outlined by the white box **(in e-h)**. This spine is targeted by two different microtubules during the time interval shown in the montage. **(i)** The distal extent of each microtubule is demarcated by green and magenta arrowheads (in the EGFP-Tubulin row). The entry of the first microtubule (green arrowheads) coincides with a transient spine head protrusion (tSHP) (52:45 – 53:55 min). The first microtubule (green arrowheads) depolymerizes (53:35 – 54:05 min) as the second microtubule polymerizes into the spine (53:35 – 55:06). **(j)** A kymograph constructed from a one pixel wide line drawn through the extent of the spine and tSHP **(k)**. The kymograph line **(k)** is linearized and compiled horizontally for each frame (10 second interval) of the one hour time-lapse (361 frames). Time is indicated on the x-axis and distance is indicated on the y-axis. White arrows in **(j)** mark the beginning of separate microtubule excursions (events) into the spine and the tSHP is indicated by the yellow arrow. **(l)** Graph plotting changes in spine area for the spine shown in e-k and microtubule invasions into that spine. Scale bar is 5μm in **(h)** and 2μm in the last DsRed2 frame of **(i)**.

Figure 1

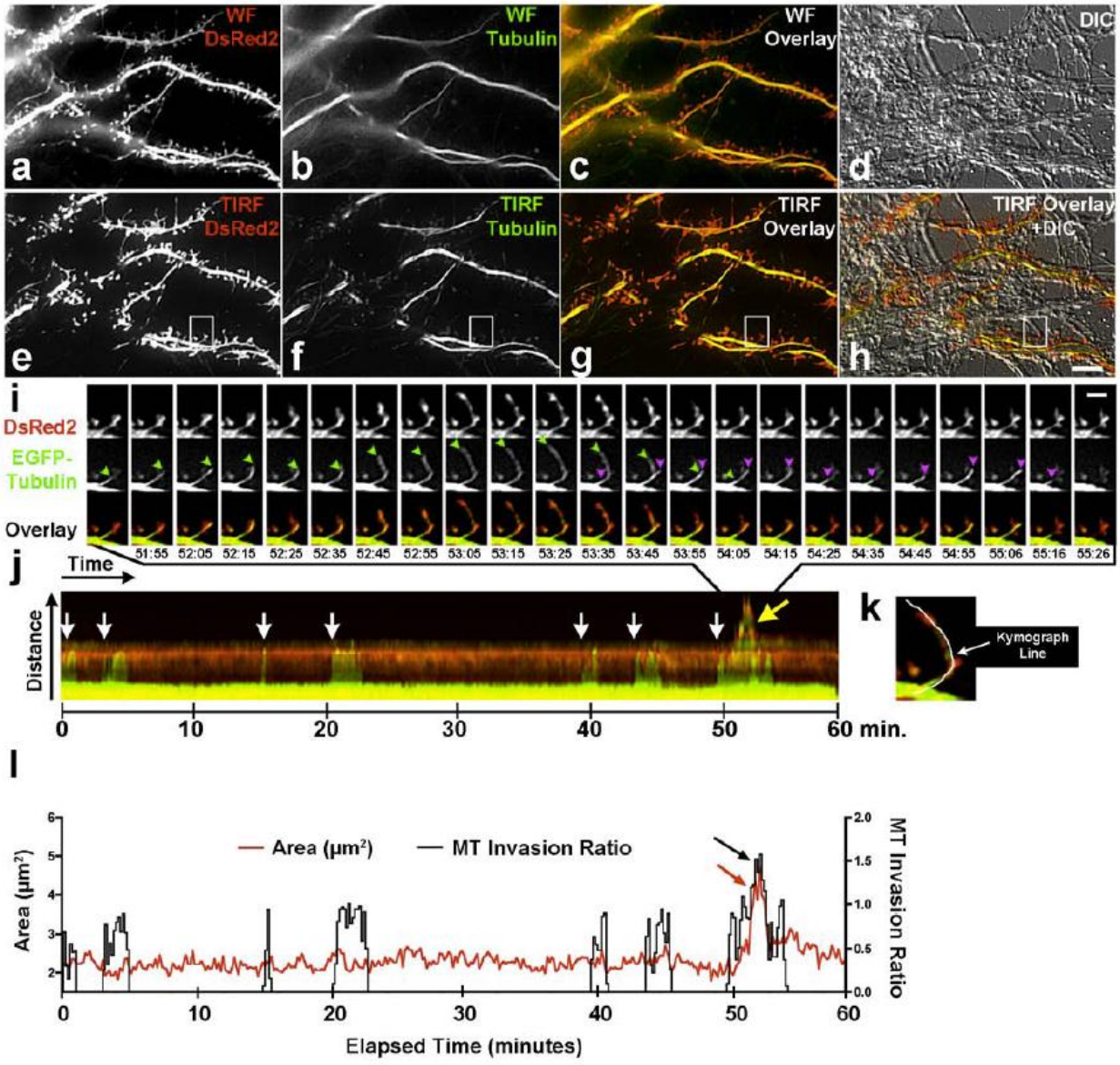
WF DsRed2
WF Tubulin
WF Overlay
DIC
a
b
c
d
TIRF DsRed2
TIRF Tubulin
TIRF Overlay
TIRF Overlay +DIC
e
f
g
h
i
DsRed2
EGFP-Tubulin
Overlay
51:55 52:05 52:15 52:25 52:35 52:45 52:55 53:05 53:15 53:25 53:35 53:45 53:55 54:05 54:15 54:25 54:35 54:45 54:55 55:06 55:16 55:26
j
Time
Distance
0 10 20 30 40 50 60 min.
k
Kymograph Line
l
Area (μm²)
MT Invasion Ratio
Area (μm²)
MT Invasion Ratio
Elapsed Time (minutes)

Figure 2. Microtubules invade spines consistently over one hour of imaging.

(a) Representative graphs of MT entry into spines as a function of time. The x axis is time (0-60 min) and the y axis is the ratio of invasion (0.0-1.0, except during tSHPs where values vary from 1.10-1.57). The asterisks above the invasions in the first graph indicate tSHPs. (**b)** Cumulative plot of all MT invasions from 69 spines (binned in ten minute intervals). Error bars are +/-SEM. There was neither a difference between any of the data points over the one hour imaging interval ($p=0.567$, repeated measures ANOVA) nor a linear trend over time ($p=0.189$, post test for linear trend).

Figure 2

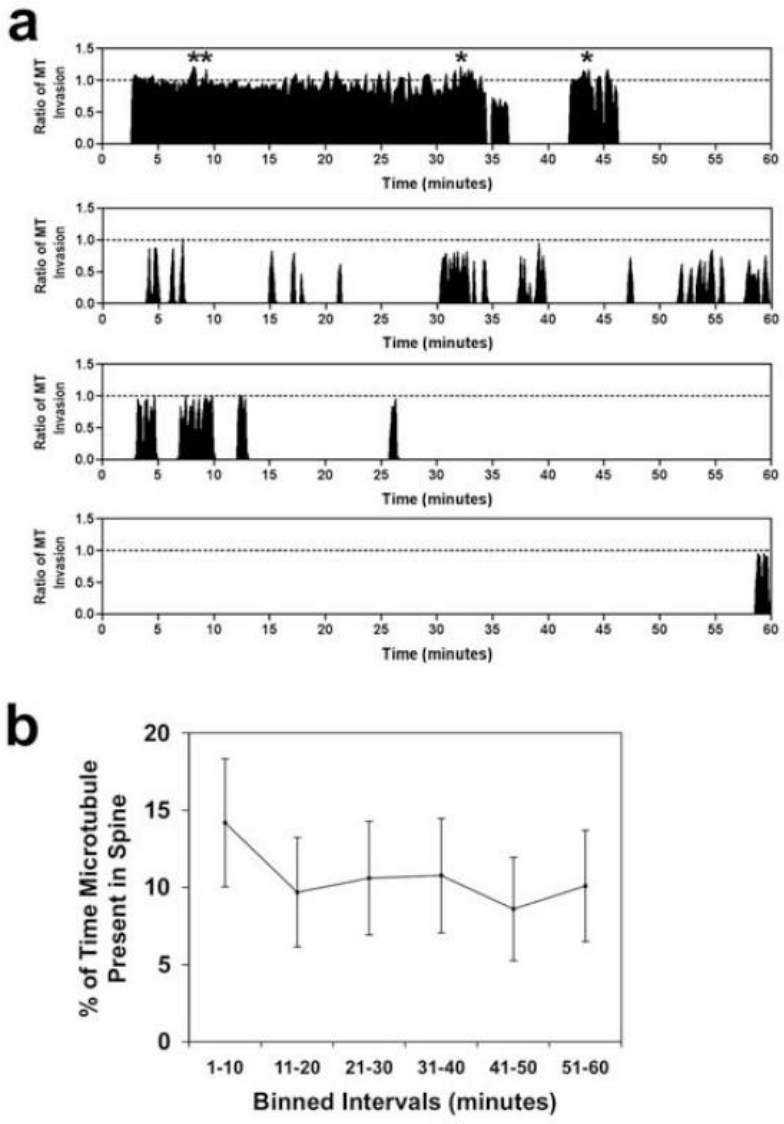
a
Ratio of MT Invasion
Time (minutes)
**
*
*
b
% of Time Microtubule Present in Spine
Binned Intervals (minutes)
1-10
11-20
21-30
31-40
41-50
51-60

Figure 3. Microtubules remain in spines longer and pause more than in stable filopodia.

(a) Bar graph showing the average percent of time microtubules are present in protrusions during a one hour interval (only spines invaded by MTs were quantified). Microtubules spend a significantly longer time in spines (Sp) than in stable filopodia (Filo) (**$p<0.01$, Student's t-test with Welch's correction). **(b)** Bar graph showing the average time a microtubule spends in a protrusion for each event (excursion). Microtubules spend a significantly longer amount of time per excursion in spines compared to filopodia (*$p<0.05$, Student's t-test with Welch's correction). **(c)** Stacked bar graph showing the percent of time microtubules spend retracting, pausing and extending while present in spines and filopodia. Microtubules in spines spend a significantly longer time in the paused state than MTs in filopodia (*$p<0.05$, Student's t-test with Welch's correction). **(d)** Bar graph showing the number of partial and full microtubule invasions into spines and filopodia per hour do not differ significantly. (n=69 spines, n=23 filopodia, from DIV20-28 hippocampal neurons)

Figure 3

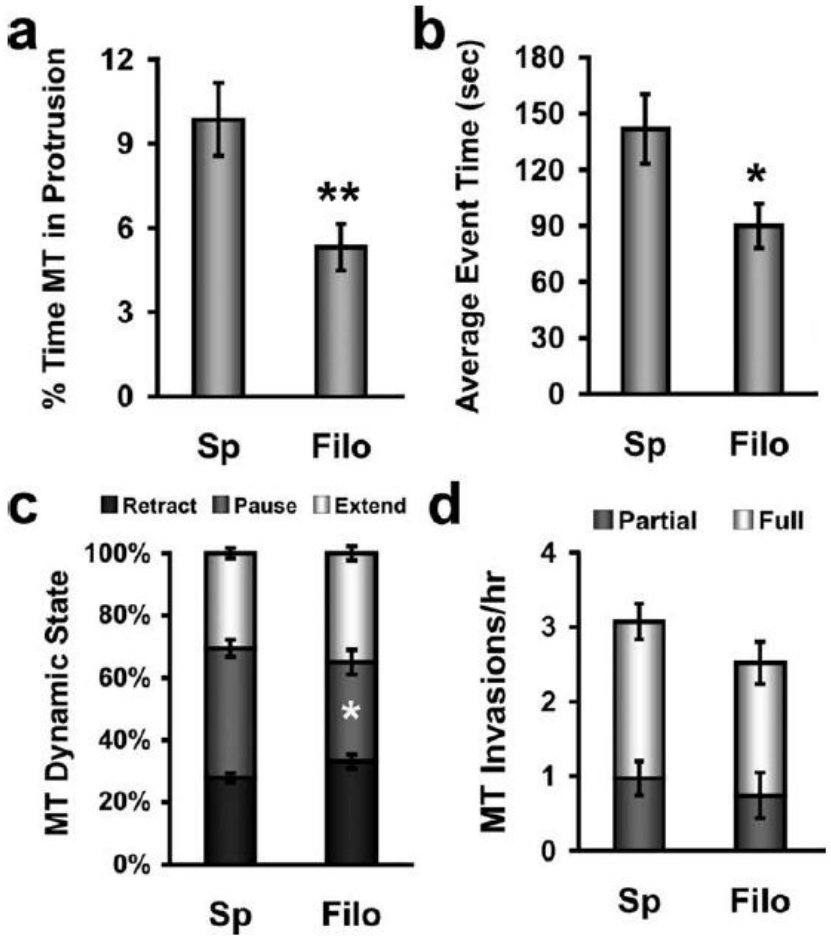
a
% Time MT in Protrusion
12
9
6
3
0
**
Sp
Filo
b
Average Event Time (sec)
180
150
120
90
60
30
0
*
Sp
Filo
c
Retract
Pause
Extend
MT Dynamic State
100%
80%
60%
40%
20%
0%
*
Sp
Filo
d
Partial
Full
MT Invasions/hr
4
3
2
1
0
Sp
Filo

Figure 4. Microtubules (EB3-labeled) enter spines from both the proximal and distal dendrite in a cortical neuron (DIV12). (a) An example of anterograde MT polymerization into a dendritic protrusion. An EB3-EGFP punctum (yellow arrowhead) starts to polymerize in the proximal dendritic shaft (0:15-0:25min), turns into the protrusion (0:30min) and polymerizes to the tip of the protrusion (0:40min). Another MT (magenta arrowhead) polymerizes in the dendrite shaft proximal to the first MT but does not enter the protrusion (0:50-1:05min). The first MT polymerizes again while in the protrusion (0:55-1:00min). **(b)** An example of retrograde MT polymerization in the same dendritic region as **(a)**. An EB3-EGFP punctum (green arrowhead) begins to polymerize in the distal dendrite shaft (6:00-6:25min), turns into a different protrusion (6:30min) and polymerizes toward the spine head (6:30-6:40min) but does not reach it (6:45min). A second MT (cyan arrowhead) polymerizes retrogradely entirely within the dendrite shaft. Time is in minutes:seconds. Scale bar is 5μm.

Figure 4

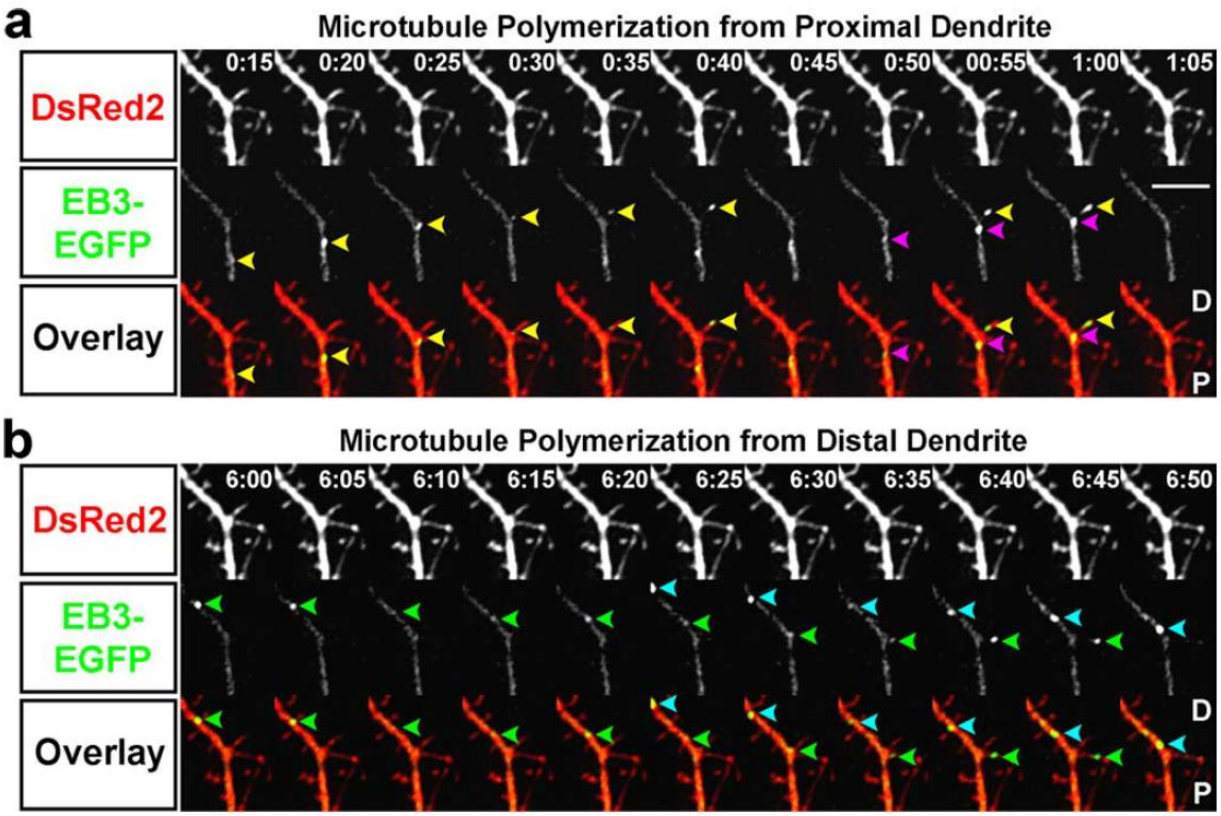
a
Microtubule Polymerization from Proximal Dendrite
DsRed2
EB3-EGFP
Overlay
0:15
0:20
0:25
0:30
0:35
0:40
0:45
0:50
00:55
1:00
1:05
D
P
b
Microtubule Polymerization from Distal Dendrite
DsRed2
EB3-EGFP
Overlay
6:00
6:05
6:10
6:15
6:20
6:25
6:30
6:35
6:40
6:45
6:50
D
P

Figure 5. EGFP-labeled and endogenous microtubules target spines from both proximal and distal dendritic regions. (a, b) Two examples of 20DIV hippocampal neurons transfected with EGFP-Tubulin (green in overlay) and DsRed2 (red in overlay), fixed and stained with an antibody to synaptophysin (blue in overlay) and imaged with wide field microscopy. The DsRed2 image was traced and the tracing was added to the anti-synaptophysin panels to show where the presynaptic endings were in relation to the dendrite. In **(a)** the microtubule is entering the spine from the proximal dendrite (P), while the microtubule in **(b)** is entering from the distal dendrite (D). **(c, d)** Two examples of spines from untransfected 20DIV hippocampal neurons that were labeled with an antibody to tyrosinated tubulin (to label dynamic MTs – green in overlay image), phalloidin (to stain filamentous actin – red in overlay image) and an antibody to synaptophysin (blue in overlay image) and imaged in TIRFM. In **(c)** the microtubule is entering the spine from the proximal dendrite (P), while the microtubule in **(d)** is entering from the distal dendrite (D). Arrows in **(a-d)** point to microtubules that are present in spines at the time of fixation. Scale bar is 2μm in a-d.

Figure 5

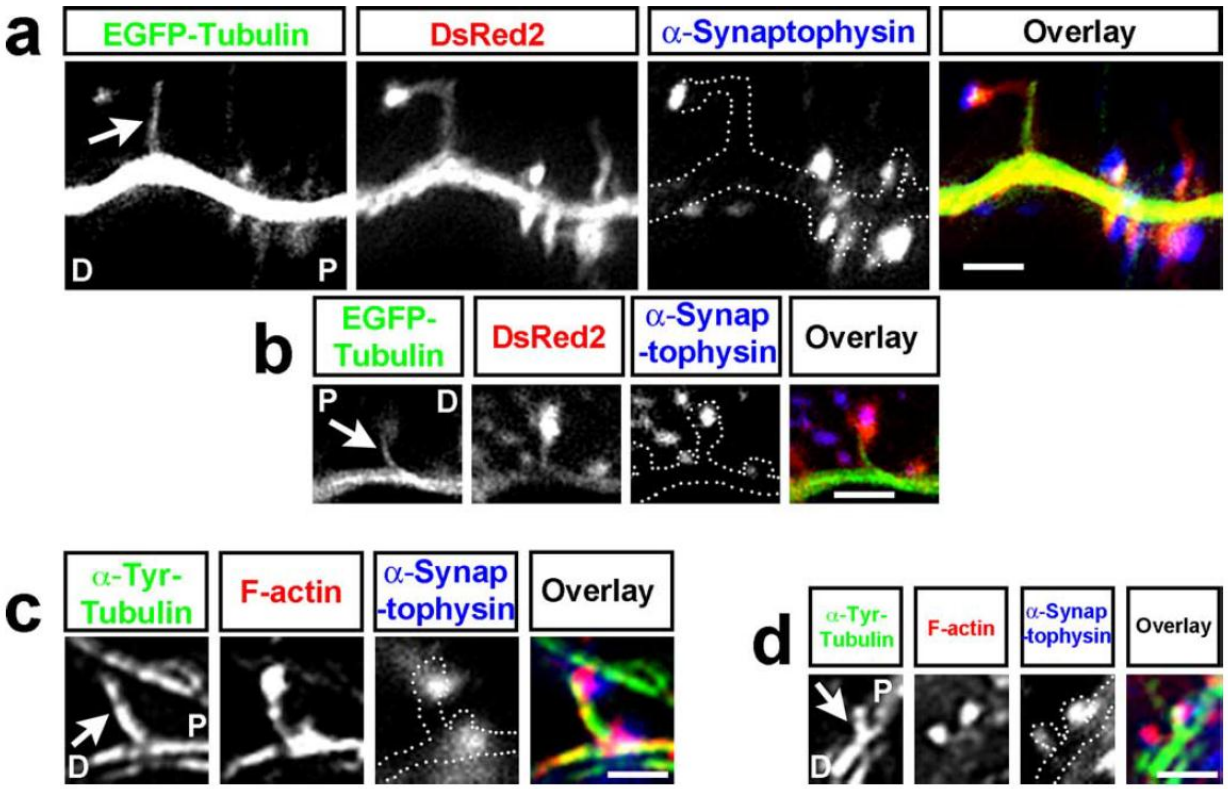
a
EGFP-Tubulin
DsRed2
α-Synaptophysin
Overlay
D
P
b
EGFP-Tubulin
DsRed2
α-Synap-tophysin
Overlay
P
D
c
α-Tyr-Tubulin
F-actin
α-Synap-tophysin
Overlay
P
D
d
α-Tyr-Tubulin
F-actin
α-Synap-tophysin
Overlay
P
D

Figure 6. Microtubules remain dynmic throughout the life of the neuron and continue to invade dendritic spines. Fluorescent images of a DIV63 hippocampal neuron transfected with mCherry-β-actin **(a)** and EB3-EGFP **(b)** at the time of plating. Arrows in **(b)** and **(c)** point to EB3 puncta (polymerizing MTs). **(c)** An overlay image of the mCherry-β-actin (red) and EB3-EGFP (green) images. **(d)** A montage of a single spine (boxed in **a-c**) from 1:29:00 -1:32:50hr in the two hour sequence. One MT polymerizes into the spine (yellow arrowheads point to an EB3-EGFP punctum in both the EB3-EGFP and overlay rows) inducing a tSHP and extending to it's tip. Another MT (magenta arrowheads point to a second EB3-EGFP punctum) polymerizes into the spine behind the first MT but only extends to the spine head. A third MT (cyan arrowheads) extends into the head of the spine (1:32:00 – 1:32:20) during the time the actin becomes markedly dynamic (1:31:10 – 1:32:40), forming transient filopodia and lamellipodia. **(e)** Kymograph of the entire two hour sequence showing no MT activity during the first hour but multiple MT excursions (short green lines) interspersed by dramatic actin-based protrusions (black arrowheads) during the second hour. **(f-g)** Same regions as in a-c except these images are composites of all 721 images in the 2hr time-lapse stacked into one image to show movement of actin and EB3. Note that there is so much activity of MTs in the dendrite shafts that they appear white, while a single frame shows only bright dots with some background of free EB3 (b). Scale bar in **(c)** is 5μm (for images a-c and f-h) and scale bar in the last mCh-Actin image of **(d)** is 2μm (for images d, e).

Figure 6

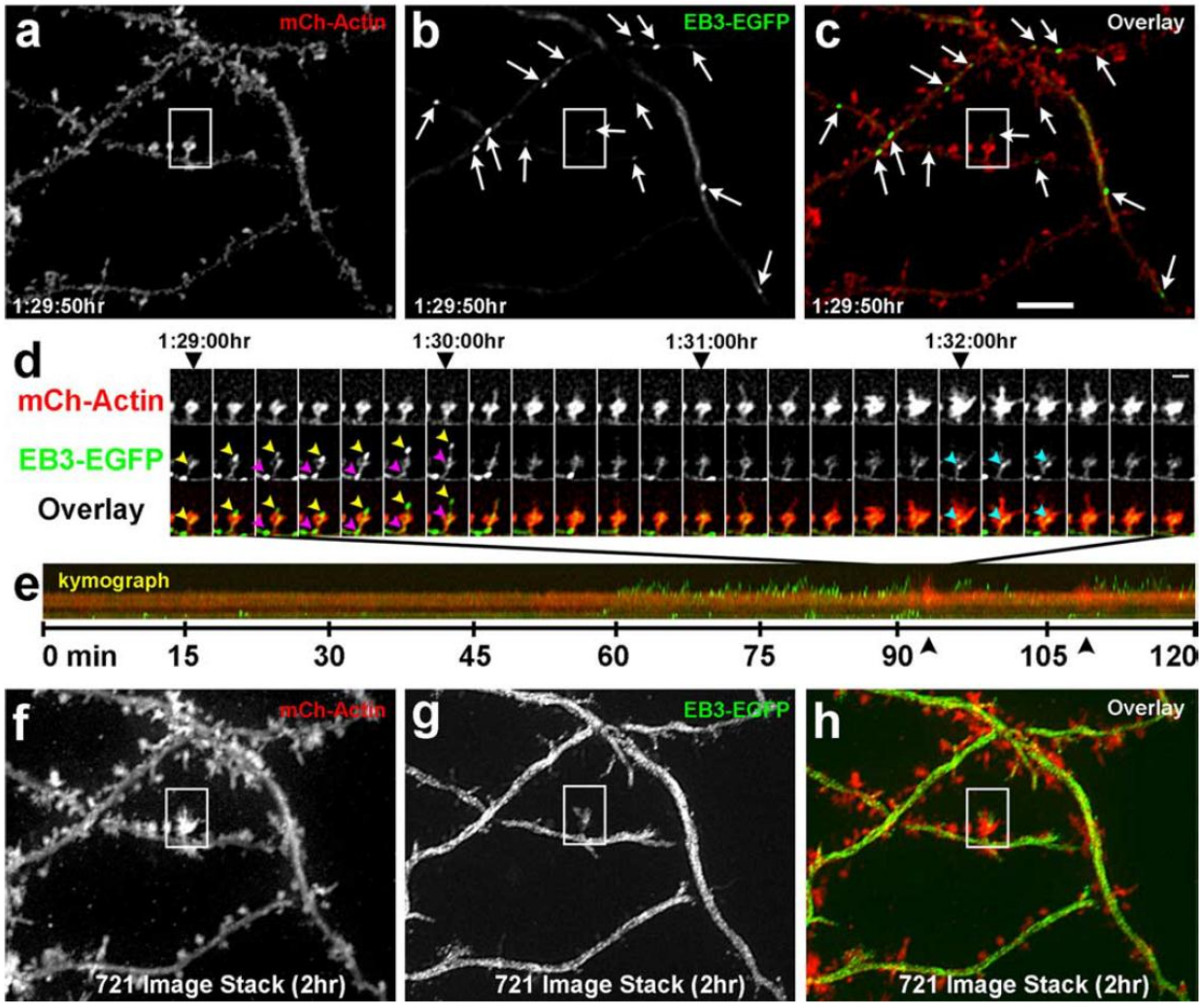
a
mCh-Actin
1:29:50hr
b
EB3-EGFP
1:29:50hr
c
Overlay
1:29:50hr
d
1:29:00hr
1:30:00hr
1:31:00hr
1:32:00hr
mCh-Actin
EB3-EGFP
Overlay
e
kymograph
0 min
15
30
45
60
75
90
105
120
f
mCh-Actin
721 Image Stack (2hr)
g
EB3-EGFP
721 Image Stack (2hr)
h
Overlay
721 Image Stack (2hr)

Figure 7. Global activity increases microtubule invasions of dendritic protrusions. (a) Diagram depicting the perfusion protocols used for 75mM KCl stimulation of global neuronal activity in DIV21 hippocampal cultures. TTX was included at 1μM. **(b)** Graph of the % of protrusions containing a MT at the time of fixation. KCl treatment induced a substantial increase in the percentage of spines containing a MT. TTX addition to the perfusate abolished this increase. P values are shown (Kruskal-Wallis test with Dunn's post hoc tests). Control, TTX and KCl+TTX were not significantly different ($p>0.05$). **(c, d)** Two examples from 34 spines (from hippocampal neurons transfected with EGFP-α-tubulin and DsRed2) that were imaged before, during and after three consecutive 75mM KCl treatments. One graph **(c)** shows an example of one without MT invasion before KCl application and substantial MT invasion after, while the second graph **(d)** shows MT invasion before KCl application and no MT invasion after. **(e-h)** Graphs quantifying the population of spines exhibiting either MT invasion before or after KCl treatment (all p values computed with Student's t-test). Spines that showed no MT invasion before or after KCl were not quantified. **(e)** MTs are present in protrusions for a significantly higher percentage of time ($p=0.020$) after KCl treatment (means are shown in boxes). **(f)** The average time a MT spends in a spine during one polymerization/depolymerization event is significantly longer after KCl treatment ($p=0.027$). **(g)** The number of MT invasions increased significantly after KCl treatment ($p=0.025$). All statistics for **e-h** were calculated with the two tailed Wilcoxon signed rank test.

Figure 7

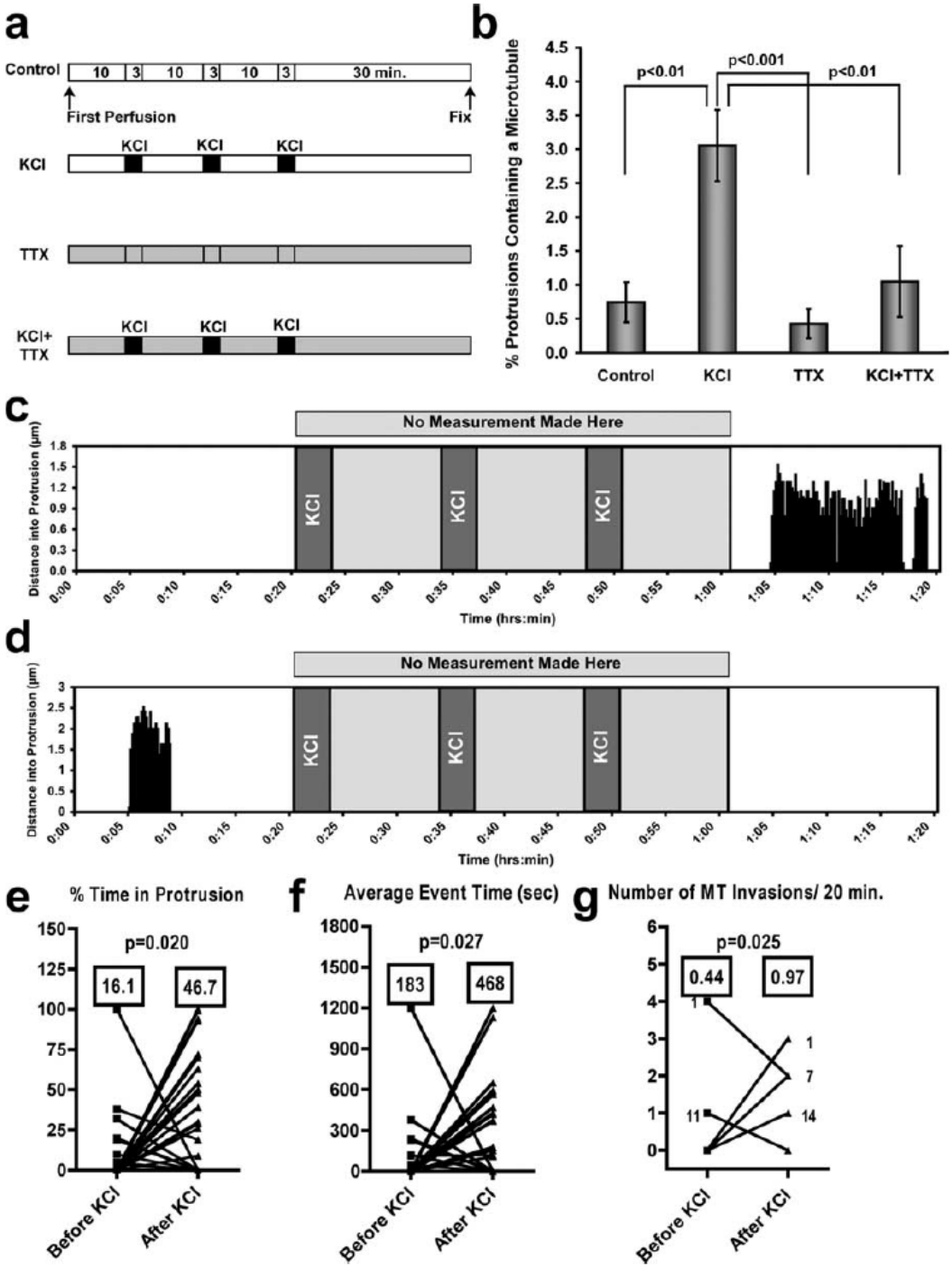
a
Control
10
3
10
3
10
3
30 min.
First Perfusion
Fix
KCl
KCl
KCl
KCl
TTX
KCl+
TTX
KCl
KCl
KCl
b
% Protrusions Containing a Microtubule
p<0.01
p<0.001
p<0.01
Control
KCl
TTX
KCl+TTX
c
No Measurement Made Here
Distance into Protrusion (µm)
KCl
KCl
KCl
Time (hrs:min)
d
No Measurement Made Here
Distance into Protrusion (µm)
KCl
KCl
KCl
Time (hrs:min)
e
% Time in Protrusion
p=0.020
16.1
46.7
Before KCl
After KCl
f
Average Event Time (sec)
p=0.027
183
468
Before KCl
After KCl
g
Number of MT Invasions/ 20 min.
p=0.025
0.44
0.97
Before KCl
After KCl

Supplemental Figure 1. Microtubules (tubulin-labeled) enter spines from both the proximal and distal dendrite in a hippocampal neuron (DIV21). (a) An example of anterograde MT polymerization into a dendritic protrusion. An EGFP-tubulin-labeled MT (cyan arrowheads point to the tip of the MT) starts to polymerize into the right protrusion from the proximal dendrite shaft (P) (4:20min), extending to the tip of the protrusion (5:01min) where it pauses (5:11min) and then rapidly retracts (5:21) back into the dendrite shaft. (b) An example of retrograde MT polymerization in the same dendritic region as (a). At a later time in this imaging session an EGFP-tubulin-labeled MT (magenta arrowheads points to the tip of the MT) polymerizes from the distal dendrite (D) into the left protrusion. The MT extends to the head of the protrusion (41:44-42:04min), where it pauses for 30 seconds (42:04-42:35) and then retracts back into the dendrite shaft (42:35-43:15min). Time is in minutes:seconds. Scale bar is 5μm.

Supplemental Figure 1

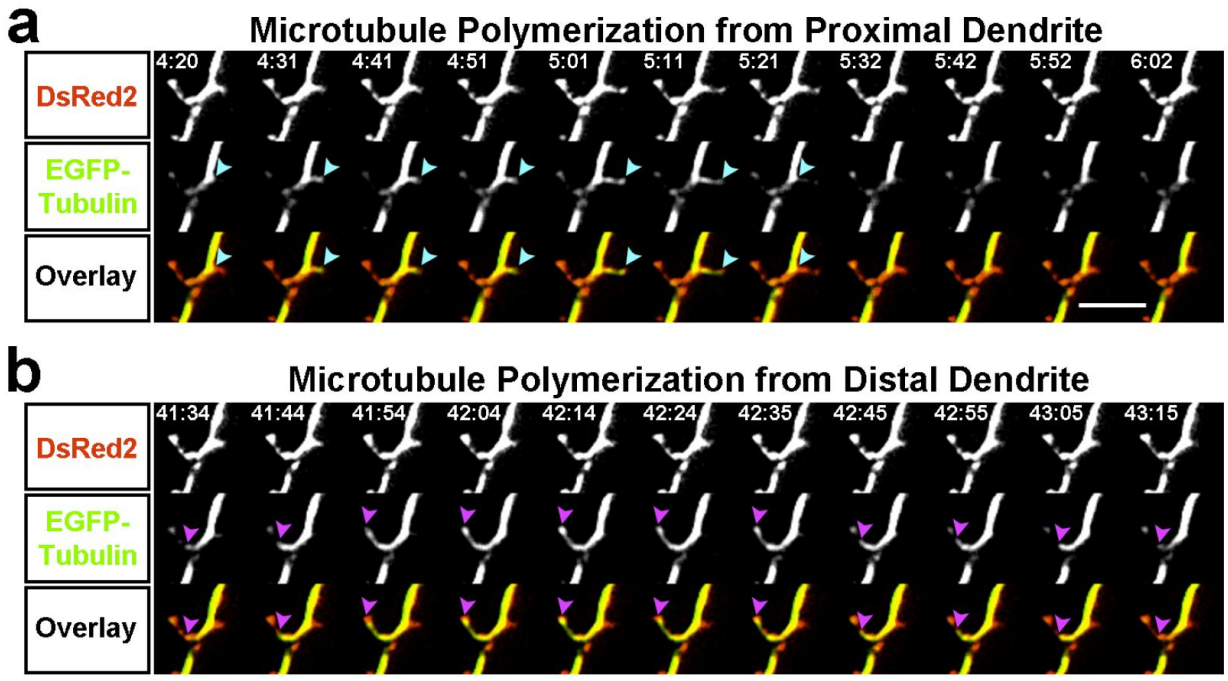

Supplemental Figure 2. Microtubules can depolymerize from their minus end while in a dendritic protrusion. A 60 second montage of a region of dendrite from a DIV20 hippocampal neuron transfected with DsRed2 (red in overlay) and EGFP-α-Tubulin (green in overlay). The microtubule had previously polymerized into the protrusion (* in overlay) at 5:19 (see movie 4) and subsequently depolymerizes from it's minus end (arrow in 13:31-14:02). Time is in minutes:seconds. Scale bar is 3μm**.**

Supplemental Figure 2

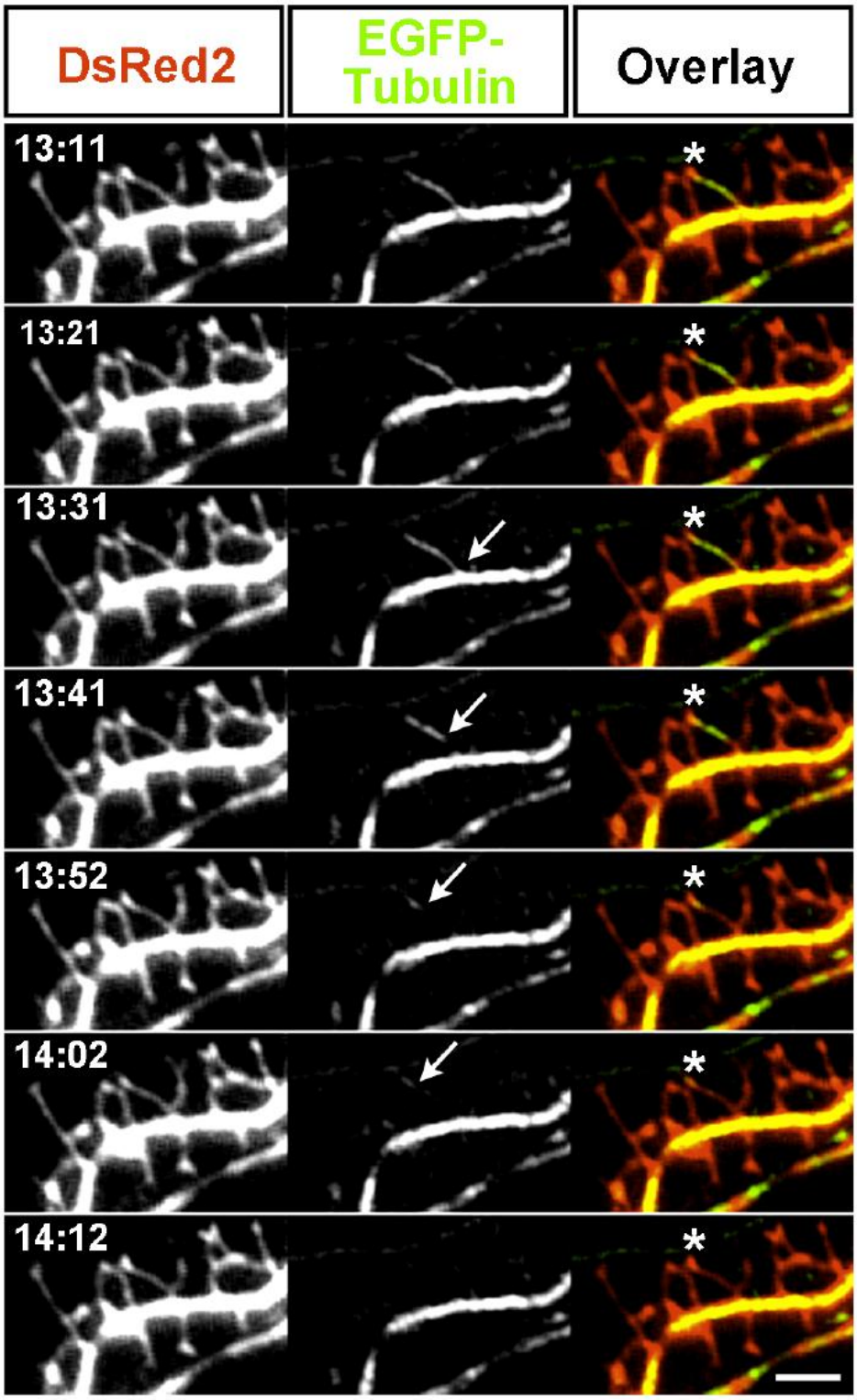

REFERENCES

Alvarez VA, Sabatini BL (2007) Anatomical and physiological plasticity of dendritic spines. Annu Rev Neurosci 30:79-97.

Baas PW, Deitch JS, Black MM, Banker GA (1988) Polarity orientation of microtubules in hippocampal neurons: uniformity in the axon and nonuniformity in the dendrite. Proc Natl Acad Sci U S A 85:8335-8339.

Bourne J, Harris KM (2007) Do thin spines learn to be mushroom spines that remember? Curr Opin Neurobiol 17:381-386.

Calabrese B, Wilson MS, Halpain S (2006) Development and regulation of dendritic spine synapses. Physiology (Bethesda) 21:38-47.

Chapleau CA, Carlo ME, Larimore JL, Pozzo-Miller L (2008) The actions of BDNF on dendritic spine density and morphology in organotypic slice cultures depend on the presence of serum in culture media. J Neurosci Methods 169:182-190.

Chicurel ME, Harris KM (1992) Three-dimensional analysis of the structure and composition of CA3 branched dendritic spines and their synaptic relationships with mossy fiber boutons in the rat hippocampus. J Comp Neurol 325:169-182.

Dent EW, Kalil K (2001) Axon branching requires interactions between dynamic microtubules and actin filaments. J Neurosci 21:9757-9769.

Dent EW, Tang F, Kalil K (2003) Axon guidance by growth cones and branches: common cytoskeletal and signaling mechanisms. Neuroscientist 9:343-353.

Dent EW, Barnes AM, Tang F, Kalil K (2004) Netrin-1 and semaphorin 3A promote or inhibit cortical axon branching, respectively, by reorganization of the cytoskeleton. J Neurosci 24:3002-3012.

Dent EW, Callaway JL, Szebenyi G, Baas PW, Kalil K (1999) Reorganization and movement of microtubules in axonal growth cones and developing interstitial branches. J Neurosci 19:8894-8908.

Dent EW, Kwiatkowski AV, Mebane LM, Philippar U, Barzik M, Rubinson DA, Gupton S, Van Veen JE, Furman C, Zhang J, Alberts AS, Mori S, Gertler FB (2007) Filopodia are required for cortical neurite initiation. Nat Cell Biol 9:1347-1359.

Ethell IM, Pasquale EB (2005) Molecular mechanisms of dendritic spine development and remodeling. Prog Neurobiol 75:161-205.

Fiala JC, Kirov SA, Feinberg MD, Petrak LJ, George P, Goddard CA, Harris KM (2003) Timing of neuronal and glial ultrastructure disruption during brain slice preparation and recovery

in vitro. J Comp Neurol 465:90-103.

Goldberg DJ, Burmeister DW (1992) Microtubule-based filopodium-like protrusions form after axotomy. J Neurosci 12:4800-4807.

Gray EG, Westrum LE, Burgoyne RD, Barron J (1982) Synaptic organisation and neuron microtubule distribution. Cell Tissue Res 226:579-588.

Gray NW, Weimer RM, Bureau I, Svoboda K (2006) Rapid redistribution of synaptic PSD-95 in the neocortex in vivo. PLoS Biol 4:e370.

Harms KJ, Dunaevsky A (2007) Dendritic spine plasticity: looking beyond development. Brain Res 1184:65-71.

Hayashi Y, Majewska AK (2005) Dendritic spine geometry: functional implication and regulation. Neuron 46:529-532.

Hirokawa N, Takemura R (2005) Molecular motors and mechanisms of directional transport in neurons. Nat Rev Neurosci 6:201-214.

Kaech S, Parmar H, Roelandse M, Bornmann C, Matus A (2001) Cytoskeletal microdifferentiation: a mechanism for organizing morphological plasticity in dendrites. Proc Natl Acad Sci U S A 98:7086-7092.

Kalil K, Szebenyi G, Dent EW (2000) Common mechanisms underlying growth cone guidance and axon branching. J Neurobiol 44:145-158.

Lebrand C, Dent EW, Strasser GA, Lanier LM, Krause M, Svitkina TM, Borisy GG, Gertler FB (2004) Critical role of Ena/VASP proteins for filopodia formation in neurons and in function downstream of netrin-1. Neuron 42:37-49.

Li Z, Okamoto K, Hayashi Y, Sheng M (2004) The importance of dendritic mitochondria in the morphogenesis and plasticity of spines and synapses. Cell 119:873-887.

Mitchison T, Kirschner M (1984) Dynamic instability of microtubule growth. Nature 312:237-242.

Mitsuyama F, Niimi G, Kato K, Hirosawa K, Mikoshiba K, Okuya M, Karagiozov K, Kato Y, Kanno T, Sanoe H, Koide T (2008) Redistribution of microtubules in dendrites of hippocampal CA1 neurons after tetanic stimulation during long-term potentiation. Ital J Anat Embryol 113:17-27.

Osumi N, Inoue T (2001) Gene transfer into cultured mammalian embryos by electroporation. Methods 24:35-42.

Richards DA, Mateos JM, Hugel S, de Paola V, Caroni P, Gahwiler BH, McKinney RA (2005)

Glutamate induces the rapid formation of spine head protrusions in hippocampal slice cultures. Proc Natl Acad Sci U S A 102:6166-6171.

Schaefer AW, Kabir N, Forscher P (2002) Filopodia and actin arcs guide the assembly and transport of two populations of microtubules with unique dynamic parameters in neuronal growth cones. J Cell Biol 158:139-152.

Schneckenburger H (2005) Total internal reflection fluorescence microscopy: technical innovations and novel applications. Curr Opin Biotechnol 16:13-18.

Spacek J, Harris KM (2004) Trans-endocytosis via spinules in adult rat hippocampus. J Neurosci 24:4233-4241.

Stepanova T, Slemmer J, Hoogenraad CC, Lansbergen G, Dortland B, De Zeeuw CI, Grosveld F, van Cappellen G, Akhmanova A, Galjart N (2003) Visualization of microtubule growth in cultured neurons via the use of EB3-GFP (end-binding protein 3-green fluorescent protein). J Neurosci 23:2655-2664.

Tada T, Sheng M (2006) Molecular mechanisms of dendritic spine morphogenesis. Curr Opin Neurobiol 16:95-101.

Toni N, Buchs PA, Nikonenko I, Bron CR, Muller D (1999) LTP promotes formation of multiple spine synapses between a single axon terminal and a dendrite. Nature 402:421-425.

Tsuriel S, Geva R, Zamorano P, Dresbach T, Boeckers T, Gundelfinger ED, Garner CC, Ziv NE (2006) Local sharing as a predominant determinant of synaptic matrix molecular dynamics. PLoS Biol 4:e271.

Vale RD, Fletterick RJ (1997) The design plan of kinesin motors. Annu Rev Cell Dev Biol 13:745-777.

van Rossum D, Hanisch UK (1999) Cytoskeletal dynamics in dendritic spines: direct modulation by glutamate receptors? Trends Neurosci 22:290-295.

Westrum LE, Blackstad TW (1962) An electron microscopic study of the stratum radiatum of the rat hippocampus (regio superior, CA 1) with particular emphasis on synaptology. J Comp Neurol 119:281-309.

Westrum LE, Gray EG (1976) Microtubules and membrane specializations. Brain Res 105:547-550.

Westrum LE, Jones DH, Gray EG, Barron J (1980) Microtubules, dendritic spines and spine appratuses. Cell Tissue Res 208:171-181.

Westrum LE, Gray EG, Burgoyne RD, Barron J (1983) Synaptic development and microtubule organization. Cell Tissue Res 231:93-102.

Wu GY, Deisseroth K, Tsien RW (2001) Spaced stimuli stabilize MAPK pathway activation and its effects on dendritic morphology. Nat Neurosci 4:151-158.

Zha XM, Green SH, Dailey ME (2005) Regulation of hippocampal synapse remodeling by epileptiform activity. Mol Cell Neurosci 29:494-506.

Zhou FQ, Waterman-Storer CM, Cohan CS (2002) Focal loss of actin bundles causes microtubule redistribution and growth cone turning. J Cell Biol 157:839-849.

Chapter 3

BDNF-induced Increase of PSD-95 in Dendritic Spines Requires Dynamic Microtubule Invasions

ABSTRACT

Microtubules (MTs) are capable of entering dendritic spines in mature hippocampal neurons through dynamic polymerization. Although these MT invasions are directly associated with neuronal activity, their function remains unknown. Here we demonstrate in mouse hippocampal neurons that MT entries into spines regulate the increase in post-synaptic density protein-95 (PSD-95) after brain-derived neurotrophic factor (BDNF) treatment. Using multi-wavelength total internal reflectance fluorescence microscopy (TIRFM) we show that BDNF prolonged the average MT dwell time in spines and this effect was dependent on TrkB receptor activation. Further examination revealed that peaks of MT polymerization into spines corresponded to rapid PSD-95 increases in the spine head. Over time, spines targeted by MTs after BDNF application, but not before, showed a robust increase in PSD-95. Conversely, spines completely devoid of MT invasions showed no significant change in the level of PSD-95. Pharmacological inhibition of MT dynamics abolished the BDNF-induced increase in PSD-95. Together these results support the hypothesis that the well known increase in PSD-95 within spines after BDNF treatment is dependent on MT invasions of dendritic spines. Thus, our study provides a direct link between dynamic MTs and the post-synaptic structure, and provides a functional role for MT invasion of dendritic spines.

INTRODUCTION

In mature cortical and hippocampal neurons MTs make rapid, infrequent excursions into dendritic spines through dynamic plus end polymerization and depolymerization (Gu et al., 2008; Hu et al., 2008; Jaworski et al., 2009). Furthermore, MT entries are promoted by neuronal depolarization (Hu et al., 2008) and pharmacological inhibition of MT dynamics blocks long-term BDNF-induced spine formation (Gu et al., 2008). These results indicate that MT entries into dendritic spines may play an important role during BDNF-induced synaptic plasticity. However, the mechanism that links BDNF-induced spine plasticity and MT invasions remains unknown.

The post-synaptic density scaffolding protein PSD-95 has been identified as a marker for synaptic strength. Overexpression of PSD-95 promotes synaptic maturation (El-Husseini et al., 2000) while knockdown of PSD-95 results in decreased synaptic strength and spine density (Ehrlich et al., 2007). PSD-95 remains mobile in mature neurons and can transit in and out of spines on the order of minutes (Marrs et al., 2001). A pool of dendritic PSD-95 molecules are shared and redistributed among neighboring spines through diffusion (Gray et al., 2006; Tsuriel et al., 2006). In visual cortical neurons BDNF can increase the size of PSD-95 puncta in spines and the overall amount of PSD-95 in dendrites within 60 minutes (Yoshii and Constantine-Paton, 2007). Thus, we hypothesized that BDNF increases the levels of PSD-95 in spines through regulation of dynamic MT invasions, and these invasions directly contribute to the accumulation of PSD-95.

To test this possibility we used dual-wavelength total internal reflection fluorescence microscopy (TIRFM) to simultaneously monitor MT dynamics and PSD-95 levels in dendritic spines of mature hippocampal neurons. TIRFM allowed us to obtain high signal-to-noise fluorescence images at rapid intervals for long periods of time (Hu et al., 2008). TIRFM has also

been shown to effectively capture changes in PSD-95 clusters by eliminating background signals from cytosolic PSD-95 molecules (Noritake et al., 2009). Here, we discovered that BDNF treatment increased the MT dwell time in dendritic spines. MT polymerization into spines also correlated with rapid increases of PSD-95 in the spine head. Within 20 minutes after BDNF treatment, only spines invaded by MTs showed a significant increase of PSD-95 levels, which was positively correlated with the probability that a MT was present in that spine. Moreover, pharmacological inhibition of MT dynamics effectively blocked the BDNF-induced increase in PSD-95. Together our results indicate that MTs directly contribute to post-synaptic structural changes by regulating the increase of PSD-95 in spines after BDNF treatment.

MATERIALS AND METHODS

Plasmids and reagents

DsRed2 and EGFP-α-tubulin in pCAX vectors were described previously (Hu et al., 2008). Newly polymerized microtubules were stained with rat anti-tyrosinated tubulin at 1:1000 (YL1/2 clone, Millipore). Alexa-conjugated phalloidin (1:50) and Alexa-conjugated anti-rat secondary antibody (1:500) were from Invitrogen. BDNF was from Promega and K252a, nocodazole and taxol were from Sigma-Aldrich.

Cell Culture and Transfection

All mouse procedures were approved by the University of Wisconsin Committee on Animal Care and were in accordance with NIH guidelines. E15.5 hippocampal neuron cultures were prepared

from Swiss Webster mice of either sex (Taconic) and transfected as described (Hu et al., 2008), with modifications (Viesselmann et al., 2011).

Live-cell TIRF Imaging and Immunocytochemistry

All imaging was performed at physiological temperatures (36-37ºC) on a Nikon TE2000E microscope as described (Hu et al., 2008). Neurons were fixed and stained as described (Dent et al., 2007). Images of fixed neurons were collected in TIRFM at a resolution of 0.063 μm/pixel. All experiments were repeated with at least three individual primary cell cultures.

Quantification of Microtubule dynamics and levels of PSD-95

Dual-wavelength time-lapse images were acquired at 10-second intervals for 20 minutes before and after the addition of BDNF +/- MT drugs, generating image stacks of 241 frames. A maximum projection image of the tubulin channel was generated by overlaying a stack of images into one image (121 frames, before or after treatment). An average projection image of PSD-95 was created to depict the morphology of dendritic protrusions. Live-cell images were collected at a resolution of 0.126 μm/pixel. For clarity, PSD-95 is shown in red and tubulin is shown in green in all figures. MT invasions into spines were determined by examining the time-lapse movies frame by frame. Parameters of MT invasions into dendritic spines were measured by tracking the polymerizing/depolymerizing plus end of MTs in the image stacks with Metamorph software (Molecular Devices) and calculated in Excel (Microsoft). MT invasion tracings were created by plotting the MT polymerization distance into spines (distance to origin) over time.

Kymographs of PSD-95 were generated by measuring the average fluorescence intensity within the width of 4-pixel wide line drawn across the long axis of the puncta. To measure PSD-95 levels, a region of interest was drawn around the entire PSD-95 puncta in the frame where it attained its largest area. The average fluorescence intensity (AFI) of PSD-95 within this region was measured at each time point. In Figure 3E, spine volume was calculated by averaging the AFI of DsRed over 1 minute (6 frames) at each time point. For the analysis in Figure 3F-I and Figure 4, PSD-95 level was calculated by taking the AFI over 1 minute. Only spines with a distinct PSD-95 punctum in the spine head were analyzed. Control spines included in Fig. 3F were chosen from the same dendritic segment as the neighboring MT-targeted spines. The percent chance of a MT being present in spine (Fig. 3J) was determined by calculating the probabilities of finding a MT in all MT-targeted spines at each individual time point (241 time points in each 40-minute time lapse). Spines in different categories (Fig. 3F-I) generated different values of "% chance of MT in spine". For the percent change in PSD-95 (Fig.3J), time points with the same "% chance of MT in spine" value were grouped together. The percent change in PSD-95 of all spines at these time points were compiled into each data point.

Statistics and graphing

All statistical tests were performed with Graph-Pad Prism. For each data set parametric or nonparametric statistical tests and *post hoc* tests were performed depending on the variance of the data sets. In all graphs p values are depicted as follows: * $p<0.05$, ** $p<0.01$, *** $p<0.001$. Graphs were compiled in Prism.

RESULTS

BDNF prolongs MT invasions into dendritic spines

Because BDNF increases PSD-95 in dendritic spines of visual cortical neurons (Yoshii and Constantine-Paton, 2007), we hypothesized that dynamic MT invasions into hippocampal dendritic spines could regulate the BDNF-induced increase of PSD-95. We first examined the effect of BDNF on the presence of endogenous MTs in dendritic spines by treating three week old hippocampal cultures with either 50ng/ml BDNF alone or BDNF with low concentrations of MT drugs for 20 minutes. We used either 10nM taxol or 100nM nocodazole to specifically inhibit MT dynamic instability, the rapid polymerization and depolymerization of MT plus ends (Dent and Kalil, 2001). After fixation, neurons were stained with an antibody against tyrosinated α-tubulin to label newly polymerized MTs, and phalloidin to label f-actin-rich dendritic spines (Fig. 1A-D). MTs were present in 0.8 ± 0.4% (all data presented are mean ± SEM) of spines under control condition (n=555 spines, 7 neurons), consistent with our previous study (Hu et al., 2008). Surprisingly, after BDNF treatment 3.8 ± 0.3% of spines contained MTs (n=768 spines, 9 neurons). The inclusion of either nocodazole or taxol abolished the increase of MTs in spines (Fig. 1C-E), resulting in 1.4 ± 0.3% of spines containing MTs (n=1030 spines, 9 neurons) for BDNF + nocodazole and 1.4 ± 0.4% for BDNF + taxol (n=769 spines, 8 neurons). These results indicate that BDNF markedly increases MT invasion of dendritic spines within 20 minutes, and these invasions are dependent on MT plus end dynamics.

We then investigated the effects of BDNF on MT dynamics in live cells using TIRFM. With TIRFM we can image cultured hippocampal neurons at 10 second intervals for over 60 minutes without inducing photodamage (Hu et al., 2008). Importantly, neurons were transfected before plating, which allowed them to mature while expressing both GFP-PSD-95 and mCherry-α-tubulin. After 2-3 weeks in culture, we selected only neurons that were expressing relatively

low levels of fluorescent proteins (the middle 25-75% brightest neurons) to minimize overexpression artifacts and phototoxicity. In these studies we imaged labeled neurons for 20 minutes before and after the application of BDNF, resulting in a 40 minute time-lapse. Treatment with BDNF increased the time MTs remained in individual spines (average MT event length) from 108 ± 14 seconds to 257 ± 37 seconds (n=101 spines, 7 neurons) (Fig. 2A, D (upper panel), E). However, BDNF application did not increase the percent of spines invaded by MTs (before, 7.9 ± 1.4 %, after, 8.3 ± 1.5 %, n=1317 spines, 7 neurons) (Fig. 2A,C), or the frequency of MT invasion (before, 1.9 ± 0.2 events/20 min.; after, 1.9 ± 0.2 events/20 min. n=101 spines, 7 neurons) (Fig. 2F). To examine the temporal change in MT dynamics in spines we measured MT dwell time, defined as the percent of time during each five minute time period that MTs were present in the MT-targeted spines (n=101 spines, 7 neurons) (Fig. 2G). Within 5 minutes of BDNF treatment, MT dwell time was significantly elevated compared to 5 minutes prior to BDNF application. MT dwell time peaked at 10-15 minutes after BDNF at a level twice that before BDNF application. These data demonstrate that BDNF treatment increases the MT dwell time in dendritic spines, resulting in a higher likelihood that MTs would be present in fixed dendritic spines (Fig. 1E).

To determine whether the BDNF receptor TrkB was responsible for BDNF-induced increase in MT dwell time, we pre-incubated neurons with the tyrosine kinase inhibitor K252a (200μM) for 24hrs to block TrkB activation. Time-lapse imaging revealed that K252a treated neurons had very few spines invaded by MTs either without (1.0 ± 1.0%) or with (0.8 ± 0.8%) BDNF treatment (n=501 spines, 4 neurons) (Fig. 2B,C), both conditions being significantly different than controls (Fig. 2C). In the handful of spines that contained MTs, MT invasions were scarce and transient (Fig. 2D, lower panel). Thus, intrinsic signaling through the TrkB receptor

is essential for basal levels of dynamic MT invasions into dendritic spines.

MT dynamics directly regulate the BDNF-induced increase in PSD-95

To study the possible correlation between MT entries and changes in PSD-95 after BDNF, we monitored MT dynamics and PSD-95 levels simultaneously in individual spines that contained a distinct PSD-95 punctum in the spine head. MT invasions correlate with "hotspots" of elevated PSD-95 levels (Fig. 3A,A') which may or may not persist following MT invasion (Fig. 3A'-C). Since MTs function as a major route of transport for a variety of intracellular cargoes in all cells, we asked whether PSD-95 is directly transported on MTs during MT entries. We examined 982 individual spines during time-lapse imaging (total imaging time = 4hrs) and found only one case in which MT invasion accompanied the movement of a PSD-95 punctum into a spine head (Fig. 3D'), followed by a subsequent increase in PSD-95 intensity in that spine head (Fig. 3D). We also documented four cases of a PSD-95 punctum moving into a spine when no MT was present (data not shown). Thus, although MT entries into spines correlated with increases in PSD-95, MTs rarely served as the direct conduit for PSD-95 transport into spines.

To better characterize the correlation between MT polymerization into spines and changes in PSD-95, we measured the average fluorescence intensity of PSD-95 in spine heads by drawing a region of interest (ROI) that included the entire PSD-95 punctum. We found that at the peak of each MT invasion, the PSD-95 level within the ROI increased by 3.0 ± 0.4% compared to the average of 1 minute prior to this time point (n=206 MT entries, 87 spines, 5 neurons). Conversely, in dendritic protrusions that did not contain a distinct PSD-95 punctum (immature spines), levels of PSD-95 remained unchanged at the peak of MT invasion (data not shown). Thus, MT invasions (red channel) do not cause bleed-through fluorescence into the

PSD-95 (green) channel.

To test the hypothesis that MT invasions are responsible for the accumulation of PSD-95, we measured the PSD-95 level in spines over a one minute interval at three time points during the 40 minute time-lapse; the start of control time period, just before and 20 minutes after BDNF addition. We measured DsRed2 intensity (as a volume marker) in spines but found no spine enlargement 20-minutes after BDNF treatment in MT-targeted spines, as well as the general population of spines (Fig. 3E). We then compared the level of PSD-95 (normalized to the start time point) over time in spines with different dynamic MT profiles. Surprisingly, we found no significant change in PSD-95 level in spines devoid of MTs before or after BDNF addition (Fig. 3F) (-1.5 ± 1.6% before, -1.4 ± 2.0% after, n=68 spines, 7 neurons), as well as spines that were invaded by MTs before but not after BDNF (Fig. 3G) (-2.0 ± 3.9% before, -6.3 ± 3.2% after, n=12 spines, 7 neurons). However, the level of PSD-95 increased significantly in spines invaded by MTs both before and after BDNF (Fig. 3H) (-0.3 ± 1.3% before, 11.5 ± 3.2% after, n=31 spines, 7 neurons). Interestingly, PSD-95 exhibited the most robust increase in spines invaded by MTs only after BDNF treatment (Fig. 3I) (1.9 ± 2.8% before, 21.6 ± 3.7% after, n=19 spines, 7 neurons). The increase in PSD-95 in this particular group of spines (Fig. 3I) was significantly higher than in all of the other three groups (Fig. 3G-I) (Two-way ANOVA with Bonferroni post-tests, $p<0.01$). No significant change in PSD-95 was detected during the control time period among all four groups of spines (Two-way ANOVA with Bonferroni post-tests, $p>0.05$). Together these data indicate that MT entries that occur after BDNF application correlate with the accumulation of PSD-95. To further test if the likelihood of MT invasion in a spine scales with the percentage change in PSD-95, we plotted the data for each of the different MT invasion scenarios mentioned above (Fig. 3F-I) and discovered that only when MT entry occurred after

BDNF application (Fig. 3J, red line) did the likelihood of a MT in a spine increase linearly with the change in PSD-95. Thus, we conclude that when BDNF causes MTs to polymerize into previously unoccupied spines, the probability of finding MTs in these spines positively correlates with an increase in PSD-95, and that over time these spines exhibit the most robust increase in PSD-95 in the spine head.

To determine if MT dynamics and invasion into spines were necessary for regulating the level of PSD-95 we used nocodazole or taxol to block MT invasions of spines and acquired time-lapse images to monitor the level of PSD-95 and MT dynamics. We discovered that inclusion of either nocodazole (100nM) or taxol (10nM) greatly diminished MT invasions after BDNF (Fig. 4A-D); only a few brief entries of MTs occurred in some spines (Fig. 4E). These drug treatments abolished the BDNF-induced increase in PSD-95 (Fig. 4F). The percent change of PSD-95 after 20 minutes in BDNF + taxol or BDNF + nocodazole was -1.5 ± 2.1% (n= 31 spines, 3 neurons) and -1.3 ± 3.4% (n= 17 spines, 3 neurons), respectively. Moreover, treatment with taxol or nocodazole alone did not result in a significant change in PSD-95 (0.6 ± 5.7% (n= 13 spines, 3 neurons), -5.4 ± 2.8% (n= 13 spines, 3 neurons), respectively). These data show that MT dynamics are necessary for the accumulation of PSD-95 in spines following BDNF treatment and suggest that MT invasion of spines plays an important role in this process. Nevertheless, the exact contributions of dendritic MT dynamics versus MT entries into spines will require the localized disruption of dynamic MTs only in the postsynaptic spine.

DISCUSSION

In this study we discovered that BDNF rapidly increased the dwell time of MTs in dendritic spines, that MT invasions were temporally and spatially associated with increases in the level of PSD-95 in mature spines, and that MT dynamics are required for BDNF-induced PSD-95 accumulation in dendritic spines. These results provide the first direct evidence that dynamic MT entries correlate with changes in the post-synaptic molecular composition during BDNF-induced synaptic plasticity. Previous studies have established that MTs remain dynamic in spines throughout the lifetime of neurons (up to 63DIV) (Hu et al., 2008). Therefore, it is reasonable to speculate that MT invasions of spines play an important role throughout the life hippocampal neurons by dynamically regulating levels of PSD-95 in spine heads in response to increases in BDNF.

Long-term BDNF stimulation (24hrs) increases spine density in hippocampal slices and dissociated cultures (Tyler and Pozzo-Miller, 2001; Gu et al., 2008; Ji et al., 2010), and induces more spines with larger spine heads in mature neurons (Ji et al., 2010). Furthermore, short-term BDNF treatment facilitates LTP induction when paired with electrical stimulation (Kovalchuk et al., 2002; Rex et al., 2007). In this study we focused on the short-term effects of BDNF treatment. We did not observe significant changes in spine density, shape or volume within 20 minutes of BDNF application. However, MT invasions into spines increased within 5 minutes of BDNF treatment, indicating that changes in MT dynamics precede longer-term structural changes of these spines (Yoshii and Constantine-Paton, 2007). The effects of BDNF on LTP maintenance and stabilization of spine growth depends on TrkB activation (Kovalchuk et al., 2002; Rex et al., 2007; Tanaka et al., 2008). We discovered that pre-incubation of cultures with the tyrosine-kinase inhibitor K252a not only eliminated the elevation of MT invasions following

BDNF application, but also significantly reduced baseline MT entries into spines. These results suggest that activation of the BDNF-TrkB signaling pathway regulates MT dynamics both under basal conditions and after application of exogenous BDNF.

Apart from its effects on structural spine plasticity, BDNF has also been shown to directly increase the size and average fluorescence intensity of PSD-95 puncta in spines within 60 minutes (Yoshii and Constantine-Paton, 2007). Time-lapse imaging studies have revealed that although a subpopulation of PSD-95 puncta are stable in spines for days, individual PSD-95 clusters appear and disappear from spines on the order of minutes to hours (Marrs et al., 2001; Gray et al., 2006; Tsuriel et al., 2006), indicating that these molecules remain dynamic in mature neurons. Using two-photon uncaging in the developing neocortex, median retention time of PSD-95 in spines was discovered to increase from ~22 minutes to ~100 minutes from post-natal day 10 to day 70 mice (Gray et al., 2006). It was proposed that the mobility of PSD-95 was due to diffusion and primarily regulated by PSD-95-interacting proteins in the spine head, such as CaMKII and Shank. Here we provide a novel mechanism whereby MT invasions regulate PSD-95 in the spine head. We discovered that spines invaded by MTs only after BDNF treatment showed a robust increase in PSD-95 within 20 minutes. When a polymerizing MT enters a spine during an activated BDNF signaling cascade, it is possible that it causes either an increased capture of diffusive PSD-95 or prolonged retention of PSD-95, ultimately leading to accumulation of PSD-95 in the spine head.

Another intriguing possibility is that PSD-95 molecules are directly associated with the plus tip protein EB3 during polymerization (Sweet et al., 2011). This could result in a polymerizing MT "delivering" more PSD-95 into spine heads during MT invasions, without PSD-95 appearing as a distinct punctum. If this was the case, PSD-95 should appear

concentrated, to some degree, at the tips of polymerizing MTs. We did not observe this in any of our studies and therefore favor a model in which MTs are delivering other, unknown cargo that cause PSD-95 to be captured or retained in the spine head. A recent study has identified a mechanism for PSD-95 movement out of spines via binding to neuroligin1, which in turn exits spines through dynein-based transport (Schapitz et al., 2010). Although not demonstrated directly, it is likely that this exit of neurolignin/PSD-95 occurs on MTs. However, whether invading MTs traffic cargo directly into spines remains unclear.

Figure 1. BDNF treatment increases endogenous MT entry into spines.

(A) Tyrosinatedα-tubulin antibody labeled MTs (yellow arrows) are detected in a small percentage of f-actin labeled spines under basal conditions (21-28DIV). (B) After a 20 minute treatment with 50ng/ml BDNF, a significantly higher percentage of spines contain a MT (yellow arrows) at the time of fixation. (C, D) Addition of 100nM nocodazole or 10nM taxol to the BDNF solution inhibits MT invasions (E) Quantification of the treatments (Kruskal-Wallis test with Dunn's post hoc tests – see Methods for significance values). Scale bar in D, 5μm.

Figure 1

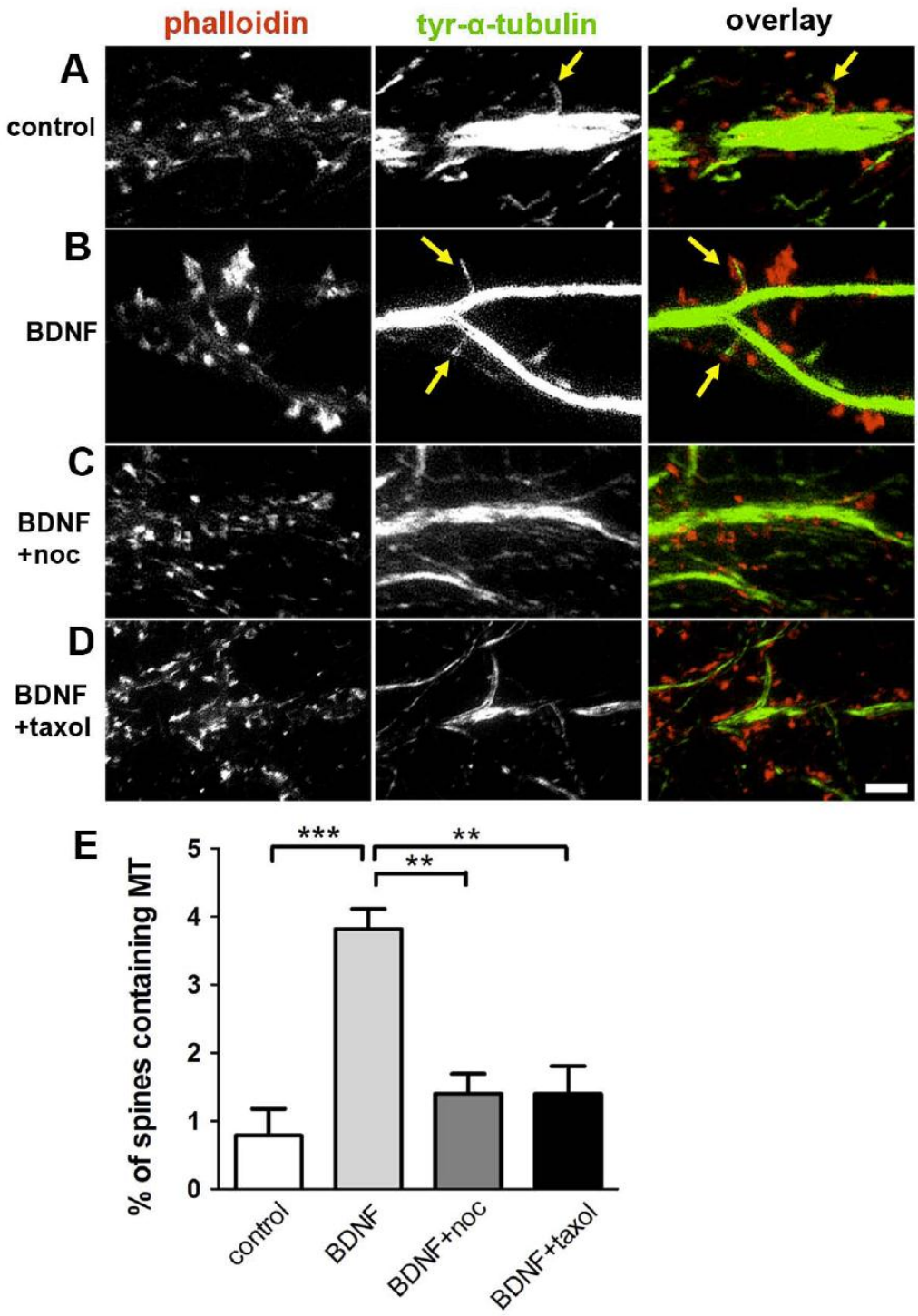
phalloidin
tyr-α-tubulin
overlay
A
control
B
BDNF
C
BDNF
+noc
D
BDNF
+taxol
E
% of spines containing MT
0
1
2
3
4
5
***
**
**
control
BDNF
BDNF+noc
BDNF+taxol

Figure 2. Live-cell TIRFM shows increased MT invasions into spines treated with BDNF .

(A) A segment of dendrite from a 16DIV hippocampal neuron, transfected with mCherry-α-tubulin and GFP-PSD-95, was imaged for 20 minutes before (control) and 20 minutes after addition of BDNF. Maximum projection of tubulin fluorescence depicts spines that were invaded by MTs (yellow arrows) during the time-lapse. Average projection of PSD-95 fluorescence acts as a volume fill. (B) A dendritic segment of a different neuron incubated with the tyrosine kinase inhibitor K252a for 24hrs prior to the experiment. (C) BDNF treatment does not change the percent of spines invaded by MTs, whereas K252a decreases MT invasions (two way ANOVA test with Bonfferoni post-tests). (D) Examples of MT invasions into two dendritic spines. (E) Average MT invasion event length is significantly increased after BDNF treatment, while the frequency of invasions among MT-targeted spines remains the same (F) (Student's t-test). (G) MT dwell time is elevated within 5 minutes of BDNF treatment, and peaks at 10 to 15 minutes (Kruskal-Wallis test with Dunn's post hoc tests). Scale bar in A an B, 2μm.

Figure 2

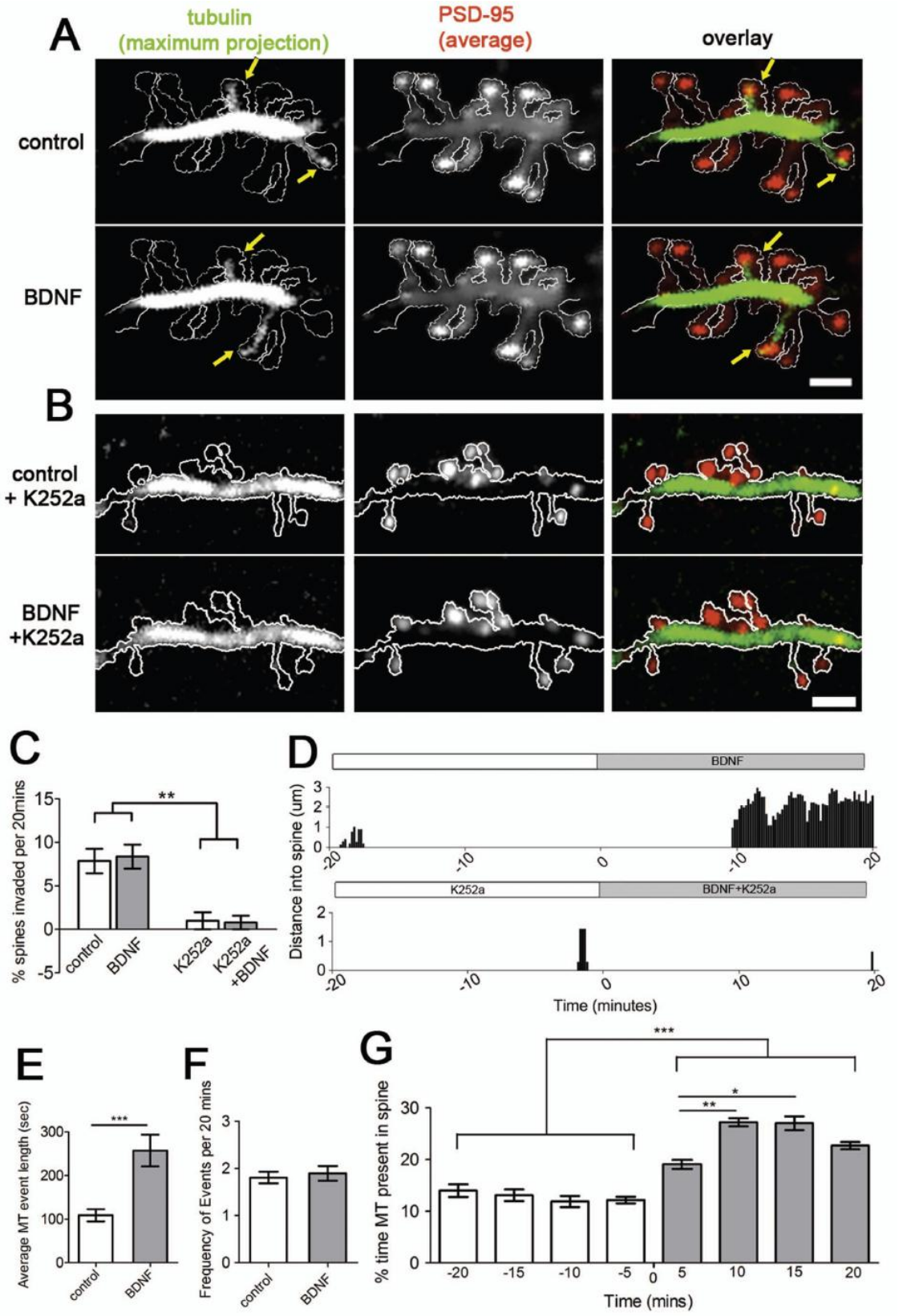
A
tubulin
(maximum projection)
PSD-95
(average)
overlay
control
BDNF
B
control
+ K252a
BDNF
+K252a
C
% spines invaded per 20mins
**
control
BDNF
K252a
K252a
+BDNF
D
BDNF
K252a
BDNF+K252a
Distance into spine (um)
Time (minutes)
E
Average MT event length (sec)
***
control
BDNF
F
Frequency of Events per 20 mins
control
BDNF
G
***
*
**
% time MT present in spine
Time (mins)

Figure 3. MT invasion of spines is correlated with BDNF-induced increase of PSD-95.

(A) An example of two hippocampal dendritic spines transfected with GFP-PSD-95 and mCherry-α-tubulin. The spine on the right is shown in a series of time-lapse images during MT entries; these time points correspond to purple arrows in A'. (A') A kymograph of the PSD-95 punctum in the spine shown in A. (B, C) Two other examples of MT-invaded spines after BDNF treatment. (D) A section of dendrite from a neuron transfected as in A. (D') A series of images showing transport of a PSD-95 punctum (purple arrowheads in top row) into a spine head. (E) Spines show no enlargement 20 minutes after BDNF treatment. (F, G) No significant change in PSD-95 level was detected at 20 minutes after BDNF treatment in spines devoid of MTs, or spines invaded by MTs only during the control time period. PSD-95 levels increased significantly both in spines that had MT entry before and after BDNF (H) and only after BDNF(I) (Student's t-test). Numbers in black boxes (F-I) show the average value of each data set. Symbol colors in F, G and H correspond to line colors in J. (J) Percent change in PSD-95 positively correlates with the percent chance of a MT being present in a spine only in spines that experience post-BDNF MT invasions. (Nonparametric correlation Spearman $R=0.6845$, $p<0.01$). Scale bars: A, 2μm, D and D', 1μm.

Figure 3

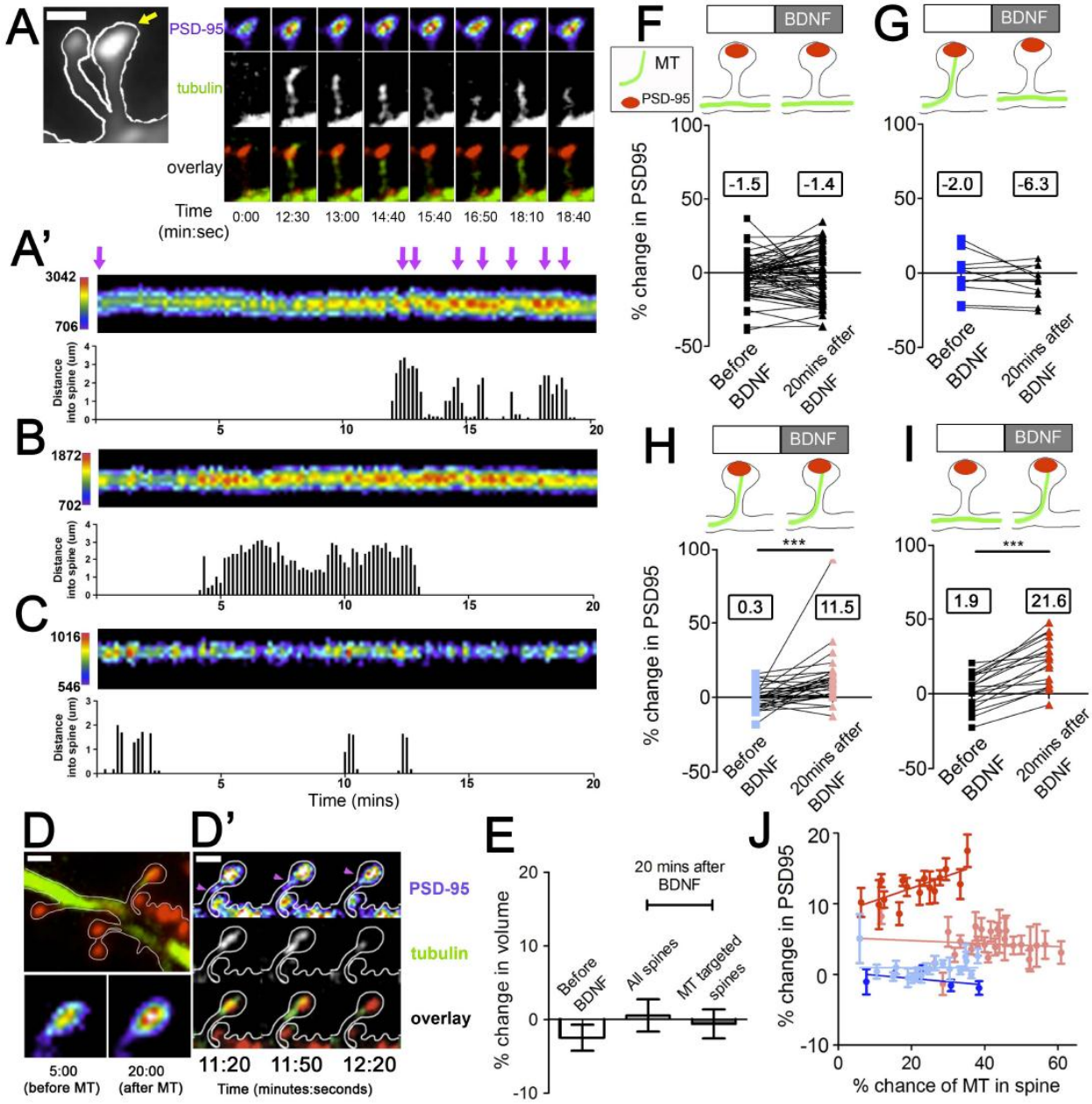
A
PSD-95
tubulin
overlay
Time (min:sec)
0:00
12:30
13:00
14:40
15:40
16:50
18:10
18:40
A'
B
C
Distance into spine (um)
Time (mins)
D
D'
PSD-95
tubulin
overlay
5:00 (before MT)
20:00 (after MT)
11:20
11:50
12:20
Time (minutes:seconds)
E
% change in volume
20 mins after BDNF
Before BDNF
All spines
MT targeted spines
F
G
H
I
BDNF
MT
PSD-95
% change in PSD95
-1.5
-1.4
-2.0
-6.3
0.3
11.5
1.9
21.6
***
Before BDNF
20mins after BDNF
J
% change in PSD95
% chance of MT in spine

Figure 4. BDNF-induced increase in PSD-95 is abolished by inhibition of MT dynamics.

(A-D) Images of maximum projection of tubulin and average projection of PSD-95 from time-lapse images, with overlays, before and after BDNF and MT drug treatments. By dampening MT dynamics MT polymerization into spines (yellow arrows) was almost completely blocked. (E) Examples of traces of MT invasions within individual spines. (F) Quantification shows no change of PSD-95 level when nocodazole or taxol were included with or without BDNF (Kruskal-Wallis test with Dunn's post hoc tests). Scale bar in A, 2μm.

Figure 4

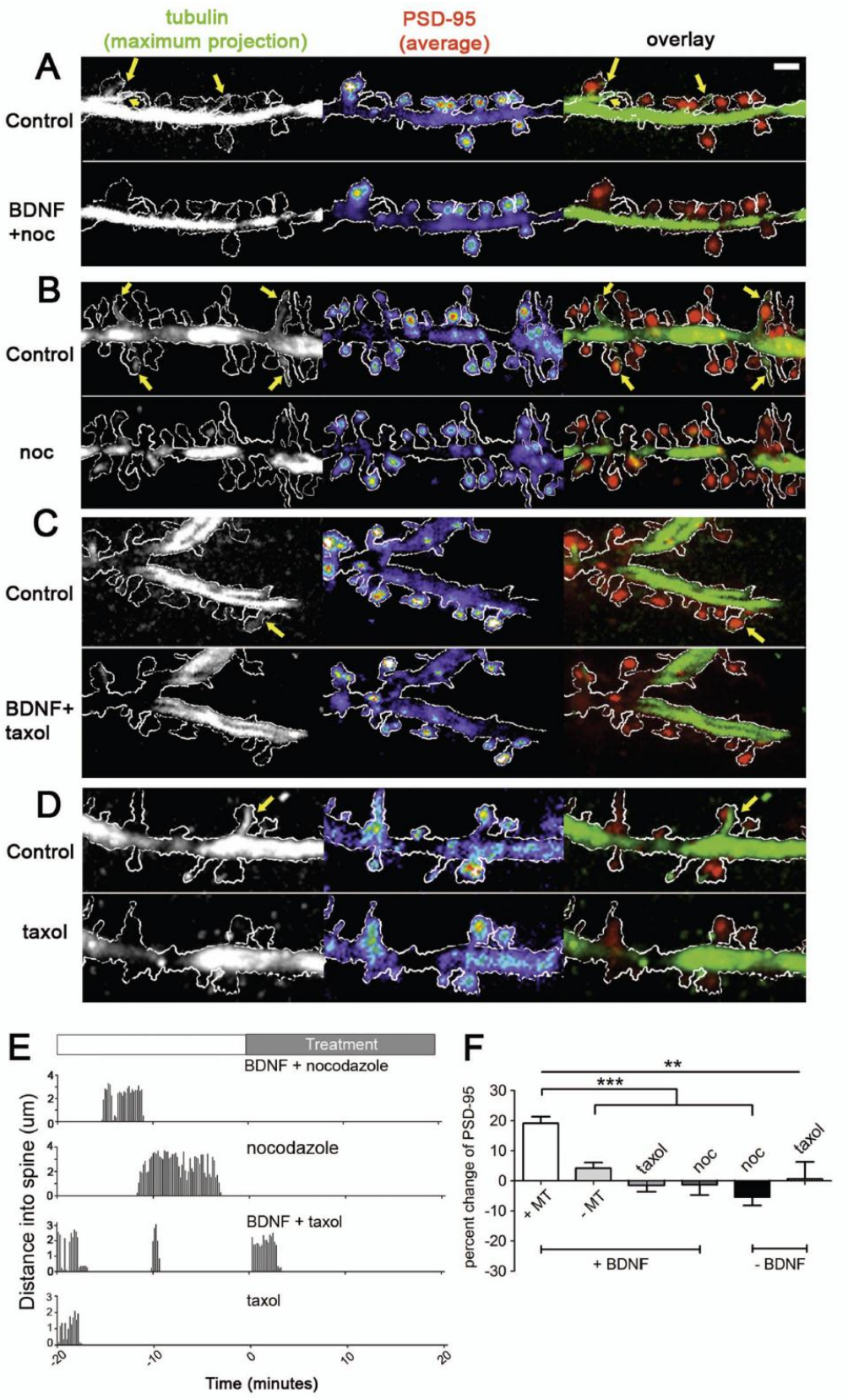
tubulin
(maximum projection)
PSD-95
(average)
overlay
A
Control
BDNF
+noc
B
Control
noc
C
Control
BDNF+
taxol
D
Control
taxol
E
Treatment
BDNF + nocodazole
nocodazole
BDNF + taxol
taxol
Distance into spine (um)
Time (minutes)
F
percent change of PSD-95
+ MT
- MT
taxol
noc
noc
taxol
+ BDNF
- BDNF
**
***

REFERENCES

Dent EW, Kalil K (2001) Axon branching requires interactions between dynamic microtubules and actin filaments. J Neurosci 21:9757-9769.

Dent EW, Kwiatkowski AV, Mebane LM, Philippar U, Barzik M, Rubinson DA, Gupton S, Van Veen JE, Furman C, Zhang J, Alberts AS, Mori S, Gertler FB (2007) Filopodia are required for cortical neurite initiation. Nat Cell Biol 9:1347-1359.

Ehrlich I, Klein M, Rumpel S, Malinow R (2007) PSD-95 is required for activity-driven synapse stabilization. Proc Natl Acad Sci U S A 104:4176-4181.

El-Husseini AE, Schnell E, Chetkovich DM, Nicoll RA, Bredt DS (2000) PSD-95 involvement in maturation of excitatory synapses. Science 290:1364-1368.

Gray NW, Weimer RM, Bureau I, Svoboda K (2006) Rapid redistribution of synaptic PSD-95 in the neocortex in vivo. PLoS Biol 4:e370.

Gu J, Firestein BL, Zheng JQ (2008) Microtubules in dendritic spine development. J Neurosci 28:12120-12124.

Hu X, Viesselmann C, Nam S, Merriam E, Dent EW (2008) Activity-dependent dynamic microtubule invasion of dendritic spines. J Neurosci 28:13094-13105.

Jaworski J, Kapitein LC, Gouveia SM, Dortland BR, Wulf PS, Grigoriev I, Camera P, Spangler SA, Di Stefano P, Demmers J, Krugers H, Defilippi P, Akhmanova A, Hoogenraad CC (2009) Dynamic microtubules regulate dendritic spine morphology and synaptic plasticity. Neuron 61:85-100.

Ji Y, Lu Y, Yang F, Shen W, Tang TT, Feng L, Duan S, Lu B (2010) Acute and gradual increases in BDNF concentration elicit distinct signaling and functions in neurons. Nat Neurosci 13:302-309.

Kovalchuk Y, Hanse E, Kafitz KW, Konnerth A (2002) Postsynaptic Induction of BDNF-Mediated Long-Term Potentiation. Science 295:1729-1734.

Marrs GS, Green SH, Dailey ME (2001) Rapid formation and remodeling of postsynaptic densities in developing dendrites. Nat Neurosci 4:1006-1013.

Noritake J, Fukata Y, Iwanaga T, Hosomi N, Tsutsumi R, Matsuda N, Tani H, Iwanari H, Mochizuki Y, Kodama T, Matsuura Y, Bredt DS, Hamakubo T, Fukata M (2009) Mobile DHHC palmitoylating enzyme mediates activity-sensitive synaptic targeting of PSD-95. J Cell Biol 186:147-160.

Rex CS, Lin CY, Kramar EA, Chen LY, Gall CM, Lynch G (2007) Brain-derived neurotrophic factor promotes long-term potentiation-related cytoskeletal changes in adult hippocampus. J Neurosci 27:3017-3029.

Schapitz IU, Behrend B, Pechmann Y, Lappe-Siefke C, Kneussel SJ, Wallace KE, Stempel AV, Buck F, Grant SG, Schweizer M, Schmitz D, Schwarz JR, Holzbaur EL, Kneussel M (2010) Neuroligin 1 is dynamically exchanged at postsynaptic sites. J Neurosci 30:12733-12744.

Sweet ES, Previtera ML, Fernandez JR, Charych EI, Tseng CY, Kwon M, Starovoytov V, Zheng JQ, Firestein BL (2011) PSD-95 alters microtubule dynamics via an association with EB3. J Neurosci 31:1038-1047.

Tanaka J, Horiike Y, Matsuzaki M, Miyazaki T, Ellis-Davies GC, Kasai H (2008) Protein synthesis and neurotrophin-dependent structural plasticity of single dendritic spines. Science 319:1683-1687.

Tsuriel S, Geva R, Zamorano P, Dresbach T, Boeckers T, Gundelfinger ED, Garner CC, Ziv NE (2006) Local sharing as a predominant determinant of synaptic matrix molecular dynamics. PLoS Biol 4:e271.

Tyler WJ, Pozzo-Miller LD (2001) BDNF enhances quantal neurotransmitter release and increases the number of docked vesicles at the active zones of hippocampal excitatory synapses. J Neurosci 21:4249-4258.

Viesselmann C, Ballweg J, Lumbard D, Dent EW (2011) Nucleofection and primary culture of embryonic mouse hippocampal and cortical neurons. J Vis Exps 47, http://www.jove.com/details.stp?id=2373 doi: 10.3791/2373.

Yoshii A, Constantine-Paton M (2007) BDNF induces transport of PSD-95 to dendrites through PI3K-AKT signaling after NMDA receptor activation. Nat Neurosci 10:702-711.

Chapter 4

Microtubule Invasions in Dendritic Spines Provide a Direct Route of Transport for Synaptotagmin-IV

ABSTRACT:

In the previous chapters, I have demonstrated that dendritic MTs are capable of rapidly entering and exiting dendritic spines through dynamic polymerization and depolymerization. MT invasions are increased by neuronal activity induced by KCl and BDNF treatment. Furthermore, MT entries are required for BDNF-induced PSD-95 accumulation in the spines. Since MTs function primarily as an intracellular transport system we hypothesized that MT entries into spines can provide a direct route of transport for postsynaptic cargoes. I screened a number of candidate dendritic and postsynaptic proteins with time-lapse total internal reflectance fluorescence microscopy (TIRFM) to identify potential cargos that are transported on MTs into or out of dendritic spines. I discovered that synaptotagmin-IV (syt-IV), a post-synaptic integral membrane protein involved in regulating vesicle fusion, is a cargo delivered directly into dendritic spines via MT-based transport. Multiple syt-IV puncta can enter a spine during one MT invasion. Moreover, syt-IV puncta can be retrieved out of the spines during MT entry, indicating that syt-IV traffics both anterogradely and retrogradely along MTs that have entered spines. Syt-IV movement into or out of the spines is abolished when MT invasions are blocked by low concentrations of the MT stabilizing drug taxol. However, transport of Syt-IV continues in the dendritic shafts, indicating transport per se is not compromised by inhibiting MT dynamic instability. I further investigated the possibility that syt-IV transport is mediated by a MT-based motor protein. A dendrite specific kinesin-2 protein, KIF17, co-localizes dynamically with syt-IV puncta trafficking in dendrites. Together these data suggest that MT invasions into dendritic spines can serve as a direct route for the transport of syt-IV into and out of spines and the anterograde transport may be accomplished through KIF17.

INTRODUCTION

The synaptotagmin family of proteins are localized to intracellular vesicles and are important members of the fusion complex during exocytic events (Chapman, 2008). Among these proteins, the synaptotagmin-IV (syt-IV) isoform has raised considerable interest. Syt-IV has been identified as an immediate early gene that is down-regulated during development in most brain regions (Vician et al., 1995). The syt-IV gene maps to the region of human chromosome 18, which is associated with developmental neural disorders such as schizophrenia (Ferguson et al., 2001). Syt-IV gene re-expression can be induced primarily in the hippocampus and piriform cortex by a form of neuronal activity that can induce seizures (Vician et al., 1995, Tocco et al., 1996). The syt-IV knockout mice exhibit memory defects during contextual fear conditioning and motor balance behavior tests, indicating that endogenous expression of syt-IV in the hippocampus and cerebellum is important for functional memory and coordinated motor behavior, respectively (Ferguson et al., 2000).

The majority of synaptotagmin proteins have been identified as Ca2+ sensors that are involved in the triggering of vesicle fusion and release. Syt-IV, on the other hand, has not been shown to be capable of direct binding to Ca2+ (Want et al., 2003). Moreover, syt-IV can inhibit syt-I mediated vesicle fusion events triggered by Ca2+ in PC12 cells (Bhalla et al., 2008). Several recent studies have shed light on the cellular functions of syt-IV in hippocampal neurons. Syt-IV has been shown to localize to both pre and postsynaptic sites in developing hippocampal neurons (Dean et al., 2009). Interestingly, syt-IV can localize to the same dense-core vesicles that contain BDNF, and was shown to affect LTP by negatively regulating BDNF release (Dean et al., 2009). Induction of neuronal activity can increase expression of syt-IV in the cell body and the trafficking of syt-IV-containing vesicles to synaptic sites (Dean et al., 2012). Moreover,

syt-IV is not exchanged between dendrites and axons (Dean et al., 2012), indicating that there are specific molecular mechanisms that regulate targeting of syt-IV to pre and postsynaptic regions. One possibility is that specific MT-based motor proteins are responsible for trafficking syt-IV-containing vesicles pre and postsynaptically.

In this chapter, I used fluorescent imaging methods to examine the mobility and trafficking dynamics of syt-IV concomitantly with MT dynamics in live hippocampal neuronal dendrites and spines. Time-lapse fluorescent images acquired at high frequency revealed that syt-IV puncta travel within the dendritic shaft at a velocity that is in consistent with motor-based trafficking on MTs. Interestingly, a small subset of syt-IV puncta can move rapidly into dendritic spines following a polymerizing MT track. MT invasions were also observed to be correlated with retrieval of pre-existing syt-IV puncta from spines into the dendritic shaft. These results strongly suggest that dynamic MT invasions into spines could serve as a direct route of transport for syt-IV-containing vesicles to and from the postsynaptic site. However, the exact molecular mechanism of this process remains to be determined.

Two major MT-based motors include cytoplasmic dynein and the kinesin superfamily of proteins (Hirokawa et al., 2010). Kinesins travel anterogradely, toward the plus-end (polymerizing end) of MTs, while cytoplasmic dynein moves retrogradely, toward the minus end (stable end). Since MTs polymerize directly into spines we focused on the kinesin superfamily. Several members of the kinesin superfamily have been identified as key motors for intracellular transport of a variety of cargos and their specific localization and function have been the focus of many studies. Of these members, a kinesin-3 isoform KIF1A has been shown to transport synaptic vesicle precursors in axons (Okada et al., 1995). Interestingly, a recent co-immunoprecipitation study revealed that syt-IV can bind directly to KIF1A (Arthur et al., 2010),

indicating that KIF1A could be the motor protein responsible for anterograde transport of syt-IV from the cell body to the axonal terminal. However, since KIF1A is specifically localized to axons (Hirokawa et al., 2010), it is likely that transport of dendritic syt-IV-containing vesicles require other kinesins.

KIF17, a kinesin-2 family member, functions exclusively in neuronal dendrites (Hirokawa et al., 2010). Recent studies have identified the NMDA receptor subunit NR2B as an important cargo that can be transported via KIF17 (Setou et al., 2000). It is believed that KIF17 recognizes NR2B containing vesicles through Mint1 (Lin10) as part of an adaptor protein complex (Jeyifous et al., 2009). Upon reaching its destination, CaMKII mediated phosphorylation of KIF17 triggers unloading of NR2B (Guillaud et al., 2008), which is subsequently trafficked to the postsynaptic site. I hypothesize that KIF17 is functioning as the molecular motor that mediates syt-IV vesicle transport in the dendritic compartment. Using live-cell imaging of fluorescently tagged syt-IV and the full-length KIF17 protein, I discovered that mobile syt-IV puncta co-localized with KIF17 puncta in the dendrites of developing neurons, suggesting that KIF17 could directly regulate fast transport of syt-IV. Moreover, the stable subset of syt-IV puncta did not co-localize with KIF17, which further supports the idea that KIF17 could recognize specific syt-IV vesicles and mediate their transport to the synaptic destinations.

METHODS:

Plasmids and reagents

mCherry-syt-IV in an N1 vector was a generous gift from Camin Dean and Ed Chapman (UW-Madison). EGFP-α-tubulin and EGFP-EB3 in pCAX vectors were previously described (Hu et al., 2008). mCerulean in a C1 vector was purchased from Clontech. KIF17FL-3XmCitrine was generous gift from Kristin Verhey. Nocodazole and Taxol were from Sigma-Aldrich.

Cell Culture and Transfection

Mouse dissociated hippocampal cultures were prepared as previously described (Viesselmann et al., 2011). For live-cell imaging of syt-IV and MT dynamics, neurons were transfected with an Amaxa electroporator before plating. mCerulean was also included in the transfection mixture to provide a fill for the dendritic shafts and spines. For imaging of KIF17 movements, neurons were electroporated with mCherry-Syt-IV and plated at high densities (20k/cm^2) without glial feeders. At 9-10DIV, neurons were transfected with KIF17FL using lipofectamine 2000 (Invitrogen) and double-labeled neurons were imaged 24-48 hours later.

Live-cell TIRF Imaging and Immunocytochemistry

Imaging experiments were performed at physiological temperatures (36-37°C) using a Nikon TE2000E microscope as described previously (Hu et al., 2008). For imaging of KIF17 dynamics, an Andor Evolve EMCCD camera was used to minimize exposure time, while achieving high frequency frame rates. Images were acquired at a resolution of approximately 0.163μm per pixel, with an EM gain of 0-500. After lipofectamine 2000 transfection, only pyramidal neurons expressing both KIF17FL-3XmCitrine and mCherry-syt-IV were selected imaged in both red and green channels in quick succession.

Quantification of syt-IV vesicle dynamics

To visualize the correlation between syt-IV pucta movement and MT dynamics in dendritic spines, kymographs were constructed from mCherry-syt-IV and EGFP-tubulin expressing neurons along the length of spines, to record changes in fluorescence intensity in both red and green channels. Syt-IV puncta trafficking trajectories in the dendritic shaft were identified by constructing a kymograph along the entire length of the dendrite within the field view. Syt-IV trafficking velocities were then calculated by dividing the total distance of travel of each punctum over the duration of the trajectory. Only actively moving syt-IV were included in the trafficking analyses. A pausing syt-IV punctum is defined by a net displacement of the center of the punctum at <0.42μm per frame for at least 2 consecutive frames (6 seconds).

For quantification in Fig.4, the subset of spines that contained immobile syt-IV vesicles were defined as spines that contained a syt-IV punctum at the start of the time-lapse. The same syt-IV punctum persisted throughout the duration of the time-lapse with no dynamic movements within or out of the spine.

Statistics and graphing

All statistical tests were performed with Graph-Pad Prism. In the graph of Fig. 4, p values are depicted as follows: * $p<0.05$, ** $p<0.01$, *** $p<0.001$. Graphs were compiled in Prism.

RESULTS:

MT invasion into dendritic spines can provide a direct route of entry and exit of synaptotagmin-IV

We have demonstrated previously that dynamic MTs are capable of entering and exiting dendritic spines through rapid polymerization and depolymerization (see chapter 2, also see Hu et al., 2008). Since the primary function of MTs is to provide a stable intracellular trafficking railway for a variety of molecular cargoes, we hypothesized that MT invasions into spines can deliver syt-IV containing vesicles directly into the postsynaptic spines. There are two mechanisms by which syt-IV vesicles could be transported on MT tracks: vesicles could be directly associated with MT plus-end complex and traffic into the spine via polymerizing MT plus-ends; another possibility is that MT invasions might create a delivery track that allows syt-IV vesicles to be delivered as cargoes associated with motor complexes. Although MT invasions were observed to be transient with an average event time of ~100 seconds it has been established that the velocity of fast trafficking motors is on the order of 1 μm/sec (Hirokawa et al., 2010), almost 10 times faster than MT plus-end dynamics. Moreover, dendritic spines are micron-sized structures with a longitudinal length typically not exceeding 3-4 microns. Thus, motor-based cargo transport from the base to the tip of spines would take less than five seconds. Therefore, it is entirely plausible that syt-IV vesicles can move into the spine on polymerizing MTs mediated by processive motors.

To test the hypothesis and examine the mechanism by which syt-IV puncta are trafficked in dendrites, I expressed fluorescently mCherry-syt-IV, EGFP-tubulin and mCerulean constructs in mouse hippocampal neurons to visualize the dynamics of presumptive syt-IV labeled vesicles (syt-IV puncta), MTs and the shape of the dendrites/spines, respectively. Neuronal dendrites

were imaged between three to four weeks in culture (21-29 DIV). Dual color time-lapse images were acquired at frequent intervals (3 seconds per frame) in order to capture fast syt-IV puncta movement in dendritic shafts and spines (Fig. 1A). MT dynamics were recorded every 3 or 9 seconds concomitantly with syt-IV to determine the correlation between the two. To determine the morphology of the neurons and dendritic spines, mCerulean was co-expressed as a volume marker and wide-field epifluorescence images of mCerulean were acquired at the beginning and the end of the time-lapse (Fig. 1A). I found that syt-IV puncta rapidly traveled in the dendrites both anterogradely and retrogradely. Interestingly, a small subset of syt-IV puncta can enter spines from the dendritic shaft (Fig. 1B). Moreover, syt-IV puncta movement into the spine often coincided with an MT invasion into the spine (Fig. 1B). In this instance a MT polymerized into the dendritic spine and a syt-IV labeled punctum then traveled toward the plus-end along the MT track (Fig. 1C, blue arrowheads). As the MT depolymerized out of the spine, the syt-IV containing puncta leave the spine (Fig. 1C, yellow arrowheads) or persist in the spine head (Fig.1C, magenta arrowheads), suggesting that syt-IV vesicles may be unloaded from the MT track upon reaching the spine head. Furthermore, these results support the notion that syt-IV puncta movement is mediated by motor-based transport rather than the MT plus-end complex. This is further corroborated by time-lapse images of the MT end binding protein EB3 and syt-IV, showing lack of colocalization of the two (data not shown).

Motor-based cargo transport depends on the polarity of specific motor proteins (Hirokawa et al., 2010). Since MTs are arranged with mixed polarity in neuronal dendrites, kinesin mediated anterograde transport can be observed in both directions. The bidirectional syt-IV puncta movement could be explained by the mixed polarity of MTs within dendrites, as well as the combination of kinesin (+ end driven) and dynein (- end driven) mediated transport. Dynein

has been shown to directly regulate retrieval of neuroligin and PSD-95 out of the spine, presumably on MT tracks present in the spine at that time (Schapitz et al., 2010). Here I also examined the retrieval of syt-IV vesicles from the spine. Time-lapse images of spines revealed that in 2 out of 3 of the cases where syt-IV puncta moved out of the spine, the event coincided with an MT invasion (Fig. 2). The syt-IV puncta could be a pre-existing vesicle in the spine head from the start of the time-lapse (Fig. 2B), or a vesicle that traveled into the spine during previous MT invasions (Fig. 1B-C). In the case of a pre-existing syt-IV vesicle, the punctum rapidly traveled along the MT track out of the spine upon MT entry, and moved retrogradely along the dendritic shaft, possibly on the same MT track (Fig. 2B-C). These results strongly support the hypothesis that MT invasions could provide a physical route of transport for fast delivery of synaptic cargos into and out of the spine. It is very likely that both kinesin and dynein are involved in the trafficking of syt-IV vesicles in the spine because we know that only plus (growing) ends of MTs enter spines and therefore transport into spines must be kinesin-driven while transport out is dynein driven (or through the one minus end directed kinesin, KIF2C) (Hirokawa et al., 2010).

Since the physical presence of MT is required for motor-based transport, it is plausible to argue that prolonged MT invasion could transport more synaptic cargo into or out of the spine. In several cases I observed that a prolonged MT invasion delivered multiple syt-IV puncta into the spine head (Fig. 3). Fluorescent time-lapse images of syt-IV puncta indicate that the second punctum entering the spine moved along the MT track toward the same sub domain in the spine head where the MT is located (Fig. 3B-C). The first syt-IV punctum remained near the postsynaptic membrane throughout the duration of the time-lapse, whereas the subsequent puncta joined their predecessors and formed one larger pool of syt-IV puncta (Fig. 3C). Taken together,

these results indicate that dynamic MTs can serve as a direct route of transport for syt-IV both into and out of the spines, possibly mediated by MT-based motor proteins kinesin and dynein, respectively. Moreover, prolonged MT invasions could correlate with repeated delivery of syt-IV containing vesicles to the same postsynaptic region, where they may subsequently fuse with the membrane.

MT invasions are responsible for the majority of syt-IV trafficking in the spine

To investigate whether MT-based transport is required for the delivery of syt-IV puncta into and out of spines, I measured the rate of transport of syt-IV labeled vesicles in the dendritic shaft as well as in dendritic spines (Table 1). Quantification showed that both anterograde and retrograde transport velocity of syt-IV puncta corresponded to the rate of movement of MT-motor based transport. Transport velocity in spines is slower than in dendritic shaft, possibly due to number of reasons. First, the intracellular space is much smaller in the spine neck compared to the dendritic shaft (Bourne and Harris, 2008), and this could result in reduced processivity of motors. Second, we have shown previously that dynamic, tyrosinated, MTs enter spines (Hu et al., 2008), but both tyrosinated and acetylated (a posttranslational modification associated with MT stability) MTs are present in dendritic shafts (Janke and Kneussel, 2010). Because several motor proteins can "read" the posttranslational state of MTs (Nakata and Hirokawa, 2003; Hammond et al., 2010), these different MT substrates could affect processivity of specific motors (Hammond et al., 2010). Therefore, the slower transport rates in spines may be due to travel along the more dynamic, tyrosinated MTs whereas the transport in the dendrite shaft may predominantly occur on acetylated MTs. Third, the imaging paradigm I used may not have captured the nuisances of puncta dynamic in spines. Given the short average length of spines

(<4 μms) and the fast nature of motor-based transport (~1μm/sec), the 3 seconds per frame imaging frequency may have missed rapid vesicle movement from the base to the tip of spine head. Interestingly, with the addition of MT stabilizing drug taxol (10nM), both MT invasion and syt-IV puncta movement into the spine were completely abolished, indicating that MT invasions are necessary for delivery of syt-IV containing vesicles into and out of the spine. Interestingly, this also slowed, but did not abolish, transport of syt-IV puncta in the dendritic shafts, suggesting that dynamic MT ends are important for efficient transport of syt-IV within dendrites.

However, I documented a few cases where a syt-IV punctum appeared in the spine without an accompanying MT entry (0.5±0.29% of all spines). There are several possible explanations to this observation. The syt-IV punctum might have resulted from endocytosis at the postsynaptic site or our imaging interval of 9 seconds for the tubulin channel, may have missed the more transient MT invasions. Another possibility is that syt-IV puncta movement may also be mediated by other means of transport, such as myosin-based transport along actin filaments.

At basal activity levels, 10.33±1.2% of spines were targeted by MTs, consistent with our previous findings (Hu et al., 2008; 2011). Of the MT-targeted spines, syt-IV containing vesicle entry or exit happened in about half of these spines (5.51±0.99% of all spines), along a polymerized MT track in the spine. In a small fraction of spines that did not contain a MT during the time-lapse, a syt-IV punctum was present in the spine head throughout the imaging interval (1.97±0.49% of all spines). When low concentrations of taxol was included this number was not significantly different than controls (2.63±1.38% of all spines contained stable syt-IV puncta; 0.63±0.63% of all spines contained mobile syt-IV puncta), suggesting the MT-independent syt-IV transport into spines remained infrequent.

Syt-IV-containing vesicles and KIF17 traffic together in dendrites

Recent studies have identified KIF17 as the dendritic MT motor protein responsible for trafficking the NMDA receptor subunit NR2B to the dendrite (Guillaud et al., 2008). NR2B-containing vesicles are transported along MTs by KIF17 and the adaptor protein Mint to the base of spine. This group proposed that upon synaptic stimulation, Ca^{2+} influx activates CaMKII, which diffuses out of the spine, into the dendritic shaft and triggers release of NR2B containing vesicles from MTs by phosphorylation of the adapter protein (Guillaud et al., 2008). In the last part of this chapter, I began exploring the possibility that KIF17 may mediate syt-IV trafficking into dendritic spines.

To study this possibility, I imaged developing dendrites expressing mCherry-syt-IV and KIF17fl-3XmCit, a full-length KIF17 protein labeled with three mCitrine fluorescent proteins to provide a brighter signal to image individual kinesin motors (Cai et al., 2009) (Fig. 4A). Full length kinesins, including KIF17, exist primarily in an auto-inhibited state (Hammond et al., 2010) and are therefore present throughout the cytoplasm. Thus, KIF17 only becomes punctate when actively moving on MTs. Nevertheless, I documented that KIF17 and syt-IV can traffic together in dendrites (Fig. 4B). Interestingly, there was no concentration of KIF17 fluorescence when the syt-IV puncta paused in the dendrite, whereas translocating syt-IV puncta colocalized with rapidly trafficking KIF17 puncta. These results suggest that only the active form of KIF17 can effectively bind to MT tracks and mediate cargo transport, whereas auto-inhibited KIF17 remains diffused in the cytoplasm. Furthermore, they suggest that KIF17 may be the motor that drives syt-IV into dendritic spines.

DISCUSSION:

To conclude, in this chapter I investigated the hypothesis that syt-IV can be trafficked into dendritic spines via dynamic MT invasions. Indeed, I found that syt-IV puncta could travel along MTs into or out of spines, indicating that syt-IV is trafficked both anterogradely and retrogradely along newly polymerized MTs. Multiple syt-IV puncta can enter a spine during one MT invasion, and Syt-IV puncta movement is abolished when MT invasions are blocked by low concentrations of taxol. Quantification of syt-IV dynamics after taxol treatment revealed that transport of syt-IV continues in the dendritic shafts, indicating transport per se is not compromised by inhibiting MT dynamic instability, but trafficking syt-IV into spines was severely affected. Results from the later half of the chapter also show that the full length version of the dendrite specific kinesin-2 protein KIF17 co-localizes dynamically with syt-IV during trafficking events in developing dendrites. Together these data strongly support the notion that MT invasions into dendritic spines can serve as a direct route for the transport of syt-IV into and out of spines. Furthermore, anterograde transport of syt-IV may be accomplished through KIF17.

Syt-IV trafficking in dendrites has been directly visualized by fluorescent microscopy in previous studies (Dean et al., 2009). It was unclear though, whether syt-IV was localized in dendritic spines in mature neurons. Based on the results in this chapter, syt-IV puncta can indeed be trafficked in and out of dendritic spines, presumably on MT tracks. We also observed colocalization of syt-IV and KIF17 puncta movement in young dendrites. Whether KIF17 is capable of transporting syt-IV directly into spines, however, remains to be tested. Among members of the kinesin superfamily of proteins, KIF5 and KIF17 have been identified as the major MT-based motors for transport in dendrites (Hirokawa et al., 2010). Previous studies have

shown that KIF5 prefers to bind to acetylated tubulin, whereas KIF17 has no preference between stable MTs and newly polymerized MTs that consist mainly of detyrosinated tubulin (Hammond et al., 2010), indicating that KIF17 is more likely to move into spines via dynamic MT invasions. Future experiments aiming at direct visualization of KIF17 puncta in spines concomitantly with MT invasions and/or syt-IV puncta movement could uncover the potential role of KIF17 in transport of postsynaptic cargos in spines.

The dynamic exchange of a variety of postsynaptic molecules have been studied. KIF17 has been demonstrated to transport NMDA receptor subunit NR2B in the dendrites towards the postsynaptic site, where the NR2B containing vesicles is proposed to be released from MT tracks and translocate into spines via diffusion or actin-based transport (Guillaud et al., 2008). Based on our results, it is possible that NR2B can be directly delivered into spines by KIF17 via MT invasions. Similarly, AMPAR trafficking has been shown to be mediated by KIF5/GRIP1 complex on MT tracks in the dendrites (Nakata and Hirokawa, 2003), and AMPAR containing recycling endosomes can be pulled into spines by myosin Vb on f-actin network (Wang et al., 2008). Although dynamics of KIF5 was not studied in this chapter, the possibility exists that KIF5 may mediate direct transport of its cargos into spines as well. Such transport events in the spine may not be exclusively based on f-actin or MT network, but can involve interaction between the two through proteins that bind to both actin and MTs.

The retrograde transport of PSD-95 and neuroligin1 complex has been shown to depend on proper function of dynein (Shapitz et al., 2010). Interestingly, a recent study also identified LIS1 and NDEL as part of the dynein adaptor protein complex involved in retrograde translocation of PSD-95 in cortical interneurons (Kawabata et al., 2012). In the chapter we showed that syt-IV vesicles can be rapidly retrieved from spines via MT invasions. It is highly likely that this

retrograde transport of syt-IV is a dynein-mediated process. It would be interesting to image dynein dynamics with syt-IV and/or MTs to investigate whether dynein is directly involved in this process.

Figure 1. MT invasion coincides with syt-IV puncta movement into dendritic spines. (A) A segment of a 19DIV hippocampal dendrite expressing mCherry-syt-IV, EGFP-α-tubulin and cerulean as a volume marker. The shapes of dendritic protrusions are outlined according to cerulean fluorescence signal in the right panel. (B) Kymographs were constructed by drawing a 3-pixel wide line along the length of the spine outlined by the white box in (A), and measuring the maximum fluorescence intensity within the width of that line. The Kymograph of EGFP-tubulin shows three MT invasion events into the spine (marked by aqua arrowheads). The last two events are accompanied by entry of two different syt-IV puncta into the spine (events outlined by blue lines). Due to slower acquisition frequencies of EGFP-tubulin (9 sec/frame) as compared to mCherry-syt-IV (3 secs/frame), individual lines of the MT kymograph appear wider. (C) Montage of images from individual frames during the time-lapse outlined by the blue line in (B). Syt-IV images are shown every third frame (2 out of every 3 frames are omitted for clarity). Upon entering the spine head along a polymerized MT, the first syt-IV punctum (yellow arrowhead) did not persist in the spine, whereas the second syt-IV punctum (magenta arrowhead) persisted in the spine head throughout the remainder of the time-lapse. Scale bars, 2μm in A and C.

Figure 1

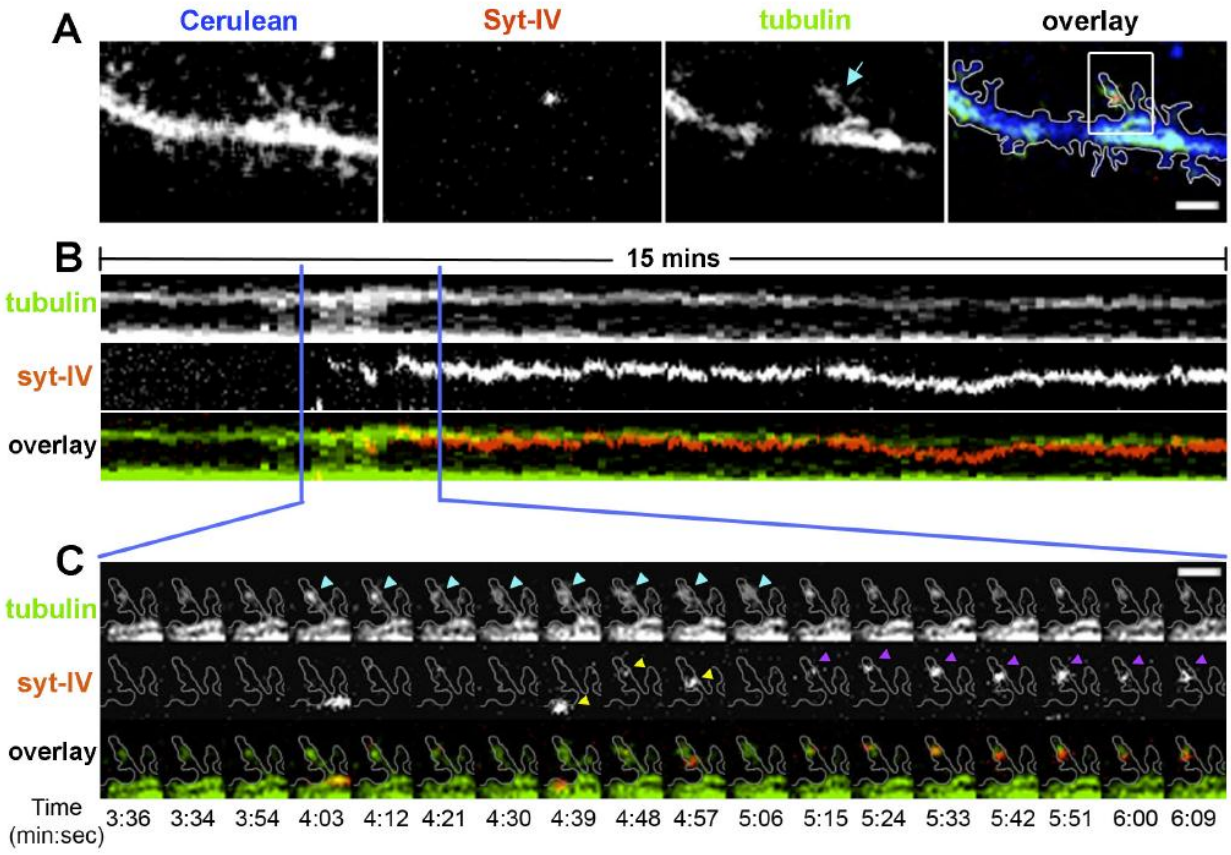
A
Cerulean
Syt-IV
tubulin
overlay
B
15 mins
tubulin
syt-IV
overlay
C
tubulin
syt-IV
overlay
Time
(min:sec)
3:36
3:34
3:54
4:03
4:12
4:21
4:30
4:39
4:48
4:57
5:06
5:15
5:24
5:33
5:42
5:51
6:00
6:09

Figure 2. MT invasion can be associated with removal of pre-existing syt-IV puncta from dendritic spines. (A) A segment of a 19DIV hippocampal dendrite expressing mCherry-syt-IV, EGFP-α-tubulin and mCerulean as a volume marker. The shapes of dendritic protrusions are outlined according to cerulean fluorescence signal in the right panel. (B) Kymographs constructed by measuring the maximum fluorescence intensity within a 2-pixel wide line drawn along the spine outlined in the white box in (A). MT invasions and syt-IV vesicle movement are revealed during the time period between the blue lines. Due to slower acquisition frequencies of EGFP-tubulin (9 sec/frame) as compared to mCherry-syt-IV (3 secs/frame), individual lines of the tubulin kymograph appear wider. (C) Montage of images from individual frames during the time-lapse outlined by the blue line in (B). Tubulin images are repeated three times whereas syt-IV images were acquired every 3 seconds. Upon MT entry into the spine (aqua arrowheads in tubulin montage), the preexisting syt-IV punctum in the spine head was removed from the spine and trafficked down the dendritic shaft retrogradely (yellow arrowheads). Scale bars in A and C, 2μm

Figure 2

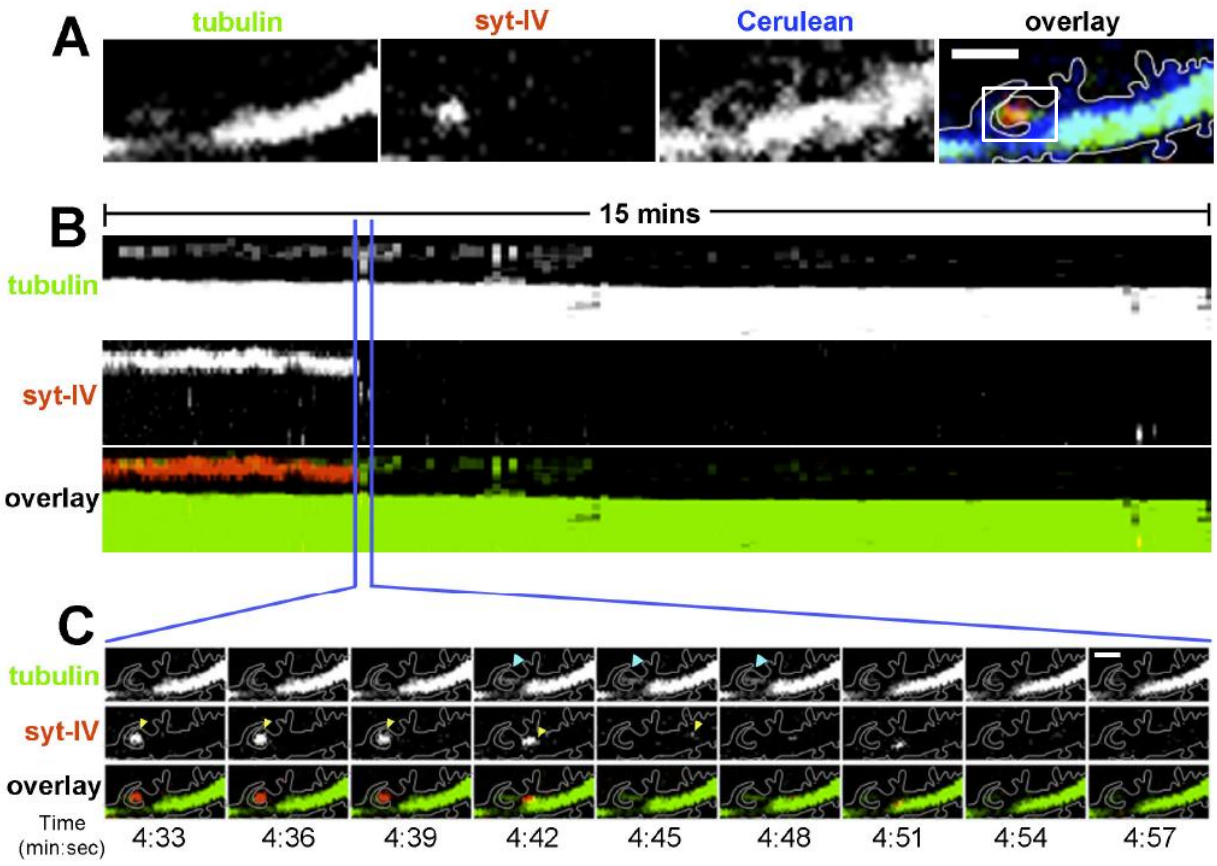
A
tubulin
syt-IV
Cerulean
overlay
B
15 mins
tubulin
syt-IV
overlay
C
tubulin
syt-IV
overlay
Time
(min:sec)
4:33
4:36
4:39
4:42
4:45
4:48
4:51
4:54
4:57

Figure 3. A prolonged MT invasion can deliver multiple syt-IV puncta into a spine. (A) Kymographs constructed by measuring the maximum fluorescence intensity within a 2-pixel wide line along the complex spine shown in (A') from a 25DIV hippocampal neuron. The MT was present in the spine neck throughout the 20-minute time-lapse and extended into the right spine head repeatedly during the later half of the time-lapse (arrows). Upon MT polymerization into the spine head, three individual syt-IV puncta moved into the spine head. (B) A montage depicting the event of the first syt-IV containing vesicle entry into the spine (as outlined by purple lines in A-1). The syt-IV punctum was trafficked along the MT present in the spine neck halfway into the spine, and then traveled along the extending MT (aqua arrowheads) into the previously unoccupied spine head (yellow arrowheads). (C) A montage depicting the event of the next two syt-IV containing vesicles entering the spine (as outlined in purple lines in A-2). Two individual syt-IV puncta (yellow arrowheads and magenta arrowheads) were delivered into the spine head by extending MTs (aqua arrowheads) and joined the pool of syt-IV containing vesicles trafficked into the spine during event 1. Scale bars, 2μm.

Figure 3

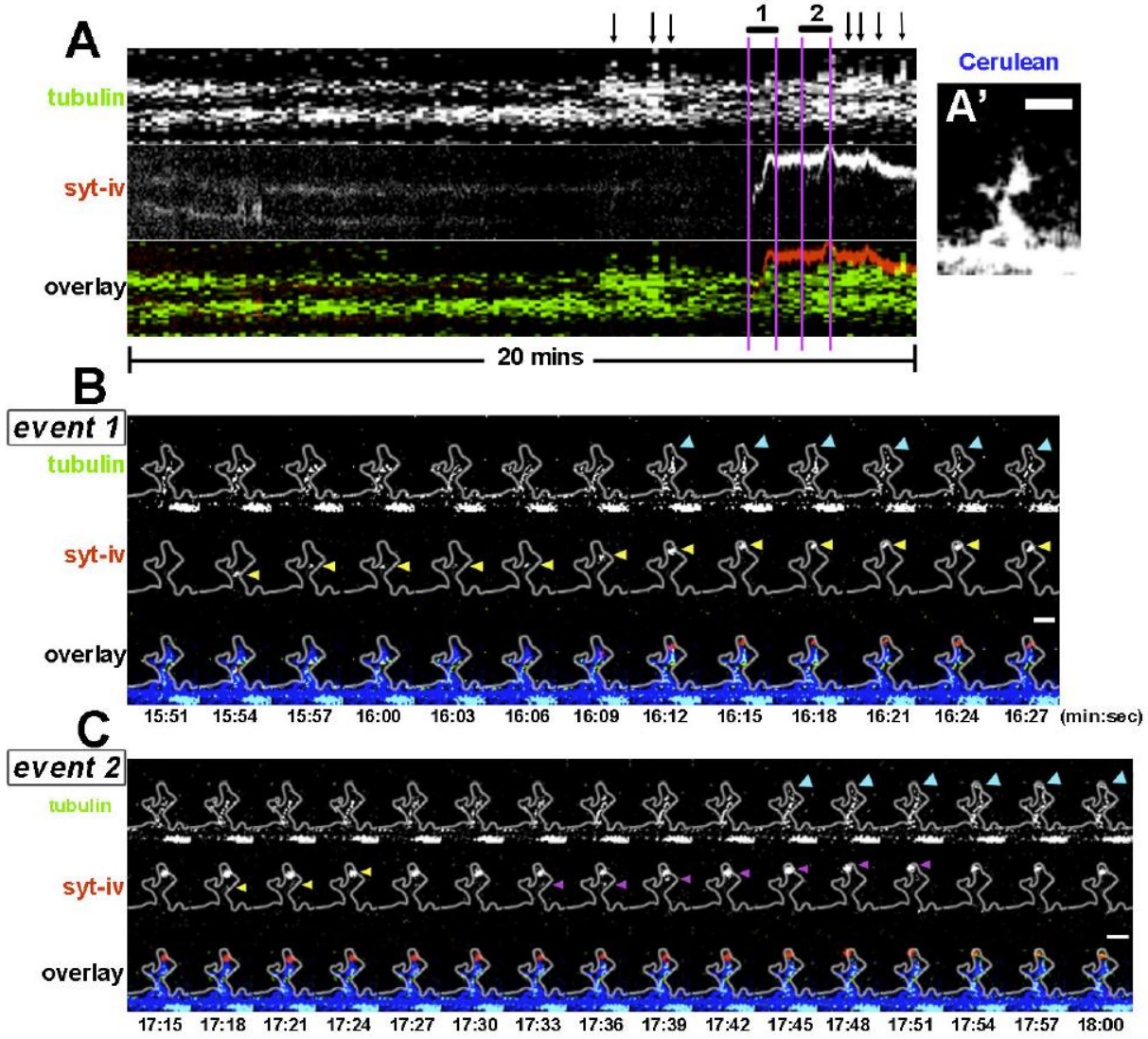
A
tubulin
syt-iv
overlay
1
2
Cerulean
A'
20 mins
B
event 1
tubulin
syt-iv
overlay
15:51 15:54 15:57 16:00 16:03 16:06 16:09 16:12 16:15 16:18 16:21 16:24 16:27 (min:sec)
C
event 2
tubulin
syt-iv
overlay
17:15 17:18 17:21 17:24 17:27 17:30 17:33 17:36 17:39 17:42 17:45 17:48 17:51 17:54 17:57 18:00

Figure 4. Full length KIF17 and syt-IV containing vesicles co-localize during trafficking events in developing dendrites. (A) Maximum projection of a DIV10 hippocampal dendrite expressing syt-IV-mCh and KIF17FL-3XmCitrine (B) Kymographs constructed from the 6-pixel wide line drawn along the dendrite (dashed lines shown in A). Kymographs are rotated 90° counter-clockwise. Note the overlay of trajectories of mobile syt-IV and KIF17FL puncta. Scale bar in A, 5μm; C, 20μm.

Figure 4

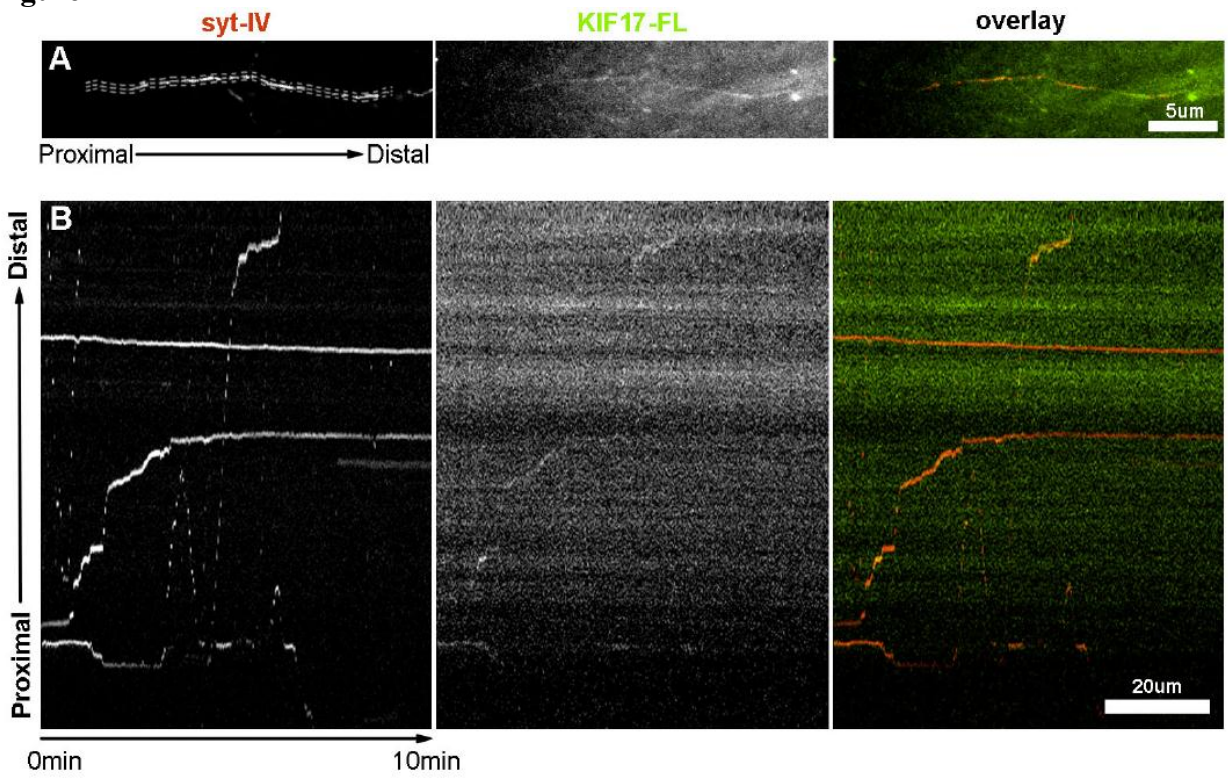
syt-IV
KIF17-FL
overlay
A
5um
Proximal
Distal
B
Distal
Proximal
20um
0min
10min

Table 1. Trafficking velocity of syt-IV containing vesicles in dendritic shafts and spines.

Syt4 trafficking velocity (um/sec)	Control		Taxol (10nM)	
	Anterograde	Retrograde	Anterograde	Retrograde
Dendritic shaft	1.05 ± 0.39 (9)*	1.00 ± .035 (7)	0.64 ± 0.07 (6)	0.57 ± 0.12 (4)
Synaptic (in spine)	0.33 ± 0.02 (8)	0.20 ± 0.05 (2)	NA	NA

*Parenthesis indicate number of puncta analyzed

REFERENCES:

Arthur CP, Dean C, Pagratis M, Chapman ER, Stowell MH. (2010) Loss of synaptotagmin IV results in a reduction in synaptic vesicles and a distortion of the Golgi structure in cultured hippocampal neurons. Neuroscience 167(1):135-42

Bhalla A, Chicka MC, Chapman ER (2008) Analysis of the synaptotagmin family during reconstituted membrane fusion: uncovering a class of inhibitory isoforms. J. Biol Chem 283:21799-21807

Bourne JN, Harris KM (2008) Balancing structure and function at hippocampal dendritic spines. Annu Rev Neurosci. 31:47-67

Cai D, McEwen DP, Martens JR, Meyhofer E, Verhey KJ. (2009) Single molecule imaging reveals differences in microtubule track selection between Kinesin motors. PLoS Biol. 7(10):e1000216

Chapman ER (2008) How does synaptotagmin trigger neurotransmitter release? Annu. Rev. Biochem. 77,615-641

Dean C, Liu H, Dunning FM, Chang PY, Jackson MB, Chapman ER (2009) Synaptotagmin-IV modulates synaptic function and long-term potentiation by regulating BDNF release. Nat Neurosci. 12(6):767-76

Dean C, Liu H, Staudt T, Markus TA, Siv V, Buckers J, Kamin D, Engelhardt J, Jackson M, Hell SW, Chapman ER (2012) Distinct subsets of Syt-IV/BDNF vesicles are sorted to axons versus dendrites and recruited to synapses by activity. J. Neurosci 32(16):5398-5413

Ferguson GD, Anagnostaras SG, Silvia AJ, Herschman HR (2000) Deficits in memory and motor performance in synaptotagmin IV mutant mice. Proc Natl Acad Sci. USA 97:5598-5603

Guillaud L, Wong R, Hirokawa N. Disruption of KIF17-Mint1 interaction by CaMKII-dependent phosphorylation: a molecular model of kinesin-cargo release. (2008) Nat Cell Biol.10(1):19-29

Hammond JW, Huang CF, Kaech S, Jacobson C, Banker G, Verhey KJ, (2010) Posttranslational modification of tubulin and the polarized transport of kinesin-1 in neurons. Mol Biol Cell 21(4): 572-583

Hammond JW, Blasius TL, Soppina V, Cai D, Verhey KJ. Autoinhibition of the kinesin-2 motor KIF17 via dual intramolecular mechanisms. (2010) J Cell Biol. 189(6):1013-25

Hirokawa N, Niwa S, Tanaka Y, (2010) Molecular motors in neurons: transport mechanisms and roles in brain function, development, and disease. Neuron 68(4): 610-38

Hu X, Viesselmann C, Nam S, Merriam E, Dent EW (2008) Activity-dependent dynamic microtubule invasion of dendritic spines. J Neurosci 28:13094-13105.

Hu X, Ballo L, Pietilla L, Viesselmann C, Lumbard D, Stevenson M, Merriam E, Dent EW (2011) BDNF-induced increase of PSD-95 in dendritic spines requires dynamic microtubule invasions. J Neurosci 31(43):15597-603

Janke C, Kneussel M (2010) Tubulin post-translational modifications: encoding functions on the neuronal microtubule cytoskeleton. Trends in Neurosci. 33(8): 362-372

Jeyifous O, Waites CL, Specht CG, Fujisawa S, Schubert M, Lin EI, Marshall J, Aoki C, de Silva T, Montgomery JM, et al. (2009) SAP97 and CASK mediate sorting of NMDA receptors through a previously unknown secretory pathway. Nat Neurosci. 12:1011–1019

Kawabata I, Kashiwagi Y, Obashi K, Ohkura M, Nakai J, Wynshaw-Boris A, Yanagawa Y, Okabe S. (2012) LIS1-dependent retrograde translocation of excitatory synapses in developing interneuron dendrites. Nat. Comm. 3(722):1-13

Merriam E.B, Lumbard D, Viesselmann C, Ballweg J, Stevenson M, Pietila L, Hu X, Dent E.W. Dynamic microtubules promote synaptic NMDA receptor-dependent spine enlargement. PLoS One 6(11):e27688

Nakata T, Hirokawa N (2003) Microtubules provide directional cues for polarized axonal transport through interaction with kinesin motor head. J Cell Biol. 162:1045-55

Okada Y, Sato-Yoshitake R, Hirokawa N. (1995) The activation of protein kinase A pathway selectively inhibits anterograde axonal transport of vesicles but not mitochondria transport or retrograde transport in vivo. J Neurosci 15, 3053–3064

Schapitz IU, Behrend B, Pechmann Y, Lappe-Siefke C, Kneussel SJ, Wallace KE, Stempel AV, Buck F, Grant SG, Schweizer M, Schmitz D, Schwarz JR, Holzbaur EL, Kneussel M. Neuroligin 1 is dynamically exchanged at postsynaptic sites. (2010) J Neurosci. 30(38):12733-44

Setou M, Nakagawa T, Seog DH, Hirokawa N (2000) Kinesin superfamily motor protein KIF17 and mLin-10 in NMDA receptor-containing vesicle transport. Science 288:1796-1802

Tocco G, Bi X, Vician L, Lim IK, Herschman HR, Baudry M (1996) Two synaptotagmin genes, Syt1 and Syt4, are differentially regulated in adult brain and during postnatal development following kainic acid-induced seizures. Brain Res Mol Brain Res 40:229-239

Vician L, Lim IK, Ferguson G, Tocco G, Baudry M, Herschman HR (1995) Synaptotagmin IV is an immediate early gene induced by depolarization in PC12 cells and in the brain. Proc Natl Acad Sci. USA 92:2164-2168

Wang CT, Lu JC, Bai J, Chang PY, Martin PF, Chapman ER, Jackson MB (2003) Different domains of synaptotagmin control the choice between kiss-and-run and full fusion. Nature 424(6951):943-947

Wang Z, Edwards JG, Riley N, Provance DW Jr. Karcher R, Li XD, Davison LG, Ikebe M, Mercer JA, Kauer JA, Ehlers MD. (2008) Myosin Vb mobilizes recycling endosomes and AMPA receptors for postsynaptic plasticity. Cell 135(3): 535-48

Chapter 5

Conclusion and Future Directions

CONCLUSIONS:

With recent advances in cell biology and high resolution imaging methods, our understanding of the neuronal cytoskeleton has been significantly improved. Actin filaments and MTs have been visualized in live neurons throughout various developmental stages of the nervous system to study their role in cell migration, neuritogenesis, neuronal polarity, synapse formation and maintenance. Because of their small size, dynamic nature and cell intrinsic functions, it is important to use a type of fluorescence microscopy protocol that can acquire images at frequent intervals without inducing phototoxicity in the cell. In my thesis study, I used TIRF microscopy to acquire time-lapse images of mature dendritic spines in cultured cortical and hippocampal neurons. I focused on the roles of dynamic MTs and investigated the hypothesis that MTs are crucial components for the maintenance and plasticity of mature synapses through regulation and transport of postsynaptic material. These results have provided novel insights into the labyrinth of intracellular mechanisms that are involved in synaptic function.

In the first chapter of my thesis, I utilized a long-term neuronal culture system to study the role of dynamic MTs in mature dendrites. We demonstrated that TIRFM could provide superior resolution, contrast and cell viability in time-lapse imaging compared to conventional microscopy methods (widefield fluorescence microscopy). Surprisingly, we documented that MTs rapidly polymerized into and depolymerized out of dendritic spines, pausing longer in spines than in filopodia, suggesting that MTs may function differently in different types of protrusions. MT invasions were transient, infrequent, plus-end driven and maintained even in very mature neurons (up to 63DIV), indicating that dynamic MTs may be associated with certain types of synaptic activity and be involved in adult spine plasticity. Moreover, KCl-induced neuronal depolarization led to prolonged MT invasions in previously unvisited spines, suggesting

that neural activity can directly regulate when and where MT invasions occur in a select subset of spines among the thousands of synapses in a dendritic compartment. These results showed for the first time that mixed polarity MTs remain dynamic in mature dendrites and are capable of entering dendritic spines from both proximal and distal regions of the dendrite. This work raised intriguing questions regarding how MTs are able to decode synaptic activity and what molecular mechanisms regulate MT interactions with other postsynaptic structures. I investigated several of these questions in subsequent chapters.

In chapter two of my thesis, I began to address the question of whether MT invasions directly function in spine plasticity. Using a BDNF treatment known to induce synapse potentiation, I recorded changes in MT dynamics and a crucial postsynaptic scaffolding protein, PSD-95, with TIRFM before and after BDNF treatment. I documented that PSD-95 puncta were very stable in mature cultures as other have shown (Gray et al., 2006), and that PSD-95 puncta movement in spines did not correlate with MT entries. However, I discovered that BDNF-induced accumulation of PSD-95 in spines is dependent on MT invasions. If these MT invasions were abolished by inclusion of nanomolar taxol or nocodazole in the medium the BDNF-induced increase of PSD-95 in spines was abrogated. Furthermore, MT entries were prolonged in spines after BDNF treatment and prolonged MT invasions directly regulated PSD-95 accumulation, possibly through changes in the postsynaptic density structure. Finally, spines that were invaded by MTs after BDNF treatment (but not before) showed the most significant increase in PSD-95. Taken together these data strongly suggest that BDNF-induced synaptic strengthening requires MT invasions into the spines.

Although PSD-95 can be regulated by MT invasions, it is unlikely that PSD-95 puncta are trafficked into spines on MT tracks. In chapter three of my thesis, I studied the dynamics of

synaptotagmin-IV (syt-IV) in dendrites and spines. Syt-IV puncta can move rapidly in mature dendrites in a motor-dependent fashion. Moreover, syt-IV puncta are capable of moving into and out of dendritic spines concomitantly with a MT track present in a spine. These syt-IV trafficking events depended on MT invasions, as low concentrations of taxol blocked both MT entries and syt-IV transport in the spine. To further examine the molecular mechanism of syt-IV trafficking, I imaged KIF17, a dendritic kinesin motor protein, together with syt-IV in young dendrites. Interestingly KIF17 co-localized with rapidly moving syt-IV puncta, but not stationary puncta, indicating that syt-IV trafficking may involve active KIF17 as a MT-based motor protein. Together these results shed light on the avenue of MT-based transport of postsynaptically destined cargos, and provide exciting candidate cargo and motor proteins that are known to be important factors in synaptic plasticity.

FUTURE DIRECTIONS:

Why do dynamic MTs enter dendritic spines?

One major question that remains unanswered at present concerns the exact cellular or synaptic events that drive MTs to polymerize into certain spines. With time-lapse imaging, we observed that only a subset of spines are targeted by MTs within a one hour time period. What makes these spines the special targets of dynamic polymerizing MTs? Are these synapses "tagged" by a specific type of activity or signaling mechanism that require participation of MTs? Based on the results in this thesis study, KCl treatment induced prolonged MT entry in spines that were previously devoid of MTs, but appeared to inhibit MT entry into spines that contained a MT before KCl treatment. Similarly, with BDNF treatment the group of spines that were targeted by MTs after BDNF showed the most robust increase in PSD-95, indicating that they may have been primed for the most significant changes in synaptic activity. Therefore, it is tempting to speculate that MT invasions are involved in the activation of certain signaling pathways that mark these spines as targets of activity-dependent plasticity. It has also been shown that NMDA receptor (NMDAR) activation can elevate MT invasions and these MT entries are required for spine enlargement following the NMDAR activation protocol (Merriam et al., 2011). MT invasions are also dependent on Ca2+ influx and an intact actin cytoskeleton in spines (Merriam et al., unpublished data). Moreover, MT plus ends of MTs, via the +TIP protein EB3, have been shown to directly associate with an actin binding protein p140cap (Jaworski et al., 2009), implicating a intimate interaction between MTs and actin in the spine. Thus, existing evidence suggests that MT invasions can be induced by a variety of synaptic potentiation protocols, and MTs interact with actin filaments to regulate structural and morphological changes in the spine.

To expand on our recent studies it is likely tight temporal and spatial control of activity would yield further insight into the mechanism by which MTs target dendritic spines. All of the experiments I completed were done by bath application of substances that potentiated all of the cells in the culture. Local application of substances or focal uncaging of neurotransmitters would allow one to test other hypotheses that could not be tested by bath application. For example, if MT invasions can be triggered by glutamate uncaging at single dendritic spines, it would support the hypothesis that MT entries are directly downstream of postsynaptic Ca2+ influx and have important roles in synapse potentiation on a single spine level. Similar experiments could be carried out with local uncaging of a function-blocking antibody to BDNF and local profusion of other activity-inducing treatments such as KCl application or locally inducing cLTP. Results from these experiments could give us valuable information on the specific type of activities that can trigger MT invasions. Moreover, existing data suggest that different aspects of MT dynamics are affected in different activity induction scenarios. BDNF treatment prolongs the average MT entry event (Hu et al., 2011), whereas NMDAR activation increases the frequency of invasions and percentage of spines targeted (Merriam et al., 2011). Therefore, local, precise activity induction could help decipher the connection between synaptic potentiation and MT invasions.

Cross-linking of MT and f-actin network in spines

Another interesting direction to pursue would be to investigate the interaction between actin in MTs in spines. Stabilizing actin with jasplakinolide led to more MT invasions, whereas actin depolymerization from the spines using latrunculin reduced MT invasions (Merriam et al., unpublished data). One potential link between MTs and actin filaments is the myosin Va protein.

Myosin Va can directly bind to KIF5 (Huang et al., 1999) and MTs through its tail domain (Cao et al., 2004) to promote cross-linking of the f-actin and MT network. It has also been implicated from myosin Va knockout studies that myosin Va is located on endoplasmic reticulum (ER) structures that are transported by MTs, where myosin Va is in turn responsible for trafficking of ER in actin-rich regions (Takagishi et al., 1996; Bridgman, 1999; Wagner et al., 2011). It would be very interesting to study whether myosin Va could directly link MTs to actin in hippocampal spines and transport polymerizing MTs into the spines on actin filaments. Myosin Va knockdown in mature neurons can be achieved using shRNA, and dynamic MTs and actin can be monitored with time-lapse imaging. If MT invasions are reduced in myosin Va knockdown hippocampal neurons, then it proves that MT invasions are correlated with proper myosin Va function. To exclude the possibility that changes in MT dynamics are downstream of defects in myosin Va-mediated ER transport in the spines, rescue experiments could be performed using wildtype myosin Va and myosin Va with a mutated tail domain that abolishes myosin Va-ER association but not myosin-MT/actin interaction. If MT invasions can be rescued by this mutant myosin Va, then it suggests that myosin Va can directly guide MT invasions into spines on actin tracks.

Recent advancements in super-resolution microscopy provide another interesting method to study potential MT/actin interaction in dendritic spines. Although dynamic MTs and actin filaments have been independently observed in dendritic spines using TIRFM (Hu et al., 2008) or super-resolution methods (Urban et al., 2011) respectively, the two structures have not been imaged together in living spines at super-resolution. It would be fascinating to capture MT invasions and simultaneously image the dynamics of actin filaments in dendritic spines. If MTs polymerize and depolymerize closely along actin bundles, it would suggest a linker protein

complex (myosin Va and KIF5 being two candidates) exists between MTs and actin filaments in the spines to facilitate MT entry. Conversely, if MT polymerization is physically distant from actin bundles in the spine, it would suggest that other cellular mechanisms are responsible for triggering MT invasions. Nonetheless, imaging MT and actin dynamics simultaneously would provide us with the first glance at how they interact with each other at the postsynaptic site at the molecular level. These imaging experiments, however, will require super-resolution techniques to break the diffraction barrier given the small size of dendritic spines and close proximity of actin/MT bundles.

How do MTs mediate transport of postsynaptic cargos?

In the third chapter of this thesis, I found that synaptotagmin-IV labeled puncta could be trafficked in spines on existing MT tracks, and the kinesin-2 family protein KIF17 puncta co-localized with mobile syt-IV puncta in young dendrites. These findings show for the first time that MT invasions could directly deliver postsynaptic cargos into spines. Future experiments are needed to provide a thorough understanding of this process.

First, one could test whether synaptic activity can alter the dynamics of syt-IV in spines, and whether these changes are correlated with MT invasions. Neuronal depolarization has been shown to increase syt-IV trafficking in dendrites, recruitment to synapses and the percentage of syt-IV puncta that co-localized with BDNF (Dean et al., 2009; Dean et al., 2012). Similar activity induction protocols using KCl, forskolin or glycine treatment can be used to study changes in syt-IV and MT dynamics in spines. Since BDNF can consistently prolong MT entries (Hu et al., 2011), it would also be interesting to determine if these prolonged MT invasions are accompanied by more syt-IV movement in the spine. This hypothesis is consistent with the

notion that syt-IV negatively regulates BDNF release from the postsynaptic site. Therefore, it is possible that BDNF treatment can upregulate syt-IV and BDNF colocalization, where syt-IV functions to prevent excess BDNF release in the spines. Since there are more syt-IV containing vesicles destined for spines and MT invasions are responsible for delivery of these vesicles, the prolonged MT retention time in the spines could be required for the upregulated syt-IV trafficking.

Second, more experiments could be done to confirm the role of KIF17 in MT-based transport in spines. Full length KIF17 exists in the neurons primarily in its auto-inhibited form as a cytoplasmic protein, and fluorescently tagged full length KIF17 appear mostly as a diffuse signal throughout the cytoplasm (Hammond et al., 2010; Jaulin and Kreitzer, 2010). Upon activation, the motor domain of KIF17 is released from its tail domain and can appear in punctate form along MT tracks (Cai et al., 2007; Hammond et al., 2010). I propose that by synaptically activating cultures by the methods outlined above one may be able to upregulate syt-IV puncta trafficking. A compensatory increase in mobile KIF17 puncta should then be observed in response to the increased demand of syt-IV transport both in the dendritic shaft and in spines. Another way to study KIF17 mediated trafficking would be to use a KIF17 point mutant (G754E) that maintains the protein in an open and therefore constitutively active form (Jaulin and Kreitzer, 2010). KIF17-G754E has been shown to actively associate with MTs while maintaining an active cargo-binding domain (Jaulin and Kreitzer, 2010). By expressing fluorescently tagged KIF17-G754E and syt-IV I predict that more punctate colocalization might be observed. However, prolonged expression of either full length KIF17 or KIF17-G754E causes deleterious effects in cultured hippocampal neurons (data now shown), which is not surprising given the importance of KIF17 during development. Therefore, it would important to

use a temporally regulated delivery system of these fluorescent proteins. Using a viral transfection system or expression of a TET-ON vector to achieve short-term expression of these motors (1-2 days before imaging) may allow imaging without affecting cellular functions.

The tail-less truncated form of KIF17 has been shown to actively bind to MTs because of the lack of auto-inhibition (Hammond et al., 2010), and can function as a dominant-negative construct. Indeed, by expressing truncated KIF17 and GFP-tubulin, I observed that KIF17 puncta could form in the base of the spine and move into the spine head along polymerized MTs (data not shown), suggesting that KIF17 can traffic along MTs that enter spines. It would be interesting to investigate whether expression of the dominant negative KIF17 can reduce syt-IV trafficking in the dendritic compartment. If fewer mobile syt-IV puncta in the dendritic shaft, or fewer syt-IV transport events in spines are observed, it would suggest that KIF17 is indeed the motor protein that is responsible for the correct targeting of syt-IV.

Third, it is tempting to speculate that a variety of postsynaptic cargo could potentially be transported on MTs in the spine. A major postsynaptic cargo associated with KIF17 is NR2B-containing vesicles (Setou et al., 2000; Guillaud et al., 2003; Guillaud et al., 2008). KIF17 has been shown to support synapse potentiation by upregulation of NR2B levels in the spine (Yin et al., 2011). It has been proposed that NR2B-containing complexes are dissociated from MTs in the dendritic shaft via CaMKII mediated phosphorylation, as the complex approaches the destined spine (Guillaud et al., 2008). However, based on my results a more plausible hypothesis may be that detachment of NR2B-containing vesicles from MTs occurs in the spine head, where the concentration of active CaMKII is likely far higher compared to the dendritic shaft. Imaging experiments observing dynamics of NR2B containing packets and MTs could be performed to study the potential of MT-based NR2B transport in dendritic spines. Similarly,

AMPA receptor trafficking has been demonstrated to be dependent on myosin Vb in spines (Wang et al., 2008). However, it is still possible that an recycling endosome-independent trafficking pathway for AMPARs could be associated with MT invasions. This could be tested by imaging MT dynamics together with a phluorin-tagged GluR1 protein to visualize the level of postsynaptic insertion of GluR1 with MT entries. Other candidate cargos include KIF5-based transport of mitochondria and TrkB containing vesicles, as well as mRNAs (e.g: fmr1, CaMKII, BDNF) that would facilitate local translation in dendritic spines.

Finally, it would be interesting to study whether dynein-mediated retrograde transport could occur on MTs that have invaded spines. A recent study demonstrated that PSD-95/neuroligin 1 complex could be retrieved from spines by dynein, possibly on MT tracks (Schapitz et al., 2010). In cortical interneurons, a dynein adaptor protein LIS1 was shown to regulate retrieval of PSD-95 prior to synapse remodeling (Kawabata et al., 2012). Dynein was also identified to be responsible for retrograde transport of $GABA_A$ receptors through an adaptor protein muskelin (Heisler et al., 2011). Since our results indicate that syt-IV puncta can be retrogradely transported out of spines by MTs, time-lapse imaging of dynein with tubulin and/or syt-IV could address the question of whether dynein moves processively on MT tracks in spines, and whether dynein puncta co-localize with syt-IV. It would also be reasonable to test if known cargo of dynein (BDNF, TrkB, Rab5-containing endosomes) can be retrieved out of spines (Colin et al., 2008; Deinhardt et al., 2006; Satoh et al., 2008; Zheng et al., 2008). A first step to take could be to image the dynamics of fluorescently tagged dynein heavy chain or dynein light chain (Tctex-1) with tubulin, to record whether retrograde movement of dynein complex occurred during MT invasions. Once MT-dependent dynein localization in spines is confirmed, time-lapse imaging of dynein and its cargos could reveal whether postsynaptic components are retrieved out of

spines via dynein-based retrograde transport. To study whether dynein is required for retrograde transport in spines, siRNA can be used to transiently knock down dynein expression in neurons. To test whether the dynein/dynactin complex is responsible for transport, dynamitin overexpression can be used to disrupt dynein/dynactin interaction in neurons (Melkonian et al., 2007; Schapitz et al., 2010).

MT invasions may be implicated in spine pathology underlying neurological disorders

Changes in spine morphology and density in cortical neurons have been observed in postmortem brain tissue of a number of neurological disorders (Penzes et al., 2011). Several studies have shown reduced spine density on cortical and hippocampal pyramidal neurons that correlate with loss of gray matter and brain volume in specific brain regions in schizophrenia patients (Sweet et al., 2009; Steen et al., 2006; Kolomeets et al., 2005). In developmental diseases, genome-wide association studies have identified mutations in the synaptic adhesion molecules neuroligin-3/4 and their ligand neurexin1 as genetic factors involved in the autism spectrum disorder (ASD) (Sudhof, 2008). Cultured neurons expressing mutant neuroligin-3/4 and neurexin1 show increased spine density that may explain the pruning defects during adolescence and hyperactivity in ASD patients (McClellan and King, 2010). Interestingly, translocation of neuroligin1 out of spines is dependent on PSD-95 and dynein-mediated retrograde transport (Schapitz et al., 2010), indicating a potential role for MT invasions in the malfunction of neuroligin/neurexin interaction. Similarly, in fragile-X-syndrome, mutation in the fmr1 gene results in elevated spine density and long, tortuous spines that may have resulted from pruning defects (Irwin et al., 2001). Since the expression of fmr1 gene has been implicated in mRNA translocation and local translation (Bagni and Greenough, 2005), it is tempting to

speculate that MT-based transport is involved in this process not only in the dendritic shaft, but also in spines. Experiments using neurons from mouse models of these disorders could reveal potential deficits in MT dynamics and MT-based functions in dendritic spines. It would be interesting to study whether MTs could directly transport FMRP mRNA into the spine, or mediate translocation of adhesion complexes containing neuroligin -3/4.

Alzheiner's disease (AD) is the most prevalent form of neurodegenerative disease. Spine loss is observed throughout the cortex and hippocampus in AD patients associated with accumulation of amyloid plaques (DeKosky and Scheff, 1990). Importantly, synaptic dysfunction shows a stronger correlation with cognitive decline than does neuronal loss (Walsh and Selkoe, 2004), indicating that synapse atrophy occurs early in AD onset and may be the driving force of disease progression. Interestingly, several recent studies have identified the MT-binding protein tau as an important factor in synapse degeneration (Ballatore et al., 2007; Hoover et al., 2010; Thies et al., 2007; Zempel et al., 2010). Tau is mislocalized from axons to dendrites and spines in mouse models of AD, where it affects proper synaptic function (Hoover et al., 2010). Since tau mainly functions as a MT stabilizing protein in the axon, it is possible that dendritic tau could dampen MT dynamics and reduce MT invasions into spines. It would be interesting to perform live cell imaging experiments using mature neurons overexpressing tau, which induces dendritic localization, and observe changes in MT dynamics in dendrites and spines. If MT invasions of spines are suppressed, which we know leads to reduced spine size and density (Hu et al., unpublished), then it is very likely that dynamic MTs are involved in synaptic dysfunction during AD onset and progression.

In summary, this work explores the new realm of MT functions in dendritic spines, and presents a promising future direction where MTs could be key regulators of synaptic plasticity by

mediating postsynaptic cargo trafficking. Since dendritic MTs remain dynamic in mature hippocampal neurons (hippocampal cultures up to 63DIV or slices 100DIV), it is likely that MT invasion of spines occurs throughout the life of these neurons as a way to deliver cargo into targeted spines. It would be fascinating to define the molecular mechanisms that underlie this transport process in spines. Future experiments directed at identifying the postsynaptic cargoes trafficked by MTs, and pinpointing the targeted spines that may be undergoing specific types of synaptic changes could provide a novel perspective in our understanding of synaptic maintenance and plasticity in the CNS.

REFERENCES:

Bagni C, Greeough WT (2005) From mRNP trafficking to spine dysmorphogenesis: the roots of fragile X syndrome. Nat Rev Neurosci 6:376-387

Ballatore C, Lee VM, Trojanowski JQ. (2007). Tau-mediated neurodegeneration in Alzheimer's disease and related disorders. Nat Rev Neurosci 8:663-672

Bridgman PC. (1999) Myosin Va movements in normal and dilute-lethal axons provide support for a dual filament motor complex. J Cell Biol. 146(5): 1045-60

Cai D, McEwen DP, Martens JR, Meyhofer E, Verhey KJ. (2009) Single molecule imaging reveals differences in microtubule track selection between Kinesin motors. PLoS Biol. 7(10):e1000216

Cao TT, Chang W, Masters SE, Mooseker MS. (2004) Myosin-Va binds to and mechanochemically couples microtubules to actin filaments. Mol Biol Cell. 15(1): 151-61

Chih B, Afridi SK, Clark L, Scheiffele P. (2004) Disorder-associated mutations lead to functional inactivation of neuroligins. Hum Mol Genet. 13:1471-77

Colin E, Zala D, Liot G, Rangone J, Borrell-Pages M, Li XJ, Saudou F, Humbert S. (2008) Huntingtin phosphorylation acts as a molecular switch for anterograde/retrograde transport in neurons. EMBO J. 27(15):2124-34

Dean C, Liu H, Dunning FM, Chang PY, Jackson MB, Chapman ER (2009) Synaptotagmin-IV modulates synaptic function and long-term potentiation by regulating BDNF release. Nat Neurosci. 12(6):767-76

Dean C, Liu H, Staudt T, Markus TA, Siv V, Buckers J, Kamin D, Engelhardt J, Jackson M, Hell SW, Chapman ER (2012) Distinct subsets of Syt-IV/BDNF vesicles are sorted to axons versus dendrites and recruited to synapses by activity. J. Neurosci 32(16):5398-5413

Deinhardt K, Salinas S, Verastequi C, Watson R, Worth D, Hanrahan S, Bucci C, Schiavo G. (2006) Rab5 and Rab7 control endocytic sorting along the axonal retrograde transport pathway. Neuron 52(6):293-305

DeKosky ST, Scheff SW. (1990) Synapse loss in frontal cortex biopsies in Alzheimer's disease: correlation with cognitive severity. Ann. Neurol. 27:457-64

Guillaud L, Wong R, Hirokawa N. (2008) Disruption of KIF17-Mint1 interaction by CaMKII-dependent phosphorylation: a molecular model of kinesin-cargo release. Nat Cell Biol.10(1):19-29

Guillaud L, Setou M, Hirokawa N. (2003) KIF17 dynamics and regulation of NR2B trafficking in hippocampal neurons. J Neurosci. 23(1):131-40

Hammond JW, Huang CF, Kaech S, Jacobson C, Banker G, Verhey KJ, (2010) Posttranslational modification of tubulin and the polarized transport of kinesin-1 in neurons. Mol Biol Cell 21(4): 572-583

Hammond JW, Blasius TL, Soppina V, Cai D, Verhey KJ. Autoinhibition of the kinesin-2 motor KIF17 via dual intramolecular mechanisms. (2010) J Cell Biol. 189(6):1013-25

Heisler FF, Loebrich S, Pechmann Y, Maier N, Zivkovic AR, Tokito M, Hausrat TJ, Schweizer M, Bahring R, Holzbaur EL, Schmitz D, Kneussel M. (2011) Muskelin regulates actin filament- and microtubule-based GABA(A) receptor transport in neurons. Neuron 71(1): 66-81

Hu X, Ballo L, Pietilla L, Viesselmann C, Lumbard D, Stevenson M, Merriam E, Dent EW (2011) BDNF-induced increase of PSD-95 in dendritic spines requires dynamic microtubule invasions. J Neurosci 31(43): 15597-603

Hu X, Viesselmann C, Nam S, Merriam E, Dent EW (2008) Activity-dependent dynamic microtubule invasion of dendritic spines. J Neurosci 28:13094-13105.

Huang JD, Brady ST, Richards BW, Stenolen D, Resau JH, Copeland NG, Jenkins NA. (1999) Direct interaction of microtubule- and actin-based transport motors. Nature 397(6716): 267-70

Hoover BR, Reed MN, Su J, Penrod RD, Kotilinek LA, Grant MK, Pitstick R, Carlson GA, Lanier LM, Yuan LL, et al. (2010). Tau mislocalization to dendritic spines mediates synaptic dysfunction independently of neurodegeneration. Neuron 68, 1067-1081

Irwin SA, Patel B, Idupulapati M, Harris JB, Crisostomo RA, Larsen BP, Kooy F, Willems PJ, Cras P, Kozlowski PB, Swain RA, Weiler IJ, Greenough WT. (2001) Abnormal dendritic spine characteristics in the temporal and visual cortices of patients with fragile-X syndrome: a quantitative examination. Am. J. Med Genet. 98:161-167

Jaulin F, Kreitzer G. (2010) KIF17 stabilizes microtubules and contributes to epithelial morphogenesis by acting at MT plus ends with EB1 and APC. J Cell Biol. 190(3): 433-60

Kawabata I, Kashiwagi Y, Obashi K, Ohkura M, Nakai J, Wynshaw-Boris A, Yanagawa Y, Okabe S. (2012) LIS1-dependent retrograde translocation of excitatory synapses in developing interneuron dendrites. Nat. Comm. 3(722):1-13

Kolomeets NS, Orlovskaya DD, Rachmanova VI, Uranova NA. (2005) Ultrastructural alterations in hippocampal mossy fiber synapses in schizophrenia: a postmortem morphometric study. Synapse 57:47-55

McClellan J, King MC (2010) Genetic heterogeneity in human disease. Cell 141: 210-217

Merriam EB, Lumbard D, Viesselmann C, Ballweg J, Stevenson M, Pietila L, Hu X, Dent EW. (2011) Dynamic microtubules promote synaptic NMDA receptor-dependent spine enlargement

Melkonian K, Maier K, Godfrey J, Rodgers M, Schroer T (2007) Mechanism of dynamitin-mediated disruption of dynactin. J Biol. Chem. 282(27): 19355-364

Penzes P, Cahill ME, Jones KA, VanLeeuwen JE, Woolfrey KM. (2011) Dendritic spine pathology in neuropsychiatric disorders. Nat Neurosci. 14(3):285-93

Satoh D, Sato D, Tsuyama T, Saito M, Ohkura H, Rolls MM, Ishikawa F, Uemura T. (2008) Spatial control of branching within dendritic arbors by dynein-dependent transport of Rab5-endosomes. Nat. Cell Biol. 10(10):1164-71

Schapitz IU, Behrend B, Pechmann Y, Lappe-Siefke C, Kneussel SJ, Wallace KE, Stempel AV, Buck F, Grant SG, Schweizer M, Schmitz D, Schwarz JR, Holzbaur EL, Kneussel M. Neuroligin 1 is dynamically exchanged at postsynaptic sites. (2010) J Neurosci. 30(38):12733-44

Setou M, Nakagawa T, Seog DH, Hirokawa H. Kinesin superfamily motor protein KIF17 and mLin-10 in NMDA receptor containing vesicle transport. (2000) Science 288(5472): 1796-802

Sweet RA, Henteleff RA, Zhang W, Sampson AR, Lewis DA (2009) Reduced dendritic spine density in auditory cortex of subjects with schizophrenia. Neuropsychopharmacology 34:374-89

Sudhof TC (2008) Neuroligins and neurexins link synaptic function to cognitive disease. Nature 455:903-911

Takagishi Y, Oda S, Hayasaka S, Dekker-Ohno K, Shikata T, Inouye M, Yamamura H. (1996) The dilute-lethal (dl) gene attacks a Ca2+ store in the dendritic spine of Purkinje cells in mice. Neurosci Lett. 215(3):169-72

Thies E, Mandelkow EM. (2007) Missorting of tau in neurons causes degeneration of synapses that can be rescued by the kinase MARK2/Par-1. J Neurosci 27, 2896-2907

Urban NT, Willig KI, Hell SW, Nagerl UV. (2011) STED nanoscopy of actin dynamics in synapses deep inside living brain slices. Biophys J. 101(5): 1277-84

Wagner W, Brenowitz SD, Hammer JA 3rd. (2011) Myosin-Va transports the endoplasmic reticulum into the dendritic spines of Purkinje neurons. Nat Cell Biol. 13(1): 40-8

Walsh DM, Selkoe DJ (2004) Deciphering the molecular basis of memory failure in Alzheimer's disease. Neuron 44:181-193

Wang Z, Edwards JG, Riley N, Provance DW Jr, Karcher R, Li XD, Davison IG, Ikebe M, Mercer JA, Kauer JA, Ehlers MD. (2008) Myosin Vb mobilizes recycling endosomes and AMPA receptors for postsynaptic plasticity. Cell 135(3):535-48

Yin X, Takei Y, Kido MA, Hirokawa N. Molecular motor KIF17 is fundamental for memory and learning via differential support of synaptic NR2A/2B levels. (2011) Neuron 70(2):310-25

Zempel H, Thies E, Mandelkow E, Mandelkow EM. (2010) Abeta oligomers cause localized Ca(2+) elevation, missorting of endogenous Tau into dendrites, Tau phosphorylation, and destruction of microtubules and spines. J Neurosci 30, 11938-11950

Zheng Y, Wildonger J, Ye B, Zhang Y, Kita A, Younger SH, Zimmerman S, Jan LY, Jan YN. (2008) Dynein is required for polarized dendritic transport and uniform microtubule orientation in axons. Nat Cell Biol. 10(10):1172-80